STRUCTURAL DYNAMICS OF TRANSMEMBRANE SIGNALING COMPLEXES BY NEGATIVE STAIN ELECTRON MICROSCOPY

by

Liliya Vasileva Mancour

A dissertation submitted in partial fulfillment
of the requirements for the degree of
Doctor of Philosophy
(Biological Chemistry)
in The University of Michigan
2013

Doctoral Committee:

Assistant Professor Georgios Skiniotis, Chair
Professor Christin Carter-Su
Professor Ari Gafni
Associate Professor Jason E. Gestwicki
Professor Janet Smith

Dedication

I dedicate this thesis to my mom, Elena Yordanova Grozdanova-Harizanova. Without her support, persistence and positive thinking I would have never gotten this far in my academic endeavors.

Acknowledgements

I would like to thank Dr. Georgios Skiniotis for giving me the opportunity to work in his laboratory during my graduate studies. I would also like to thank my committee members, Christin Carter-Su, Ari Gafni, Jason Gestwicki and Janet Smith. I was very fortunate that they all agreed to support me throughout my thesis work. I have received their unconditional advice, mentorship and dedication well beyond their duties of committee members and I am eternally grateful for all of their support.

I also would like to acknowledge my laboratory mates, both past and present, for all of their support, helpful discussions and simply sharing my experiences in the laboratory. I specifically want to thank Gerwin Westfield who has been there for me since the commencement of our graduate school studies and for all of his help with the computational side of my projects.

Of course, I could have not made it throughout the last five years without the help and support of my friends , both here in Michigan and elsewhere. I became friends with an extraordinary group of people here at University of Michigan, and I hope they all remain my friends for life.

Last but not least, I would like to acknowledge the immense support of my family who kept my sanity and my focus during hard times. I would like to thank my mom who has provided me with her unconditional support and everything that anyone could have given me in order to come this far. Also, my husband, Matthew Mancour who never lost faith in me and has always encouraged and supported me with anything that I have taken upon.

Table of Contents

List of Figures

List of Appendices

List of Abbreviations

aa	amino acid
ATP	adenosine triphosphate
β_2AR	β_2-adrenergic receptor
cAMP	cyclic adenosine monophosphate
CCC	Cross-correlation coefficient
CHR	cytokine homology region
CTF	contrast transfer function
DAG	diacylglycerol
EM	electron microscopy
EPO(R)	erythropoietin receptor
FNIII	fibronectin III
GCSF(R)	granulocyte colony stimulating factor (receptor)
GPCR	G-protein coupled receptor
IgG	Immunoglobulin G
IL-	interleukin
IP_3	inositol 1,4,5-triphosphate
JAK	Janus kinase
LC	Liquid chromatography
LEPR	leptin receptor
LIF(R)	leukemia inhibitory factor (receptor)
MOR	μ-opioid receptor
MS	Mass spectrometry
MW	Molecular weight
Ni-NTA	Nickel nitrilotriacetic acid
PAGE	polyacrylamide gel electrophoresis
PDB	protein data bank
PTPase	phosphatase
SDS	sodium dodecyl sulfate
STAT	signal transducer and activator of transcription
TEV	Tobacco etch virus

Abstract

As an integral part of the cell's communication system, membrane proteins play an essential role in relaying signals between cells and their environment. For example, binding of ligand on the extracellular portion of a cell surface receptor induces conformational changes that are transmitted through the membrane and activate numerous signaling pathways. I have utilized negative stain electron microscopy and single particle analysis to investigate and characterize the structural dynamics of transmembrane protein machineries.

The hormone leptin is a key regulator of metabolism and body weight. The leptin receptor (LepR) is a single pass transmembrane receptor that is capable of instigating intracellular signaling *via* the JAK/STAT pathway upon leptin binding to the extracellular side of LepR. Both stimulation and inhibition of LepR have implications in disease treatment and represent important drug targets. I characterized the architecture of the leptin/LepR signaling complex and proposed a mechanism of activation upon binding of ligand. LepR displays significant flexibility in a hinge region within the leptin binding domain while the C-terminal "legs" remain rigid. In the context of a liganded receptor, there is no flexibility at the hinge region and the C-terminal, membrane proximal "legs" become positioned in a certain orientation that we propose is a key mechanism for transmitting the signaling across the membrane.

This work also characterizes a signaling complex between the μ-Opioid receptor (μ-OR) and its cognate Gi subunit. The results reveal the dynamic nature of the Gα subunit of Gi, which appears to be a common feature of G-protein activation. As opioid drugs are highly addictive and their clinical efficacy restricted, understanding the activation mechanism of the μ-OR will facilitate more targeted drug development.

Chapter 1 Introduction

1.1 Structure and Function on Membrane Proteins

Membrane proteins are biologically very important groups of proteins because they connect the extracellular environment to the intracellular environment of the cell. Membrane proteins are involved in immune response and recognition, transport of molecules across the phospholipid bilayer, cell adhesion and signal transduction. There are two major categories of membrane proteins based on the membrane interaction - integral and peripheral. Integral membrane proteins are characterized by at least one membrane-spanning domain with many hydrophobic side chains in their amino acid composition, allowing them to make contact with the fatty acyl groups of the phospholipids. Integral membrane proteins penetrate the phospholipid bilayer through α-helices or β-barrels, making these regions both structural and functional components of the cell membrane. On the other hand, the peripheral membrane proteins do not directly interact with the hydrophobic core of the phospholipid bilayer but instead are connected to the membrane through polar head groups (Lodish et al., 2000) (Figure 1-1). Ligand binding on the extracellular side of an integral membrane protein can lead to conformational changes, which are then transferred to the intracellular side, and the signal is converted to a physiological response. Membrane proteins comprise an extremely sophisticated set of cellular machineries whose intricate functions depend largely on the chemical makeup of the amino acids displayed on their surfaces.

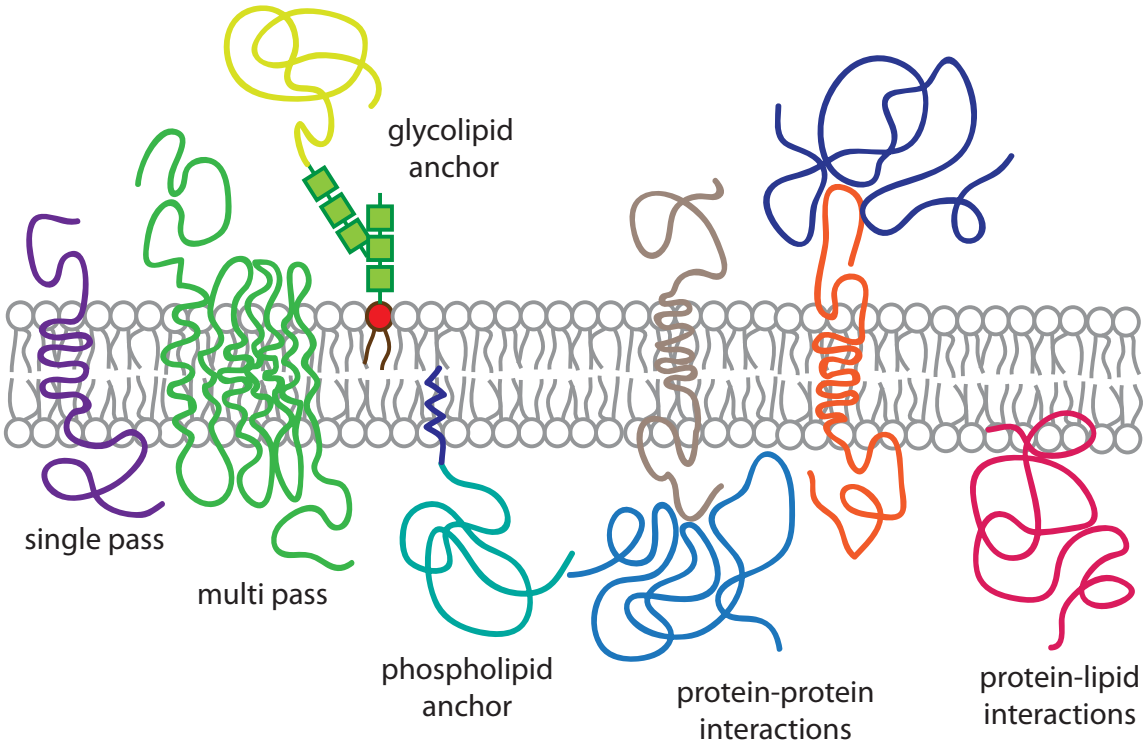

Figure 1-1 An illustration of different types of membrane – protein associations. There are two major groups of membrane-associated proteins, based on their interaction with the membrane. Peripherally associated proteins only make a contact with the membrane and have an access either to the intracellular or the extracellular space. Examples are protein-lipid interactions and glycolipid-anchor. The integral membrane proteins are mainly single or multiple pass proteins making access to both the extracellular and intracellular space.

In addition, their specific protein fold has a crucial significance in positioning a precise set of amino acids at the ligand binding pocket, governing the interactions with extracellular signals. The three-dimensional structure of proteins changes upon interaction with environmental stimuli. Following reversible or irreversible series of chemical shifts in their three dimensional structure is a way of providing a mechanism for exertion and regulation of cell processes. Exactly how the integral membrane proteins are able to transmit an extracellular signal in the form of a conformational change through the membrane and initiate physiological response is still poorly understood.

Although membrane proteins constitute about 30% of the proteome, their solved structures are highly underrepresented, making up only about 2% of the total structures in the Protein Data Bank (PDB) (Figure 1-2).

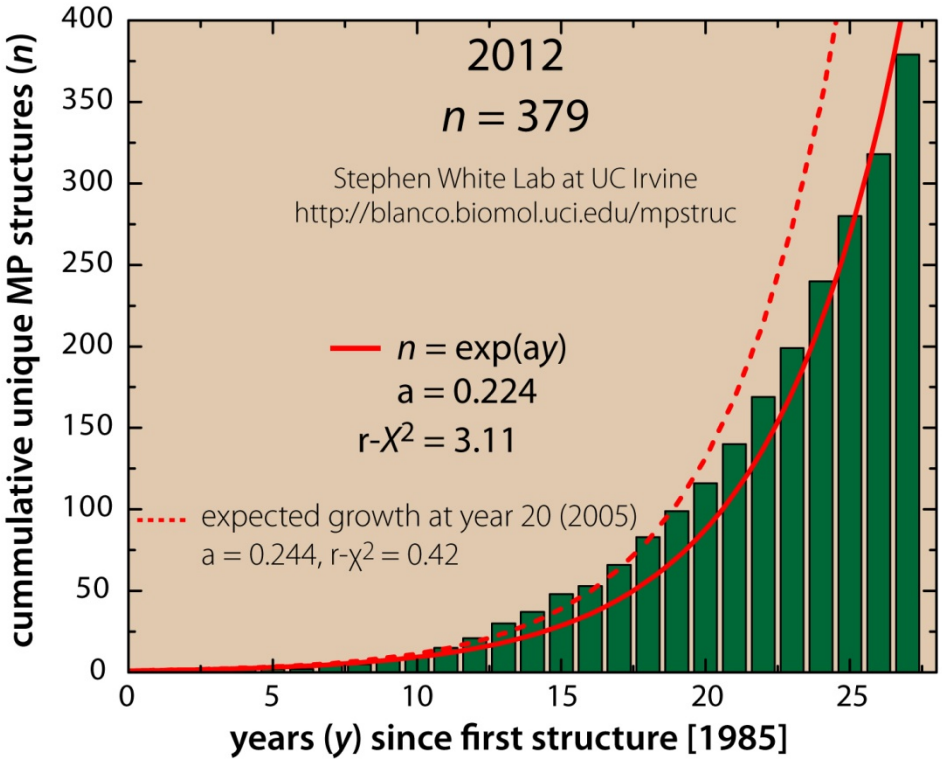

Figure 1-2 Number of known membrane protein structure in PDB up to date (http://blanco.biomol.uci.edu/mpstruc/listAll/list)

The technical difficulties in expression, solubilization and purification are responsible for the low number of solved membrane protein structures. Recent advances in protein engineering had aided the successful crystallization of a few challenging membrane proteins, shedding new light into our understanding of structure-function relationship.

1.2 Membrane proteins as signal transduction units

A cell communicates with its environment by receiving, processing and responding to specific chemicals that can trigger signal transduction. The sensing and processing of stimuli is termed a signal transduction cascade whereby the cell is able to detect, amplify and integrate various external signals in order to generate diverse biological responses. For example, extracellular stimuli can modulate receptor and/or enzyme activity, ion-channel activity or the expression of certain genes which may lead to disease (Berg et al., 2002).

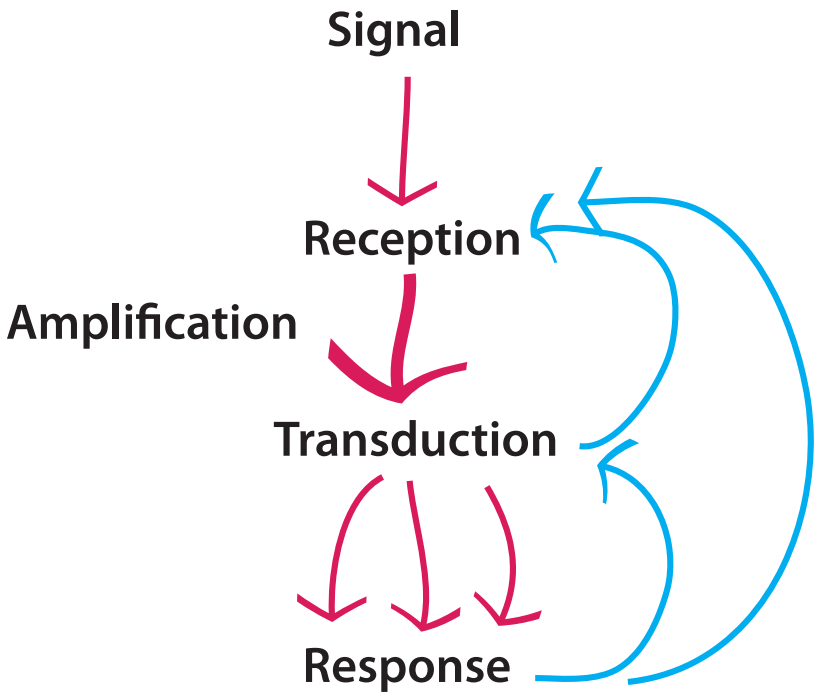

Figure 1-3 Signal propagation diagram.
A signal in the form of any stimuli is received by the cell surface receptor (reception), amplified by the second messengers and transduced to downstream signaling effectors. As a result, a cellular response is generated in the form of transcriptional activation, for example.

The main principles of signal transduction can be summarized in (Figure 1-3). An environmental signal, termed primary messenger, arrives at the cell membrane and since it is usually unable to cross the membrane, it interacts with a cell-surface receptor. Following the receptor interaction, the signal is relayed to the cell by a way of a conformational change in the receptor protein and further converted into an intracellular chemical response. On the intracellular side and in the cytosol, the signal is usually amplified by other small molecules, termed secondary messengers. The secondary messengers stimulate downstream effector molecules which in turn are able to trigger a physiological response. Second messengers are very important in signal transduction because they not only amplify the signal generated by a few activated membrane receptors but also travel to a variety of cellular compartments and signal in multiple pathways. Some of the important second messengers include cyclic AMP (cAMP), cyclic

GMP (cGMP), calcium ion (Ca^{2+}), inositol 1,4,5-triphosphate (IP_3) and diacylglycerol (DAG) (Stryer 2002) (Figure 1-4).

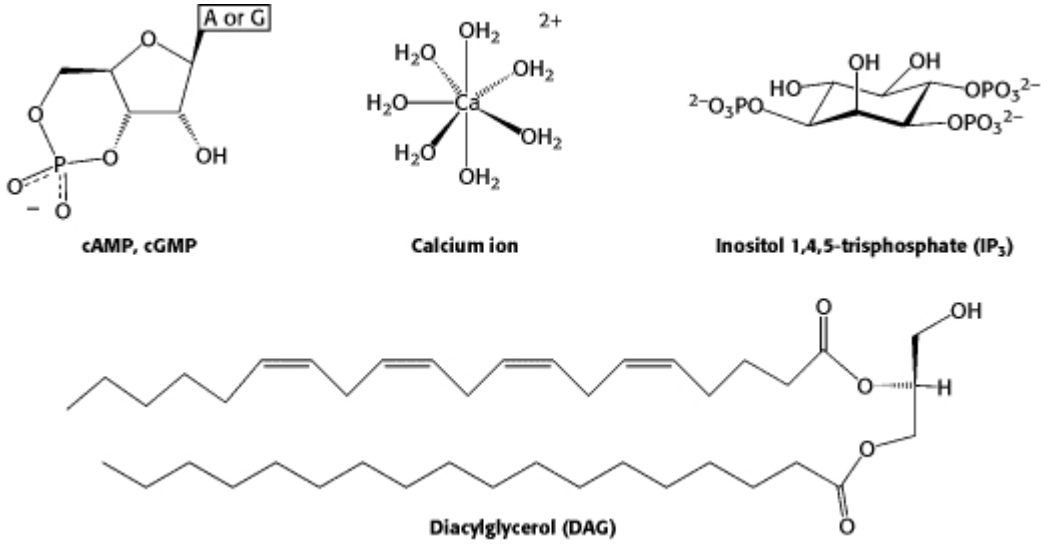

Figure 1-4 Structures of some important second messengers.

The concentration of these small molecules changes in response to extracellular stimuli and since they are readily diffusible through other cellular compartments, they can modulate diverse biochemical processes in the cell. Moreover, many cell surface receptors share the same second messengers in multiple signaling pathways which can often lead to cross talk, affecting the local concentration of second messengers. It is important to mention, however, that cross talk can not only lead to more precise regulation of cellular activity but also it may cause potential problems if the second messengers are misinterpreted by the cell (Berg et al., 2002). In addition, this signaling cascade can be modulated by feedback mechanisms by which the cell's response is able to inhibit or change the initial signal reception.

Some small non-polar molecules such as certain hormones can diffuse through the cell membrane and instigate signaling. Most of the time, however, the cell surface receptors are responsible for making the first contact with the environmental stimuli. Thus, large and polar molecules that are otherwise incapable of entering the cell are transmitting the information they are carrying into the intracellular space.

In addition, information transduction can be in the form of protein phosphorylation where second messengers activate protein kinases. In this case, an enzyme transfers a phosphoryl group from an adenosine triphosphate (ATP) to a serine, threonine or tyrosine residue of a protein. Protein phosphatases may reverse this change by dephosphorylating the protein and terminating the signal (Figure 1-5).

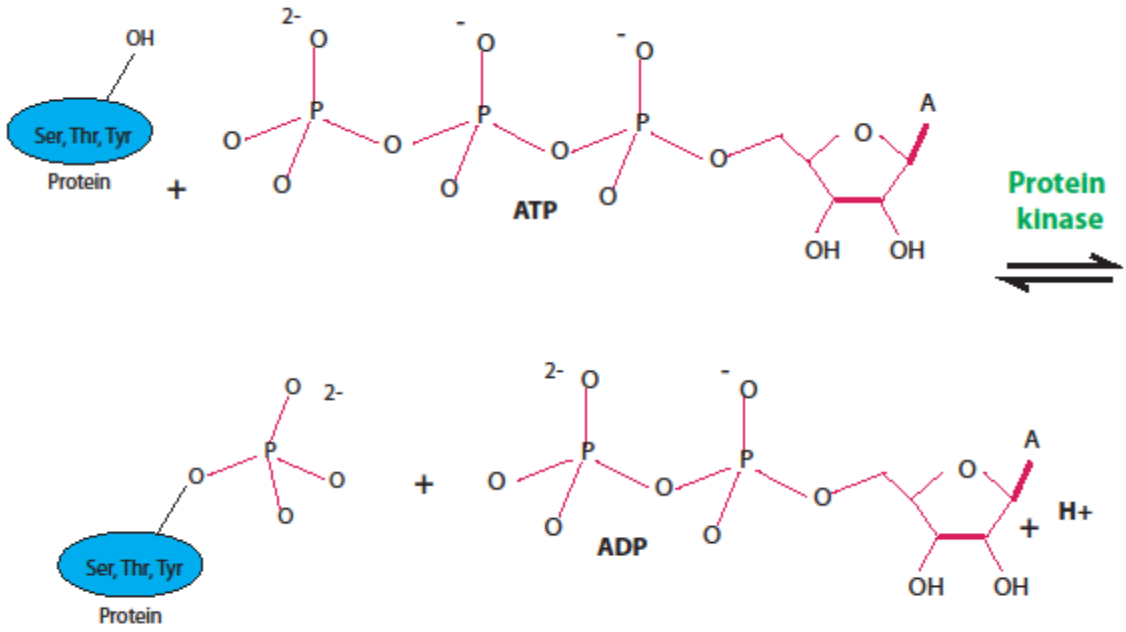

Figure 1-5 Phosphate transfer.
Graphical representation of the γ phosphate transfer from an adenosine tri-phosphate (ATP) to a Serine, a Threonine or a Tyrosine residue on a protein.

Signal termination is needed in order for the cell to respond to new signals. However, when the signal cascade fails to be terminated, the cell can undergo uncontrolled growth or even become cancerous. Other mechanisms for signal transduction termination can be exerted in the form of negative feedback processes. A well-documented example of negative feedback used as a regulatory mechanism is the signaling of insulin. Insulin signals to liver cells to reduce the production and release of glucose thereby contributing to lowered blood glucose levels. In addition, insulin signals to fat and muscle to take up glucose at a greater rate. Insulin binds and activates transmembrane receptor tyrosine kinases which upon activation are phosphorylated on certain Tyrosine residues. Tyrosine phosphatases (PTPases) are enzymes capable of dephosphorylating the receptor and attenuating the insulin-induced signaling. A negative feedback mechanism of insulin

signaling is the insulin-mediated transcriptional activation of PTPases, which dephosphorylate the insulin receptors and attenuating the signal (James et al., 2005; Saltiel and Kahn, 2001).

Some integral membrane proteins serve as ion channels, cellular transporters of cargo binding to them, energy pumps, enzymes catalyzing reactions at the cell membrane surfaces or receptors that transmit chemical information. The work in this thesis concentrates on the topics of how two different classes of integral membrane receptors, specifically, single and multiple pass receptors, are able to communicate signals through the cell membrane in response to extracellular stimuli and instigate physiological processes. Understanding the conformational dynamics of how these complicated membrane machineries are able to transduce information through the membrane is the primary aim of my studies.

1.3 Cytokines and signal transduction

Cytokines and their receptors

The formation of a ligand-receptor complex at the membrane is the prerequisite for instigating intracellular signaling cascades. Cytokines are pleiotropic signaling molecules that regulate important biological responses such as immune response, cell proliferation, differentiation and apoptosis (Wang et al., 2009). Both ligands and receptors that belong to the cytokine superfamily share common structural features. Class 1 cytokines are most abundant and are characterized by a typical "four-helical" bundle fold (Bazan, 1990a) with their hydrophilic residues oriented on the outside and the hydrophobic ones forming the core of the helical bundle (Sprang, 1993). To signal, cytokines bind to their corresponding transmembrane receptors and instigate intracellular downstream signaling by stimulating an array of cytosolic molecules. According to their structure, the cytokine receptors can also be classified into several groups - class I, class II, TNF receptor superfamily, IL-1 and chemokine receptor family with class I being the largest (Thomson and Lotze, 2003). Because of their structural similarities, receptors can engage similar ligands, thus, involving redundant biological processes. Receptors belonging to this class, also known as the hematopoietin receptor family, are single pass

transmembrane proteins having an N-terminal extracellular, ligand-binding portion and C-terminal intracellular tail. Members of this family include granulocyte colony stimulating factor receptor (GCSF-R), leukemia inhibitory factor receptor (LIF-R), leptin receptor (Lep-R) and glycoprotein 130 (gp130) (Baumann et al., 1996; Tamada et al., 2006; Wang et al., 2009) and others. The extracellular regions of class I cytokine receptors are grouped into modules, consisting of an array of fibronectin type-III (FNIII) fold domains. A membrane distal cytokine homology region (CHR) motif is associated with ligand-binding and is necessary for signaling (Eastell et al., 1998) (Bazan, 1990b; de Vos et al., 1992). In some members of this class such as the human Growth Hormone receptor (hGHR) and the erythropoietin receptor (EPOR), the basic CHR is sufficient to engage the ligand and initiate receptor homodimerization (de Vos et al., 1992; Sprecher et al., 1998). However, an Ig-like domain is an additional prerequisite for ligand-binding and signal induction in other cytokine receptors such as gp130, GCSF-R, LIF-R and LepR (Chow et al., 2001; Huyton et al., 2007; Tamada et al., 2006; Fong et al., 1998). Additional membrane-proximal FNIII type domains connect the ligand-binding region to the membrane. Following a single transmembrane helix, these receptors are characterized by a short intracellular tail also marked by conserved regions. Box 1 and box 2 motifs, for example, found in close proximity to the membrane, serve as docking sites for constitutively bound kinases, required to propagate the signal initiated by ligand binding (Tanner et al., 1995; Usacheva et al., 2002) (Figure 1-6a). Class I cytokine receptors are not active kinases themselves. Instead, they rely on constitutively bound Janus kinases (JAK's) to execute the tyrosine kinase activity needed for signal transduction (Darnell et al., 1994; Leonard and O'Shea, 1998; Murray, 2007). Ligand-binding on the outside is followed by a conformational change which results in a critical re-orientation of the intracellularly bound kinases which are activated upon their transphosphorylation.

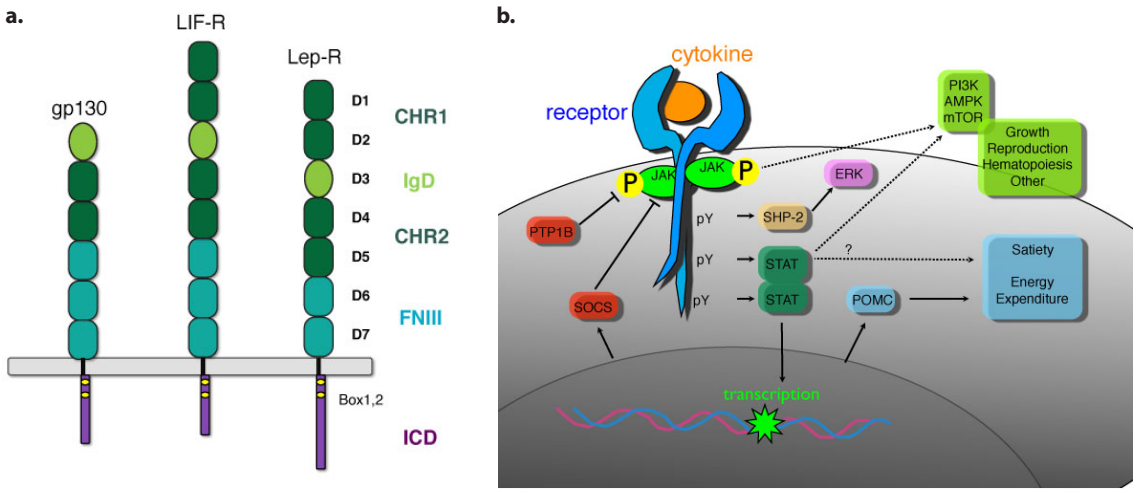

Figure 1-6 Overall domain organization of some class I cytokine receptors and their signal transduction.
a, Domain organization of class I cytokine receptors – receptors belonging to class I are composed of an array of fibronectin III fold domains at their extracellular region; cytokine homology region (CHR) and immunoglobulin-like domain are involved in ligand binding; conserved Box 1, 2 motifs on the intracellular receptor tails serve as Janus Kinases binding sites; b, Signaling pathways activated by class I cytokines – Jak/Stat pathway is the primary pathway instigated upon ligand biding to class I cytokine receptors. Secondary signaling pathways involved in growth, reproduction and energy expenditure can also be activated as a result of cytokine signaling. (b, Courtesy of Georgios Skiniotis)

Once activated, the JAKs phosphorylate certain residues on the receptor tail which serve as docking sites for a second family of proteins, the signal transducer and activator of transcription (STAT) proteins. STATs bind to the receptor tail and their JAK-mediated phosphorylation and activation results in subsequent dissociation from the receptor and dimerization in the cytoplasm. In turn, STATs translocate into the nucleus and activate transcription of variety of genes (Ihle, 2001; Schindler et al., 2007). In addition to the JAK-STAT signaling pathway, the class I cytokine receptor family can instigate and signal through many other pathways such as the PI3K kinase and/or the RAS/MAP kinase pathway (Cantley, 2002; Dong et al., 2002). However, how the structural changes upon ligand binding are transmitted on the other side of the membrane to instigate signaling as well as the structural dynamics surrounding the JAK-STAT communication during receptor signaling are poorly understood (Figure 1-6b).

Janus kinases

Janus kinases (JAKs), a distinct family of tyrosine kinases, are required for signal transduction for class I cytokine receptors (Baker et al., 2007; Darnell et al., 1994). In addition to JAKs' role in cytokine signal transduction, it has been suggested that they may promote cell surface expression of cytokine receptors by binding to the receptor (Huang et al., 2001). The JAK family includes four members, JAK1 (Wilks et al., 1991), JAK2 (Harpur et al., 1992), JAK3 (Rane and Reddy, 1994) and TYK2 (Firmbach-Kraft et al., 1990).

According to their sequence similarities there are seven regions of homology named Jak homology (JH) regions 1-7 (Figure 1-7a) (Yeh and Pellegrini, 1999). The two carboxy terminal JH domains 1 and 2 retain high homology to tyrosine kinases. However, only JH1 retains kinase activity while JH2 lacks critical functional amino acids rendering it a pseudo-kinase (Duhe and Farrar, 1995; Feng et al., 1997). The pseudo-kinase domain has an essential regulatory function as a cytokine-inducible switch and can regulate JAK2 activation. Despite the lack of structural information, biochemical studies suggest that regulation of the kinase activity is mediated possibly through an intramolecular interaction between JH1 and JH2 (Saharinen and Silvennoinen, 2002). The N-terminal region contains a Four-point-one/Ezrin/Radixin/Moesin (FERM) (JH4-JH7 and half of JH4) domain, which is responsible for receptor recognition and association (Frank et al., 1995; Zhao et al., 1995). Mutagenesis and kinase chimeric experiments combining regions from different JAKs have suggested that a minimum receptor recognition region may be concentrated to the first 200 residues of the N-terminus (Feng et al., 1997; Richter et al., 1998). A Src homology-2 like (SH2-like) domain (JH3-JH4) is located between the FERM and the pseudo-kinase domains (Figure 1-7a)(Wilks et al., 1991). The SH2-like domain does not function as a conventional phosphotyrosine binding domain and may be involved in mediating association with the membrane proximal regions of the cytokine receptors but its exact functions remain unclear (Haan et al, 2006).

Ligand binding to the extracellular site of cytokine/growth factor receptors results in juxtaposition of JAKs leading to their auto- trans-phosphorylation on key tyrosine

residues (Remy et al., 1999). Activation of JAKs, in turn mediates downstream signaling through phosphorylating specific tyrosine residues on the receptor tail that serve as docking sites for SH2 domains containing molecules such as signal transducers and activators of transcription (STATs) (Figure 1-6b).

Mutations in JAKs that lead to the constitutive activation of the kinase domain and cause serious pathological diseases such as myeoloproliferative neoplasms (MPNs) and leukemia (Haan et al., 2010; Vainchenker et al., 2011), imply negative regulation of JH2 on JAK activity. However, in a recent study it was suggested that JH2 may also have a positive regulatory function because a JH2 deletion mutant was able to maintain JAK2 basal activity but could not be further stimulated by the cytokine (Ungureanu et al., 2011). The crystal structures of both JH1 (Jak3) and JH2 (Jak2) are available (Bandaranayake et al., 2012; Boggon et al., 2005) although the precise regulatory nature of interactions of JH2 on JH1 remains elusive. In addition, it is also possible that in the context of preformed receptor dimers, constitutively bound JAKs interact in an inhibitory manner, through their JH2 domains. Upon ligand binding, conformational changes in the receptor perhaps lead to stimulatory rearrangements within the JH2 domains of JAKs and activate downstream signaling.

How the structural information is carried from the activated receptor to JAK is still poorly understood due to the lack of structural information on both full-length JAK and the receptor/kinase complex.

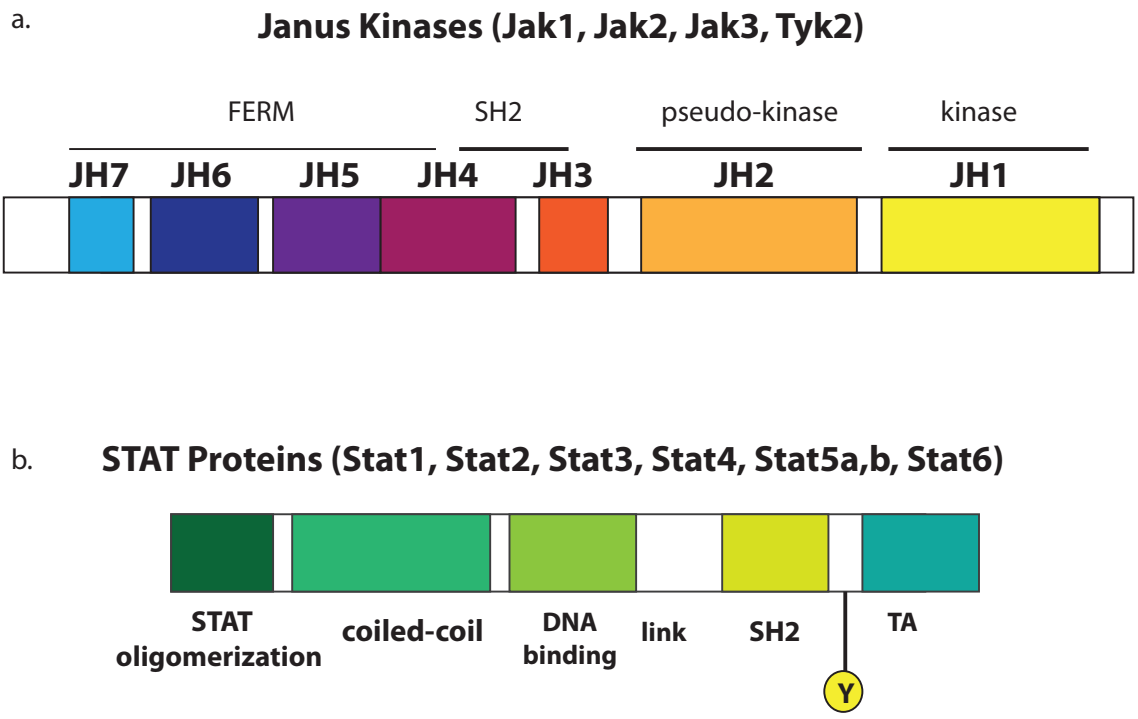

Figure 1-7 Domain organization in JAKs and STATs
a., representation of Janus kinases (JAKs) domain organization showing JAK homology domains (JH) 1-7, based on the sequence similarities of the four known JAKs. N-terminal FERM domain comprises regions JH7 through JH5. Src homology 2-like domain (SH2-like) spans the JH3-JH4 region. JH2 is the pseudo-kinase domain and JH1 is the C-terminal kinase.. b. Signal transducer and activator of transcription (STAT) domain organization – the six Stats share several functional domains. An amino terminal oligomerization domain, a coiled-cooil domain, a DNA-bidning domain, an SH2 domain and a transcriptional activation domain at the C-terminus.

Structural information of the cytokine/receptor/JAK complex could provide important information regarding the structural rearrangements that take place upon ligand binding and lead to the activation of the Janus kinases.

Signal transducers and activators of transcription and their targets

The signal transducers and activators of transcription (STATs) are a family of proteins consisting of seven members in mammalian cells and originally described by Darnell et al. (Darnell et al., 1994) as ligand-induced transcription factors. Different members of the STAT family share domain organization. There are a total of seven domains that exhibit modular structure (Figure 1-7b) – a conserved N-terminal domain, a coiled-coil domain, a

DNA-binding domain, a linker region, a tyrosine activation and a C-terminal activation domain (Jatiani et al., 2010). The amino terminal domain is critical for STATs' function as small deletions in this region lead to inability of the STATs to become phosphorylated. In addition, this domain plays a role in nuclear import, export, receptor binding and interaction with the DNA binding domain (Mertens et al., 2006). The coiled-coil domain is involved in receptor binding and interaction with regulatory proteins (Kisseleva et al., 2002). The DNA binding domain, as its name implies is involved in binding to DNA to activate transcription and is highly conserved among STATs. A linker region is located between the DNA binding domain and the SH2 dimerization domain to ensure proper conformation. The SH2 domain is critical for signaling and the recruitment of STATs to the activated receptor complexes and is highly conserved. Through this domain STATs can homodimerize and heterodimerize and in turn localize to the nucleus and bind DNA. The C-terminal transactivation domain is the most variable between different STATs and it modulates transcriptional activation of target genes (Figure 1-7b) (Jatiani et al., 2010; Neculai et al., 2005).

When cells are resting, STATs exist as a preformed homodimers in the cytoplasm (Mertens et al., 2006). Upon ligand binding to receptor, intracellularly bound JAKs also become activated and phosphorylate specific tyrosine residues on the receptor tails. The phosphotyrosyl residues, in turn, serve to direct the SH2-dependent recruitment of STATs to the receptor. Once recruited to the receptor tails, STATs become phosphorylated by the activated JAKs and get released into the cytoplasm where they rearrange into anti-parallel dimers through the SH2 domains. Furthermore, STAT dimers translocate to the nucleus, bind certain enhancer elements and initiate gene transcription (Baker et al., 2007; Schindler et al., 2007).

Moreover, Stats are capable of forming not only homodimers but also heterodimers, tetramers and other higher order complexes (Ward et al., 2000). It has been suggested that JAKs do not exhibit specificity for certain STATs because the same STATs can get activated at different receptors, associated with different JAKs (Darnell, 1997). In addition, some experiments with chimeric receptor molecules with different JAK binding sites but with the same STAT-binding sites were found to activate the same STATs

(Kotenko et al., 1996). Therefore, it is likely that the specificity for STATs depends on their docking sites on the receptors rather than the JAK kinases. There are multiple details that yet remain to be resolved in the JAK-STAT signaling pathway which would require further structural and mechanistic information.

Other signaling pathways activated by cytokines

In addition to the JAK-STAT pathway, cytokines are able to activate multiple other signal transduction pathways, exerting their divergent actions. For example, it has been suggested that the protein tyrosine phosphatase SHP-2 is implicated in mediating the leptin receptor activation of MAPK (Bjorbaek et al., 1999). In addition, some cytokines can also induce JAK/STAT mediated phosphorylation of ERK and AKT (Saxena et al., 2007). Moreover, experimental evidence suggests that AKT can also be activated via cytokine mediated stimulation of the lipid kinase phosphoinositol 3 kinase (PI3K) (Reddy et al., 2000).

Negative regulation of cytokine pathways

Excessive signaling and overstimulation of cytokine signaling can lead to autoimmune disorders and cancer. Therefore, it is crucial for the cell to exert tight regulation on the signaling pathways mediated by JAK/STAT. There are a few ways in which the cell is capable of turning off the signaling, initiated by cytokines. Src-homology phosphatase (SHP-1) can directly dephosphorylate JAKs. Three protein families, particularly the suppressors of cytokine signaling (SOCS), protein inhibitors of activated STATs (PIAS) and cytoplasmic phosphatases have been implicated in the negative regulation of cytokine signaling. SOCS are found to be able to compete with STATs for binding to the receptor (Seki et al., 2002) or directly interact with JAKs (Khwaja, 2006) to mediate negative regulation of cytokine signaling. PIAS proteins, on the other hand, can regulate the amount of available STAT for enhancing the transcription of available genes by directly binding to STAT dimers (Baker et al., 2007). Protein tyrosine phosphatases (PTP) can negatively regulate JAK-STAT pathways by dephosphorylating tyrosine residues (Pallen et al., 1992). The mechanism of regulation involves dephosphorylation

of both JAKs and activated receptors, thereby preventing STATs from associating with the receptors and their activation.

1.4 G-protein Coupled receptors as signal transduction units

GPCRs are by far the largest family of membrane proteins, with more than 800 members in the human genome, and are involved in signal transduction that mediates the majority of cellular responses to a variety of ligands, ranging from nucleotides and amines, to peptides and hormones (Strader et al., 1994). In addition, GPCRs are responsible for vision, olfaction and taste and many other vital physiological events. A seven transmembrane (7TM), α-helical region spanning the membrane with an extracellular amino terminal and a carboxy intracellular tail is a characteristic signature of all GPCRs. There are five main families of GPCRs grouped based on their amino acid sequence and three-dimensional structural similarities: rhodopsin, secretin, glutamate (family A, B and C, respectively), adhesion and Frizzled/Taste2 (Fredriksson et al., 2003). Although, the receptors are very similar in their overall topology, GPCRs, like cytokine receptors, can be involved in a variety of unique signal transduction pathways, both dependent and independent of different associated G-protein subtypes.

GPCR overall structural topology

There are three extracellular and three intracellular loops connecting the 7TM α-helices which also represent the most variable regions among the family of GPCRs (Kobilka, 2007). The extracellular loops contain conserved cysteine residues that are capable of forming disulfide bonds to stabilize the receptor tertiary structure. In addition, the extracellular domain contains asparagine residues and motifs for N-glycosylation which are implicated in intracellular trafficking of the receptors to the membrane (Tuteja, 2009). The greatest diversity is displayed at the amino termini where the sequence can range in size from few amino acids for the monoamine and peptide receptors to few hundred amino acids for the glutamate receptors (Kobilka, 2007). In contrast, the greatest structural homology in GPCRs is within the transmembrane helical segments. The α-helices embedded in the membrane are arranged to form a tight, ring-shaped hydrophobic structure which is important for receptor stability and ligand-induced conformational

changes. Thus, any mutations or perturbations in this structural organization could be deleterious.

Common modes of activation of GPCRs

As in other transmembrane signaling systems, the interaction between ligand and the extracellular portion of a GPCR is the prerequisite event in signal transduction. The major course of events upon ligand binding can be depicted in Figure 1.8. Once the ligand and the receptor form the signaling complex, the receptor is activated and ready to propagate the information in terms of structural rearrangement through the membrane.

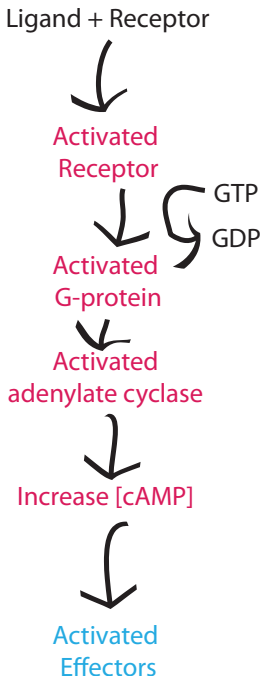

Figure 1-8 Signal Transduction through GPCRs.
Ligand binds to the extracellular side of the receptor and activates the receptor. GDP is released and GTP comes in, activating the G-protein, bound on the intracellular side of the receptor. Activated G-protein, interacts with effector molecules such as adenylate cyclase and leads to increase in concentration of second messengers such as cAMP. Second messenger diffuse to other cellular compartments and interact with other downstream effectors, initiating cellular responses.

Briefly, ligand binding to the extracellular side of receptor initiates the G-protein interaction with the intracellular side of the receptor. Nucleotide exchange, specifically the exit of GDP and the subsequent binding of GTP within the α subunit, activates the G-

protein and drives the dissociation of its heterotrimer into Gα and Gβγ subunits (Berg et al., 2002). Signaling is terminated by the hydrolysis of GTP by the GTPase activity in the α-subunit. The resulting GDP-bound α-subunit re-associates with the βγ-complex to enter a new cycle if activated receptors (Wettschureck and Offermanns, 2005).

The ligand recognition is by far the most important and crucial part of activating the receptor and downstream signaling. As mentioned earlier, the extracellular loops (ECL) are the structures that display most heterogeneity and their characteristic folds are receptor specific. For example, in the β_2 adrenergic receptor (β_2AR), ECL2 forms a compact helical shape, close to the transmembrane region and allows soluble ligands to readily diffuse toward the binding site inside of the receptor (Rosenbaum et al., 2007). In contrast, the crystal structure of sphingosine 1 phosphate 1 receptor (S1P1) reveals that the ECL2 appears to block the access from the outside and seals off the ligand-binding pocket (Hanson et al., 2012). These different binding modes have important implications during receptor activation, suggesting that there is no unique switch for all GPCRs. On the contrary, by interacting with different regions of the receptors, ligands can modulate and/or converge to common active states (Audet and Bouvier, 2012).

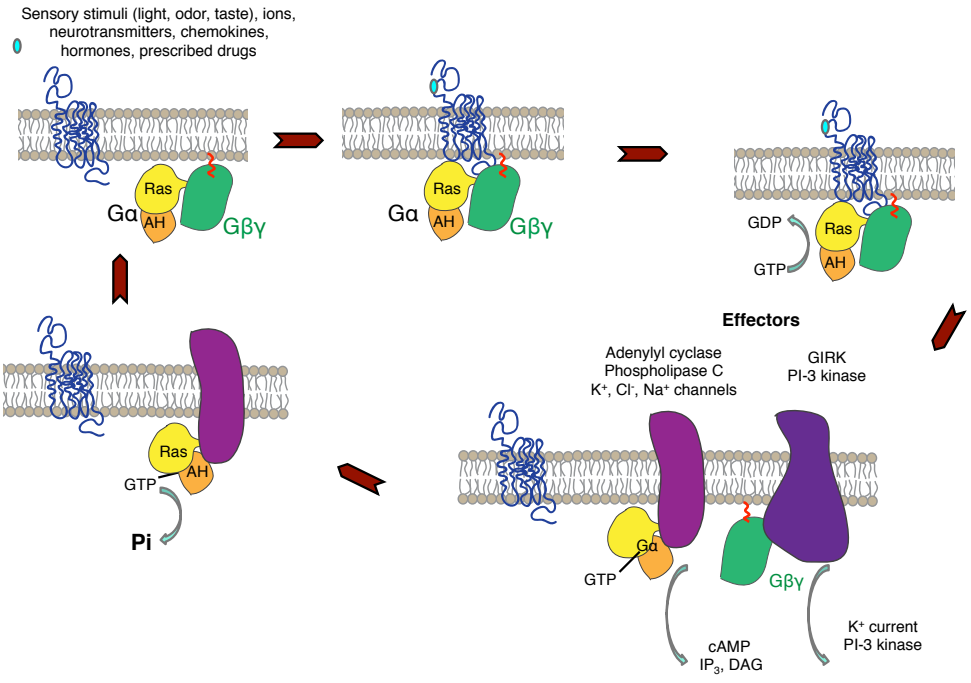

Figure 1-9 G-Protein coupled receptor signaling initiation.

A stimuli binds to the receptor extracellular portion and causes association of the receptor to its cognate G-protein. Nucleotide exchange of GTP for GDP leads to dissociation of the heterotrimeric G-protein into an α and a βγ subunits. In turn, the α and the βγ can interact with downstream effectors and lead to an increase in concentration of second messengers such as cAMP and DAG. Hydrolysis of GTP leads to re-association of the α and the βγsubunits into a G-protein heterotrimer and the cycle can be repeated again.

Activation of the receptor leads to the association of the heterotrimeric G-protein on its intracellular side (Figure 1-9). Further, nucleotide exchange decreases the affinity of Gα to Gβγ and Gα is freed from the complex and allowed to interact with downstream effectors with the canonical effector being adenylyl cyclase. In addition, the βγ-subunit can also modulate the activity of other effector proteins (Clapham and Neer, 1997). Some of the downstream signaling targets of βγ subunit are isoforms of adenylate cyclase, phospholipase C and phosphoinositide-3-kinase (Exton, 1996; Sunahara et al., 1996; Vanhaesebroeck et al., 2001). Moreover, most GPCRs are able to activate more than one subtype of G-protein which results in the activation of several different pathways both through the α and the βγ subunits. However, the interaction between the receptor and the G-protein appears to be selective and cell type specific (Wettschureck and Offermanns, 2005).

G-proteins composition

G-proteins are the mediators of signaling from the activated receptors to the downstream effectors. The adenylate cyclase is the original model system for studying G-proteins whereby it can be either activated or inhibited by different G-proteins. G-proteins consist of three subunits: a guanyl nucleotide binding α subunit (39-52kDa), a β subunit (35-36kDa) and a γ chain (8kDa) (Stryer and Bourne, 1986). G-proteins cycle between GDP-bound inactive to GTP-bound active state. In the guanyl nucleotide, GDP-bound form, the G-protein is a trimer composed of all three α, β and γ subunits. There are many subtypes of G-proteins that modulate the functional versatility of GPCRs. The heterotrimeric G-proteins are divided into four groups depending on the sequence similarities in their Gα subunits (Gαs, Gαi, Gαq and Gα12) (Oldham and Hamm, 2008).

The α-subunit is a member of the P-loop NTPase and involves guanyl binding (Berg et al., 2002). Gα contains a conserved region composed of a GTPase domain, responsible

for the GTP hydrolysis and an α-helical domain (Oldham and Hamm, 2008). The GTP-ase domain is conserved in all G-proteins and is also involved in the binding interface with the βγ dimer.

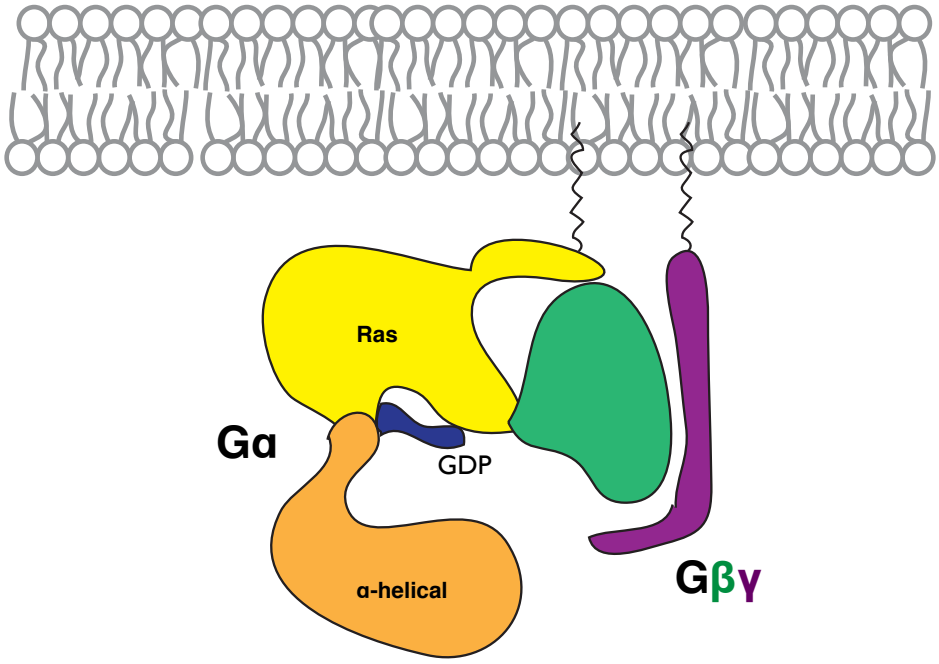

Figure 1-10 Heterotrimeric G-protein.
Gα consist of a Ras domain (yellow) and an α-helical domain (AH) (orange). A nucleotide binding pocket is at the interface of the Ras and α-helical domain. Gβ is represented in green and the Gγ in purple, wrapping around the β subunit. Both the GαRas and the Gγ can mediate interactions with the membrane.

The β subunit is characterized by a β-propeller fold, composed of seven WD40 sequence repeats (Wall et al., 1995). The γ subunit wraps around the β subunit and forms a coiled-coil at its N-terminus (Figure 1-10). In addition, it bears an isoprenyl post-translational modification at its C-terminus, possibly with a farnesyl group that allows for membrane interactions (Zhang and Casey, 1996).

In addition, a combination of 5 different β-subunits and 12 different γ-subunits, can compose the βγ-complexes adding even more complexity to GPCRs signal transduction (Wettschureck and Offermanns, 2005).

Stimulatory Gαs subunit

The Gαs proteins are ubiquitously expressed and facilitate the activation of adenylyl cyclase resulting in the subsequent increase in the second messenger cAMP (Berg et al., 2002). In turn, the increase of cAMP is able to modulate a variety of cellular processes by activating protein kinase A (PKA). This enzyme is composed of two regulatory chains (R) and two catalytic chains (C). When cAMP binds to the active chains, the catalytic chains are released and are then able to phosphorylate specific serine and threonine residues on multiple targets (Berg et al., 2002). The bacterial toxin, *Cholera toxin* (CTX), from *Vibrio choleare* can ADP ribosylate the Gαs subunit, rendering the G-protein catalytically inactive in the GTPase function (Freissmuth and Gilman, 1989). The ADP-ribosylated Gα subunit is therefore left constitutively active thus constantly stimulating the AC, cAMP production and protein kinase A (PKA) activation. Finally, PKA opens chloride channels which leads to increased water secretion and can result in diarrhea (Gabriel et al., 1994).

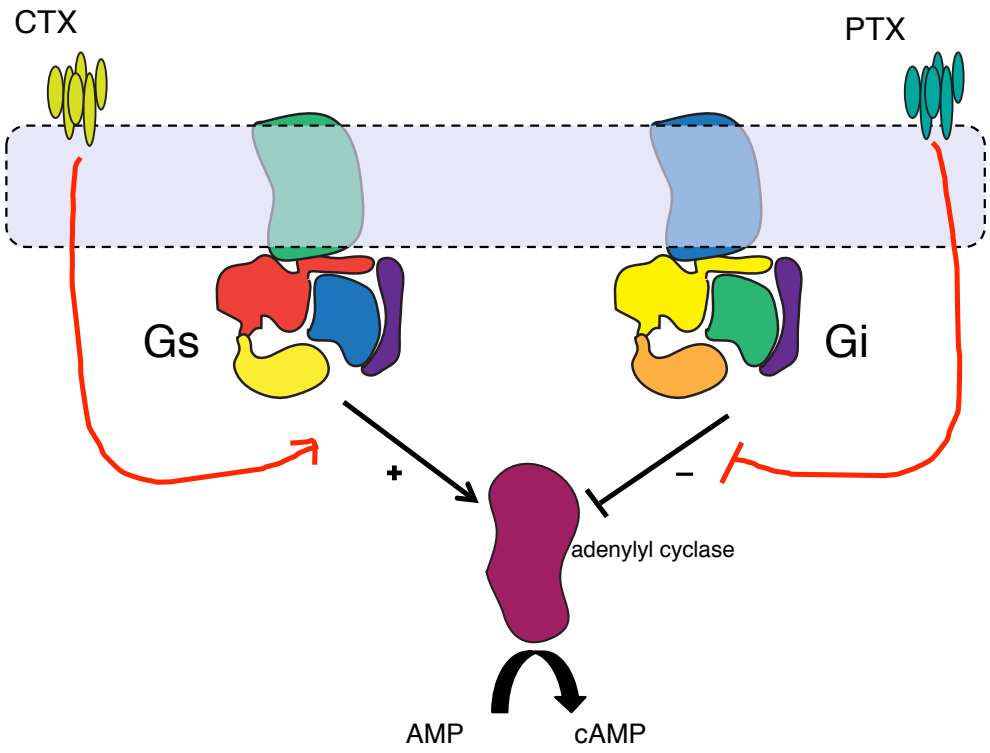

Figure 1-11 Effect on G-protein signaling by bacterial toxins.
Cholera toxin (CTX) ADP-ribosylates the α subunit of Gs, leaving it constitutively active, thus, constantly stimulating adenylyl cyclase. *Pertussis toxin* (PTX) ADP-

ribosylates the α subunit of Gi, rendering it inactive and no longer able to inhibit adenylyl cyclase. Therefore, both toxin, act through different mechanisms but lead to constitutive activation of AC and increase of cAMP concentrations.

Inhibitory Gαi subunit

The Gi/Go G-protein family is widely expressed throughout different tissues, where the α-subunit is implicated mostly in the inhibition of adenylyl cyclases (Sunahara et al., 1996). It is also believed that the major signaling processes in the Gi/Go family are mediated by the βγ-complexes that are released from the G-protein (Clapham and Neer, 1997). Studies on this family of G-proteins with *Clostridium botulinum* (pertussis toxin; PTX) show that the PTX can ADP-ribosylate the carboxy terminal of the Gαi, preventing the α-subunit from interacting with AC. In turn, AC is constitutively activated and this leads to an increase in intracellular concentration of cAMP and activation of potassium channels (Figure 1-11).

Shutting off the signal transduction

Halting the signal from the activated ligand-receptor-G-protein complex can be accomplished in several ways (Figure 1-12). First, the recycling of GTP for GDP increases the affinity of the α for the βγ subunits and reforms the G-protein heterotrimer, thus turning off the signal. Second, the ligand concentration in the extracellular space also plays a role in receptor disensitization. At lower concentrations, the likelihood of a 7TM receptor rebinding a ligand is smaller and the receptor is predominantly in inactive form. G-protein coupled receptor kinases (GRK) can phosphorylate Ser and Thr residues on the C-terminal receptor tail. The phosphorylated residues serve as binding sites for β-arrestins which in turn can prevent the re-association of the G-protein to the receptor and inhibit signaling (Berg et al., 2002).

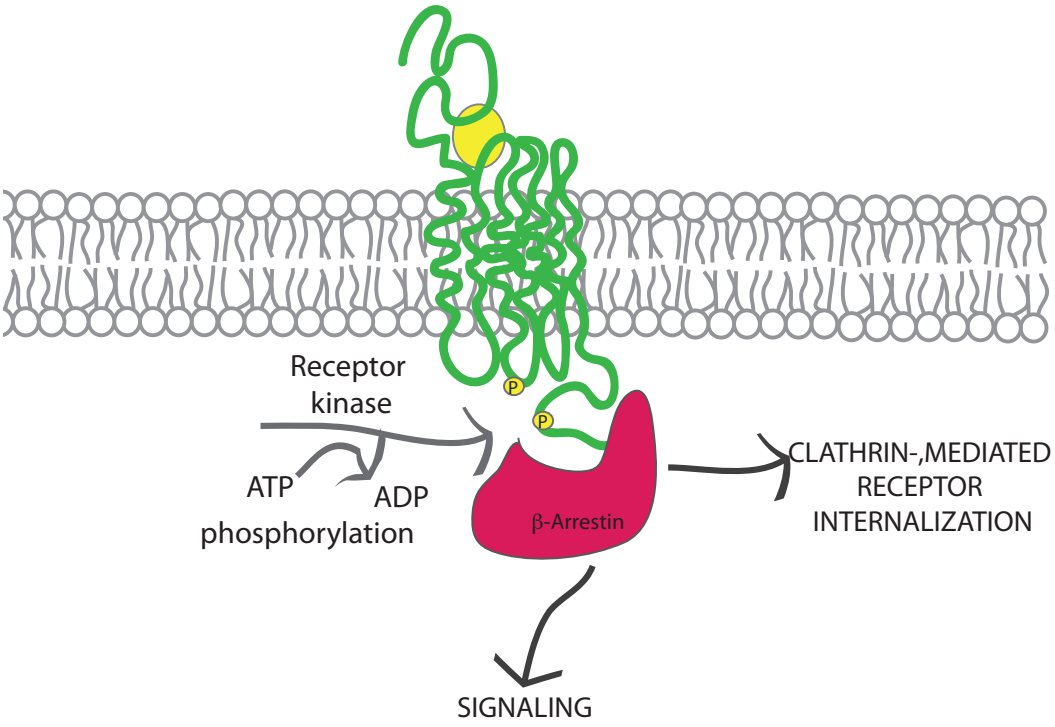

Figure 1-12 Regulation of signal transduction of GPCRs by arrestins.
Arrestins can bind to phosphorylated receptor tails and serve as both regulatory subunits, by internalizing the receptor, or signaling subunits.

It is important to mention that signaling pathways of GPCRs can also be mediated in a G-protein independent manner, making the regulation and modulation of GPCR signaling cascades even more complicated (Azzi et al., 2003; Lefkowitz and Shenoy, 2005).

1.5 Structural techniques and challenges in studying membrane proteins

Lipid-protein interactions

The cell membrane is essential for life as it provides a barrier between the intracellular space and the extracellular matrix. Biological processes such as respiration, photosynthesis, motility and signal transduction are executed by the interactions between membrane proteins and the lipid bilayer. Protein production, purification, stability and homogeneity are the major challenges in studying membrane proteins. Membrane proteins are embedded in the lipid bilayer and need to be resolubilized by detergent in order to be studied. Lipids play important roles not only in stabilizing the proteins but

also in their function, folding and even membrane insertion. Understanding the lipid-protein interactions is crucial to delineate the native environment of membrane proteins and their functions (Lee, 2003, 2004). The association between the lipids and the membrane proteins is very tight. During protein purification, most of the lipids are lost in the process and those that remain are usually those most tightly bound ones. That is why in many cases lipids are added during purification in order to keep the proteins stable as in the case of human β2-adrenergic G protein-coupled receptor (Cherezov et al., 2007; Raunser and Walz, 2009).

Methods overview to study the structure of membrane proteins

There are a variety of methods available to study membrane proteins' structure. All methods have their own advantages and disadvantages and the suitability of each depends on the identity and the characteristics of the protein of interest. Membrane proteins are very challenging targets for structural determination for a variety of reasons. The expression, purification, solubilization, inherent flexibility, hydrophobicity and size are just of the few of the reasons that make membrane proteins difficult to study. An overview of some of the most widely used techniques to study membrane protein structure is given below.

X-ray crystallography

X-ray crystallography is the primary technique used in protein structure determination with the majority of protein structures in the data bank being solved by this method. After the protein is purified and crystallized, it is subjected to an intense X-ray beam which is diffracted by the proteins in the crystal resulting in a characteristic pattern of spots, containing the information about the electron distribution in the protein. X-ray crystallography is a very powerful technique that can provide an atomic resolution detail for the molecules incorporated into the crystal. Crystallography is an excellent method for studying rigid proteins, of modest size, that can form nicely ordered crystals. However, flexible proteins, such as the membrane proteins, are more difficult to crystallize because they cannot all align in the same orientation to form a crystal. In addition, locally flexible regions in a protein that is successfully crystallized can be

invisible in the electron density maps because their electron density is smeared over a large space. NMR can provide information about the protein in solution and thus also provide information for the flexible regions of a protein that are otherwise disordered in crystal structures. Recent advances in protein engineering and purification have tremendously accelerated x-ray chrystallography as a technique to study membrane protein structures. For example, the concept of the lipidic cubic phase (LCP) where membrane proteins can freely diffuse in a continuous lipid bilayer for nucleation and crystal growth was introduced (Landau and Rosenbusch, 1996). Further, the insertion of an N-terminal recombinant lysozyme for the successful crystallization of human β-adrenergic G-protein coupled receptor complex (Zou et al., 2012) as well as the introduction of a stabilizing nanobody for the crystallization the β2AR-Gαs complex (Rasmussen et al., 2011a; Rasmussen et al., 2011b) have transformed the field of membrane protein crystallography.

Nuclear Magnetic Resonance (NMR)

Both solution and solid state NMR have been used to study membrane proteins' structure and dynamics of membrane proteins. The main advantage of NMR is that the proteins of interest can be studied in various environments including different salt concentrations, pH, temperature, organic solvents or synthetic micelles. One of the challenges with this technique is the requirement for large amounts of very pure protein, usually in the milligram scale. As mentioned earlier, the purification and solubilization of membrane proteins is difficult and obtaining large quantities of such can be expensive, time-consuming and sometimes impossible. What distinguishes the solution from the solid-state methods in NMR is the motional properties of the protein-lipid sample (Montaville and Jamin, 2010). Because large protein assemblies (larger than ~ 40kDa) have slower molecular tumbling, they are more difficult to study with solution NMR. In contrast, the addition of specific stable-isotope to the protein is the limiting factor in solid-state NMR. Further, membrane proteins are characterized by high repetitiveness of hydrophobic amino acids spanning the membrane, forming primarily α-helices or β-strands. The signal overlaps from these structures further complicate the NMR spectra and make the solution of membrane protein structure more challenging using NMR.

Electron microscopy

Electron microscopy has become a very powerful tool for characterizing protein structures. There are different methods in electron microscopy used to determine the three dimensional shape of proteins. For example, in cryo-EM, the sample is suspended in vitreous ice, and in negative stain, the proteins are embedded in heavy metal salt. If the protein forms 2D crystals, electron diffraction can be used to generate a 3D density map and to solve the structure of the protein (Unwin and Henderson, 1975). Cryo-electron microscopy has also made tremendous advances in the study of membrane protein structures as a result of instrument and data processing improvements. Generally, it is very applicable to supramolecular assemblies that are either too flexible to crystallize for X-ray diffraction analysis or too big for NMR to characterize. Thus, the combination of cryo-EM with single particle analysis allows for the determination of structures of supramolecular machineries in their native environment even in their transient states (Zhou, 2011). Viruses are particularly good candidates for cryo-EM because of their large size intrinsic symmetry, which allows for signal redundancy and easier averaging in single particle analysis. Viral structures have contributed to some of the highest resolution structures characterized by single particle analysis, cryo-EM (Cheng et al., 2010; Zhang et al., 2010). However, as a result of the lower contrast in cryo-EM, proteins that are smaller than ~ 200 kDa are difficult to visualize. Therefore, negative staining EM may be a more suitable technique to study their structure.

In negative staining, the sample is embedded and fixed in a solution of a heavy metal salt and subsequently dried on the EM grid. The stain embedding provides better contrast in comparison with cryo-EM but has its limitations as well. The dehydration of the proteins as a result of the negative staining may result in flattening and distortion of the three dimensional conformations (Vahedi-Faridi et al., 2012). In addition, this technique can provide information only about the surface characteristics of the protein and not their internal features. Nevertheless, the negative staining method is an excellent tool to assess the quality of purified samples, their homogeneity and purity, a test that is even more stringent than SDS gels, gel filtration or even dynamic light scattering. Negative stain electron microscopy cannot provide the atomic resolution of X-ray crystallography and

NMR. However, it allows us to study the overall shape of large and flexible molecular assemblies, in their native state.

Applying Negative Stain EM for Structural Analysis of Proteins

Image Formation

After emitted from the source, the electron beam is deflected through a set of condenser lenses ensuring that the beam is parallel (Figure 1-13a). Then, the electron beam passes through the specimen by which the electrons are either scattered or not (Figure 1-13b). The inelastically scattered electrons provide the background noise of an image. The areas where the electrons are scattered, are in the range of grey and where the electron are unscattered the image is brighter (Frank, 2006; Williams and Carter, 1996). In contrast, in the regions where the electrons do not pass through the sample the image appears dark. However, in negative staining, as the name suggests, things are reversed. Background areas, covered in stain appear dark, while proteins appear brighter and are stain excluded. The scattered electrons interact further with the magnetic field of the objective, followed by an intermediate and projector lenses which in turn form an image (Figure 1-13). The image is then viewed on a fluorescent screen or can be recorded by a charge-coupled device (CCD) camera or conventional film (Williams and Carter, 1996). Because no lens is perfect the achievable resolution of an image is partly depended on the lens aberrations. There are three main sources of aberrations - spherical aberration, chromatic aberration and astigmatism. In the case of spherical aberration, the peripheral electrons are deflected more than the electrons closer to the center. This aberration can be improved with thinner samples.

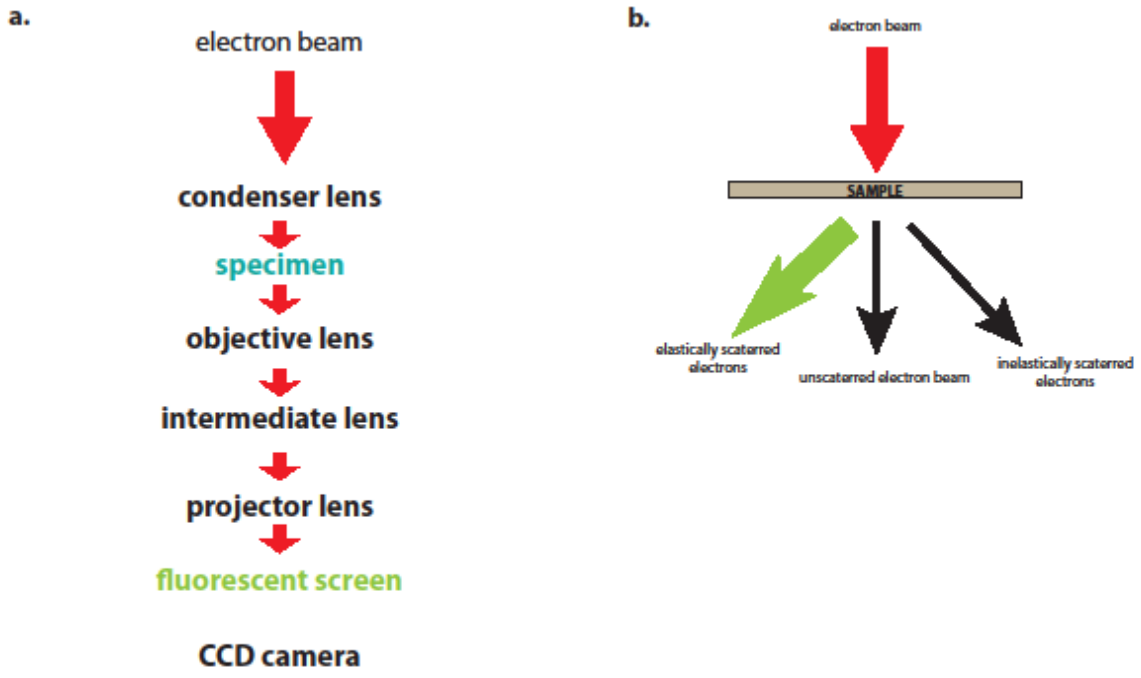

Figure 1-13 TEM lens organization and electron path through the sample.
a, Lens organization in the column of the EM. Red arrows represent the electron path. b, Electron diffraction path through the sample.

Chromatic aberration is related to the energy of the electrons which emerge from the gun with different energies and are subsequently bent by the objective lens to different degrees with the ones with less energy being bent more. This is the aberration that most significantly defines the performance of the objective lens. Both types of aberrations result in a disk rather than a point where all the rays converge which makes the image blurred and may reduce contrast. The astigmatism is caused by the inherent property of the electromagnetic lens lacking a perfect cylindrical symmetry. Thus, this aberration affects the ability to focus an image but could be easily corrected by the stigmators (Frank, 2006). In addition, the resolution limit is also dependent on the nature of the biological sample. For example, because higher electron dose could damage biological samples, obtaining high sample contrast and better resolution is dependent on the dose rate. Furthermore, sample heterogeneity can also lead to lower resolution structures.

Single Particle Analysis

Single particle analysis aims to determine the structure of macromolecules from images of individual particles, termed single particle projections. In negative staining the particles are fixed on a carbon support, embedded in heavy metal salt. Furthermore, based on their shape and charge they can assume preferred orientation on the carbon support. The single particle analysis method is a compilation of a few computerized image processing techniques used to analyze the images from TEM. Generally, the micrographs from the electron microscope are characterized by a very low signal-to-noise ratio. Therefore, the integral part in image processing is to improve signal-to-noise ratio by averaging large number of particle projections. With single particle analysis, the structure of a macromolecular protein complex can be determined from the images of individual particles (Frank, 2006). The homogeneity of the protein sample is critical in single particle analysis although, samples with conformational heterogeneity can also be analyzed.

Reference-free alignment and classification

The purpose of the alignment of several images is to increase the signal-to-noise ratio. After the particles have been boxed out, the averaging is carried out through translational and rotational alignments of the particle projections using reference-free procedures (Frank, 2006). In this method, multiple views from particles of a particular data set are separated into classes by comparatively aligning the particle projections to randomly chosen particles from the same data set. In essence, the randomly chosen initial projections are used as models and the remaining particles are grouped with them based on cross-correlation values. All the particles in each group are averaged out and the resulting class average is then used as a new reference. The alignment procedure is performed iteratively with multiple cycles until class averages are produced with no further change in the overall image shifts and rotations (Ohi et al., 2004). Each average contains similar particle projections, creating improved signal-to-noise ratio, and allows for clearer visualization of the protein's features. In addition, the number of required classes can be chosen based on the heterogeneity of the sample. That is why initially, it is

good to start with few classifications containing different number of classes. A good indication would be if there are more output averages that represent a significant number of projection structures and the raw particle projections resemble their class averages. Further, unique classes can be selected from the classification and used for subsequent classifications to improve the model and enrich the population of particles in the specific group. There are few software packages capable of performing image alignment, classification and also multireference alignment such as IMAGIC (van Heel et al., 1996), SPIDER (Frank et al., 1996) and EMAN (Ludtke et al., 1999).

Contrast transfer function

The electron microscope distorts the structural information from the protein sample by changing the amplitudes and phases of the recorded electron waves. These artifacts are dependent on the microscope's objective lens spherical aberration coefficient, the voltage and defocus values used as well as the spatial frequency. The contrast transfer function (CTF) defines the transfer of contrast from the sample to an image by defining the relationship between the Fourier transform of an object's image and the Fourier transform of an object's Coulombic potential multiplied by the contrast transfer function (Wade, 1992). The CTF is an oscillating function with amplitude that can be plotted against the resolution in inverse angstroms (Figure 1-14). The CTF oscillates from positive contrast transfer to negative contrast transfer as it passes through zero, where the information about the object is lost due to no transmittance or contrast transfer.

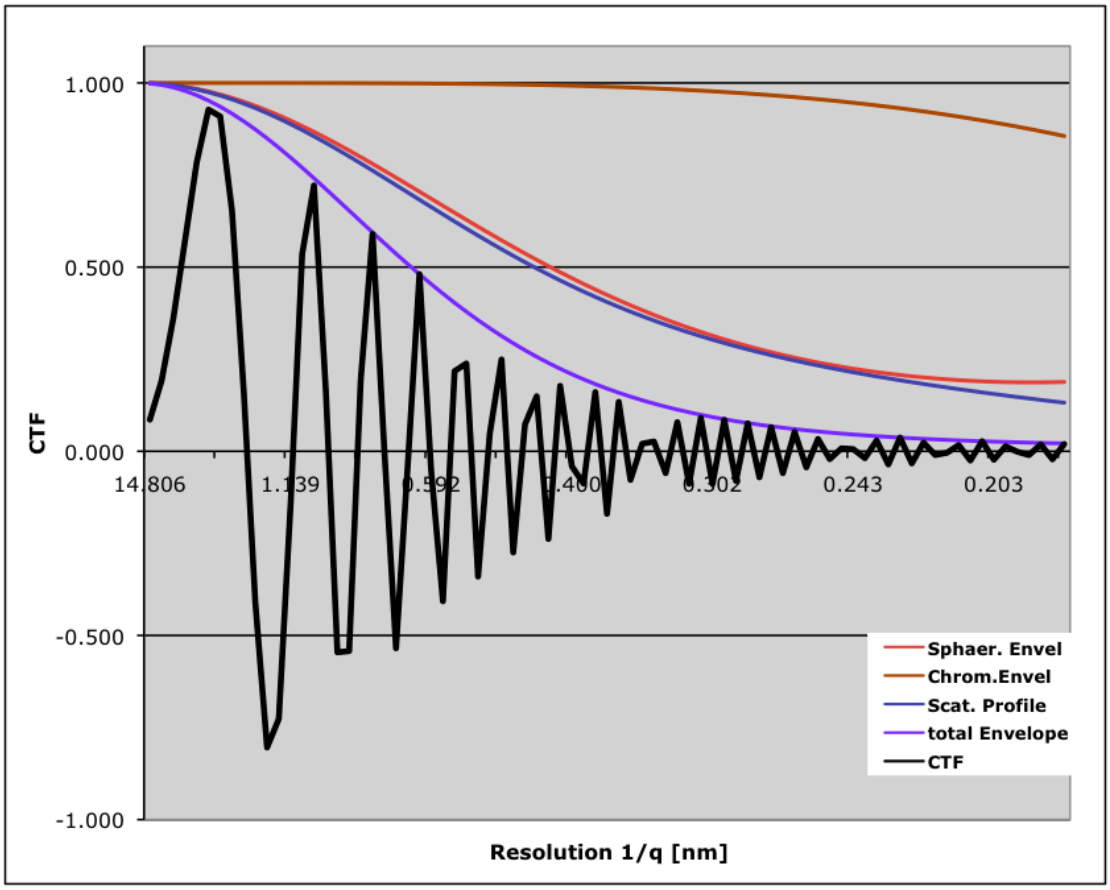

Figure 1-14 Contrast transfer function (CTF) curve.
This is an example of a contrast transfer function curve for a TEM operating at 200 kV, with Cs=2 and for a defocus value of 1000 nm. The signal amplitude is plotted against the resolution in inverse angstroms (x-axis). The experimental contrast transfer curve is in black and oscillates from positive to negative values, while the signal gradually with increasing resolution (Courtesy of Georgios Skiniotis).

Since the exact location of the zero crossings depends on the defocus values, by collecting images at different defoci, the resolution limit of a 3D reconstruction could be improved. Another way to correct for the lost image information is to obtain a constant positive phase values by inverting the negative values of the micrograph's CTF. The so-called "phase-flipping" can be performed by determining the values of the parameters, contributing to the shape of the CTF of each micrograph and using these values to flip the negative regions of the curve to positive ones (Zhu et al., 1997).

Three dimensional reconstruction

Among the mathematical operations to be carried out in the computer are alignment, determination of particle orientation (by random conical technique, common lines or reference to an existing density map), classification, reconstruction and correction of the contrast transfer function (CTF). A three dimensional reconstruction from the protein's 2D projections is achieved with several algorithms and approximations where the 2D projections along a 3D object contain sufficient information to restore the original object. For this purpose the orientation angles of each projection must be known. As the protein particles interact with the carbon support they form different projections which must fully fill Fourier space from all directions (Llorca, 2005). Therefore, the requirement to resolve the 3D structure of a protein is to establish the orientation of each projection image with respect to some reference coordinates. The orientation can be characterized by the projection's Euler angles which are directional angles used to define the position of a particle around a common center. For this procedure, the data set needs to be of a sufficient size as well as to contain particles in the same conformation and different orientations on the carbon support. In cases when the protein falls on the grid in a preferred orientation or because it has an inherent conformational flexibility, different views cannot be unambiguously assigned to a specific conformation. The random conical tilt procedure in such situations can provide a solution to this and generate a 3D volume for each type of view (Llorca, 2005; Radermacher and Ruiz, 2006).

Random conical tilt reconstruction

The Random Conical Tilt (RCT) method is used to generate a reconstruction of a three dimensional image, taking advantage of the preferred orientation of the specimen with respect to the plane of the grid (Radermacher et al., 1987). In this approach, one micrograph is taken at 0° and another at a high tilt angle of 60° (could also be 50°-70°) degrees) (Figure 1-15a). The two images are digitized and put side put side-by-side where the same particles at different angles are selected (Figure 1-15b). The images of the untilted particles are then correlated to their tilted counterparts by the direction of the tilt axis and the tilt angles. After the untilted particles have been aligned and classified, the

angles and shifts are also applied to the corresponding particles from the tilted images. Thus, their orientations in space are determined (Figure 1-15c). The projections of the tilted particles will form a cone with a fixed tilt angle of 60° degrees and a random azymuthal angle series that can be extracted for the untilted particles and used for the reconstruction. By back-projecting the tilted particle projections, the initial model can be reconstructed (Figure 1-15d). One of the advantages of this method is that no initial model is needed and thus it can be used to generate one for subsequent reconstructions from negative stain and/or cryo EM.

Angular refinement

Angular refinement is an iterative process used to increase the visible details of the model obtained in the previous step by better defining the angular position of each experimental projection. In this method, the initial reconstruction serves as an initial reference structure from which two-dimensional projections are computed and then compared to the experimental projections, yielding refined angles. From the refined angles a new reconstruction is obtained which is consequently used as a reference for the next cycle. The process is repeated iteratively until no further improvement in the 3D model is observed and the orientation angles have been stabilized. (Fuller et al., 1996; Zhu et al., 1997). A new reconstruction is calculated based on these parameters and it is used as an initial model for the subsequent iterations.

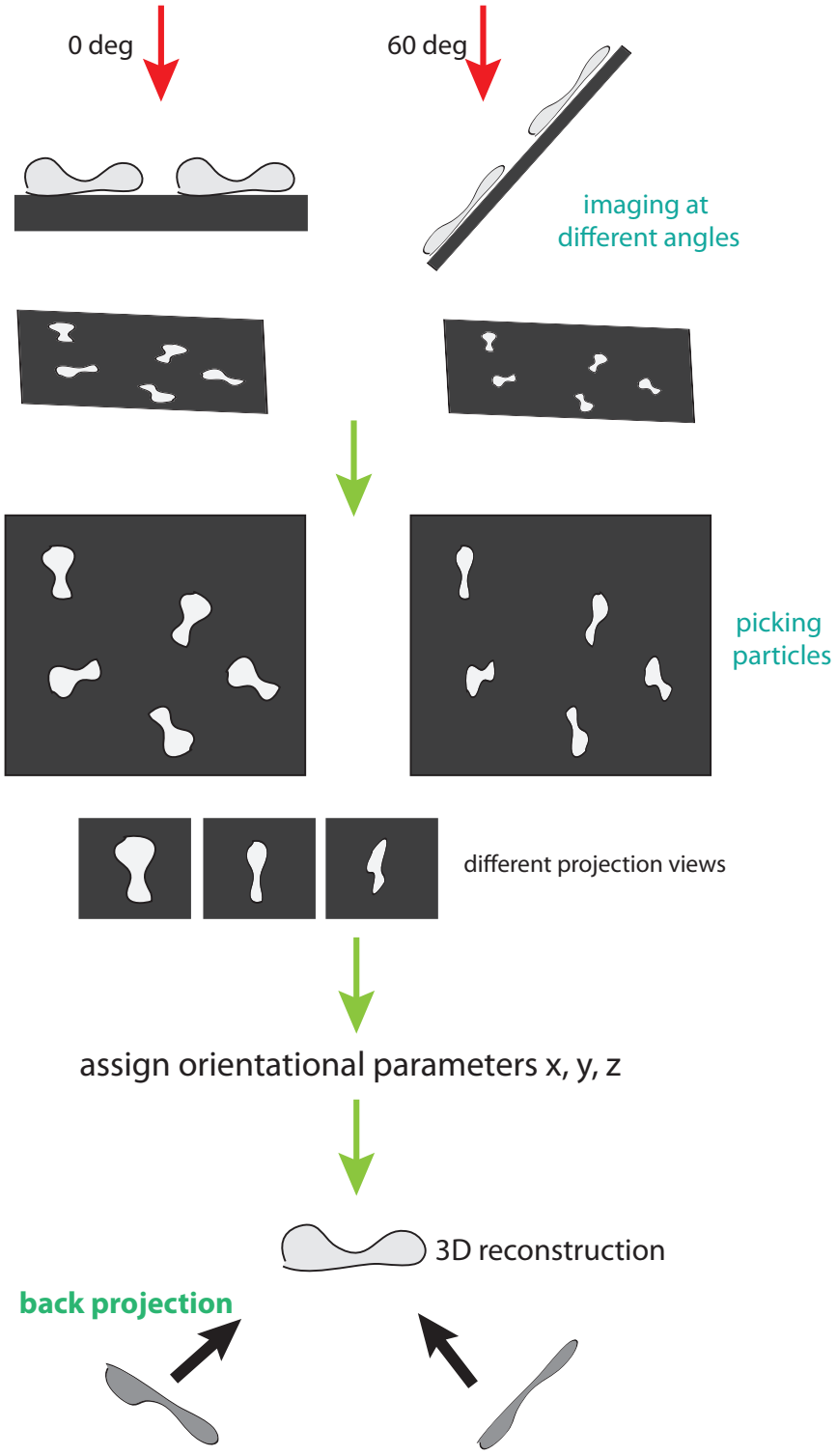

Figure 1-15 Random Conical Tilt.
a., Red arrows show the electron path through the sample imaged at 0° and 60° degrees. b., Micrographs containing multiple single particle projections from the 0° and 60° degree are collected and the individual particles and picked and excised. c., Orientational

parameters of tilted particles are assigned based on their relationship to the untilted particles. d., After back-projecting the different views, the original image of the specimen can be restored.

This process is repeated until the Fourier shell correlation (FSC) curve is converged. Figure 1-16 is a sample angular distribution plot of a 3D reconstruction of the single chain LepR, where the particles are spread in angular space around a reference model. Each mark inside the circle indicates the position of a matched projection with the ones near the center corresponding to the untilted particles and the ones surrounding the ring to the tilted particles. The more dots, the more representative views of the protein have been imaged and ideally the whole space should be filled.

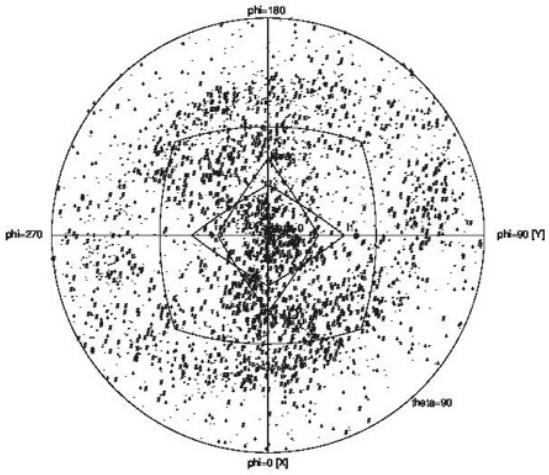

Figure 1-16 Angular plot of single chain extracellular LepR.
The graph represents the angular distribution of particles, relative to a reference volume of the single chain LepR. Each dot marks a reference projection that has a matched experimental particle.

In addition, when the particles have preferred orientation their corresponding 2D averages will contain more particles. This in turn will increase signal-to-noise ratio for a particular class, potentially increasing the resolution in the direction of space corresponding to the preferred orientations. The final resolution of the 3D reconstruction is calculated when the data set is split into two randomly selected subpopulations and two corresponding 3D maps are calculated. The Fourier Shell Correlation curve (FSC) is

calculated between the two volumes (a comparison in Fourier space) and the reconstruction's resolution limit is determined at the FSC value of 0.5 (FSC=0.5).

1.6 The leptin receptor system - a brief historical perspective

The first documented case of genetically obese animals, the *ob/ob* mice, dates back to the 1950s (Ingalls et al., 1950). However, it was not until later that another group discovered a nonsense mutation in the ob/ob mice (Zhang et al., 1994). The gene bearing the nonsense mutation makes the 16 kDa leptin hormone, normally expressed in the white adipose tissue. The mutation causes a truncation in the hormone making it unable to be secreted and causing extreme obesity in the mice (Zhang et al., 1994). Interestingly, the authors also reported that the expression of the ob gene in mice is greatly enhanced compared to their wild-type counterparts (Zhang et al., 1994). To identify the high affinity binding site of leptin or in other words the leptin receptor (LepR), Tartaglia and colleagues used a radioactively labeled leptin in mouse tissues and performed binding assays to identify the major sites of leptin binding. After constructing a cDNA library, the authors were able to isolate and clone the LepR which they characterized as a single pass membrane receptor similar to glycoprotein 130 (gp130), Interleukin-6 receptor (IL-6R), granulocyte colony stimulating factor receptor (GCSF-R) and leukemia inhibitory factor receptor (LIF-R) (Tartaglia et al., 1995).

Leptin

The hormone leptin belongs to the hematopoietin family of cytokines because of its shared structural homology to interleukin-6 (IL-6), leukemia inhibitory factor (LIF) and cilliary neutrophic factor (CNTF), to name a few (Zhang et al., 1994). Because the native leptin peptide is very prone to aggregation, its poor solubility proved its crystallization to be very challenging. Systematic site-directed mutagenesis during the crystallographic trials led to the discovery of a single amino acid substitution at its surface having a dramatic effect on its solubilization. The yielded analog, leptin-E100, bearing a single amino acid substitution of Glu for Trp at position 100, finally allowed its crystallization (Zhang et al., 1997).

The hormone leptin and the leptin receptor (LepR)

Structurally, leptin bears striking similarity to other four-helical bundled cytokines such as LIF (Robinson et al., 1994) and G-CSF (Hill et al., 1993). In addition to many similarities, the structure of leptin also has a few notable differences from other cytokines. For example, G-CSF and LIF have well pronounced kinks in the middle of helix A and D, respectively, in order to maximize helix contacts in these structures. Leptin, on the other hand, has only a small kink at the end of helix D (Zhang et al., 2005). Like other class I cytokines, leptin possesses three binding epitopes at sites I, II and III which can be potentially engaged with receptor interactions and activation (Bravo and Heath, 2000; Iserentant et al., 2005). Peelman and colleagues showed that epitope II of leptin constitutes the primary binding site to the receptor (Peelman et al., 2004). However, the existence of the two more putative binding epitopes has led to substantial controversy in terms of the formation of the leptin/LepR signaling complex (Couturier and Jockers, 2003; Mistrik et al., 2004; Peelman et al., 2006).

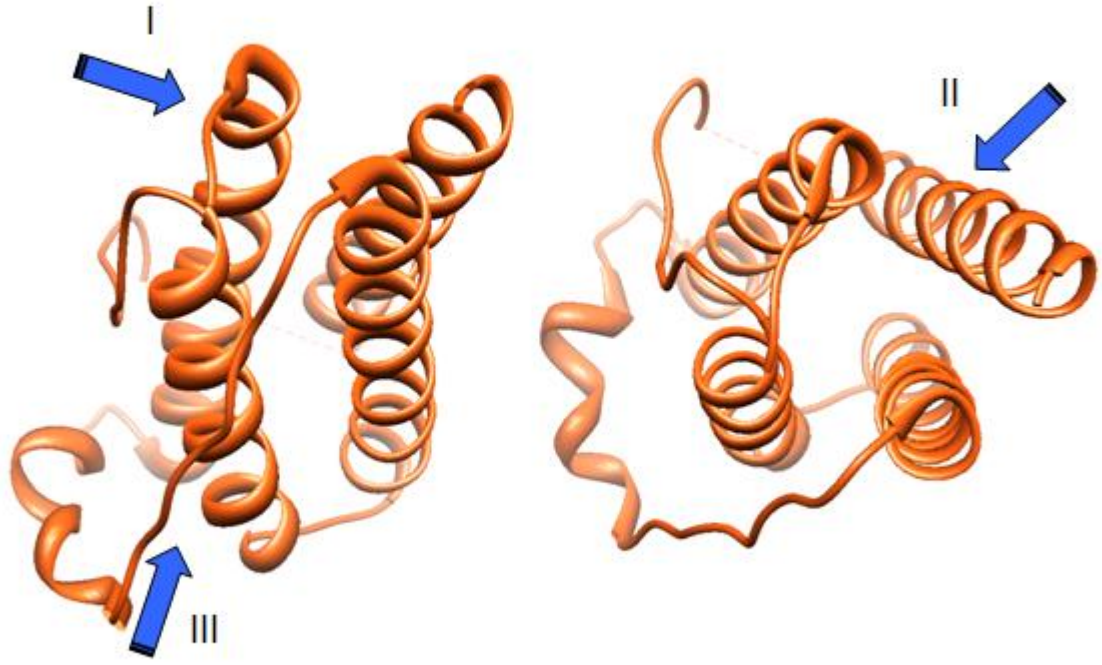

Figure 1-17 Ribbon diagram of the crystal structure of leptin.

A four-helical bundle conformation of human leptin. Blue arrows point to putative binding epitopes based on structural similarities to other four-helical bundle cytokines.

LepR belongs to class I cytokine receptors which includes glycoprotein 130 (gp130), the LIF receptor (LIF-R), the CNTF receptor (CNTF-R), the granulocyte colony stimulating factor receptor (GCSF-R), and others (Tartaglia et al., 1995) (Wang et al., 2009). Receptors from this class are characterized with conserved signature domain organization at their extracellular end. LepR has seven domains grouped into modules on the extracellular side of the membrane. Along with oncostatin M receptor (OSM-R) and LIF-R, LEP-R is an unusual class I receptor since it contains not one, but two CHR modules. The N-terminal CHR1 and the C-terminal CHR2 are membrane-distal and separated by an immunoglobulin-like domain (IgD). Each CHR module consists of two domains with a characteristic fibronectin type III (FnIII) fold that contain the classical motif for cytokine binding (Wang et al., 2009). In addition, both CHR modules represent potential ligand binding sites, however, only CHR2 has been shown to be required for leptin binding (Fong et al., 1998; Iserentant et al., 2005; Peelman et al., 2004). Furthermore, unlike LIF-R and gp130, LEP-R possesses two, rather than three, FNIII membrane-proximal domains. Although the IgD (D3) and the two membrane-proximal FnIII domains are not prerequisites for high-affinity leptin binding, they have been shown to be essential for LEP-R activation (Zabeau et al., 2005; Zabeau et al., 2004).

To this end, there are at least five known isoforms of LepR (a-f) produced by alternative splicing of the db gene (Lee et al., 1996; Tartaglia et al., 1995). All isoforms are identical at their extracellular region but differ in length at their C-terminal tails. The shortest, isoform e, is truncated proximally to the membrane-spanning domain and functions as a soluble circulating leptin-binding protein. In addition, the longest isoform b is the only one having signaling capabilities (Friedman, 1998). LepR is primarily expressed in the hypothalamus, at the areas involved in the regulation of energy balance such as the arcuate and ventromedial nuclei (Elmquist et al., 1998). Therefore, leptin's ability to regulate food intake can be primarily attributed to its actions in the hypothalamus.

Class I cytokine receptors are not kinases themselves. Instead, they rely on constitutively bound Janus kinases (JAKs), at their intracellular domains (ICD) for activation. There are two highly conserved motifs on the LepR ICD, termed box 1 and box 2 which are required for Jak2 binding and activation (Kloek et al., 2002). A few studies have suggested that ligand-binding on the extracellular portion of the receptor is a prerequisite for Jak2 signal instigation by way of stabilizing the transmembrane region in a certain conformation and thus favorably orienting the JAK2s toward each other (Couturier and Jockers, 2003; Murray, 2007).

Signal transduction pathways activated by leptin

Ligand-binding to the leptin receptor can lead to the activation of numerous downstream signaling pathways. Once activated, JAK2 phosphorylates multiple tyrosine residues on the intracellular receptor tail which serve as binding site for downstream signaling effectors. Some of the pathways that lepin activates include JAK/STAT, SHP-2, MAPK, phosphatidylinositol 3 kinase (PI3K and AMP-activated protein kinase (AMPK) (Zhang et al., 2005). Leptin signaling through the JAK/STAT pathway has been well studied. STAT3 binds on the receptor tail upon phosphorylation of Tyrosine1138 which results in JAK2-mediated phosphorylation and subsequent release into the cytoplasm, dimerization and translocation to the nucleus. In the nucleus, the STAT dimer binds DNA and instigates transcription of genes predominantly involved in expression of numerous neuropeptides involved in feeding and regulating body energy balance (Zhang et al., 2005). Activation of LepR also induces the expression of SOCS3 in the hypothalamic area by direct binding of STAT3 to the response element (Bjorbaek et al., 1998). SOCS3 is an SH2 domain-containing protein, capable of binding phosphorylated Tyr985 on JAK2 inhibiting JAK2 activity and abolishing LepR signaling (Bjorbaek et al., 1999). In addition, leptin-mediated MAP kinase activation is promoted through SH2-containing phosphatase 2 (SHP-2) which binds to the phosphorylated LepR and simultaneously inhibits STAT3 activation (Banks et al., 2000). Moreover, there is a strong correlation between leptin and insulin signaling pathways. It has been suggested that the hypothalamic leptin receptor signaling couples to the intracellular insulin-receptor substrate (IRS)-PI3K pathway via JAK2-mediated phosphorylation of IRS and Grb-2

protein (Villanueva and Myers, 2008). Also, it has been postulated that leptin can regulated lipid metabolism through fatty acid oxidation by activating AMPK (Minokoshi et al., 2002).

Biomedical significance of leptin/LepR system

Leptin is a pleiotropic adipokine and its receptors are located not only in the hypothalamus but also in peripheral tissues such as monocytes, lymphocytes, vascular tissue, pancreas, skeletal muscle and myocardium (Margetic et al., 2002). Given the broad expression of the receptors and plethora of pathways activated upon leptin signaling, it is not surprising that perturbations in the leptin system lead to serious illnesses. After the discovery of leptin and its successful crystallization, scientists thought that the solution for treating obesity would be a straightforward one. However, the initial recombinant leptin treatment for obesity did not yield the expected results. Leptin administration was shown to successfully suppress appetite and reduce excessive fat in obese humans with genetic leptin deficiency (Farooqi et al., 2002). In contrast, leptin therapy in the majority of human obese patients only resulted in modest weight reduction (Mantzoros and Flier, 2000). Interestingly, most obese individuals exhibit elevated circulating leptin concentrations, indicating leptin resistance rather than deficiency (Considine et al., 1996).

Lipodystrophy is another rare disease characterized by low leptin levels and associated with insulin resistance, hyperglycemia, hyperinsulinemia and hepatic steatosis (Garg, 2000). Treating lipodystrophic patients with leptin leads to an improvement in their glycemic control and decreases triglyceride levels. In addition, leptin deficiency contributes to insulin resistance and other abnormalities associated with severe lipodystrophy (Oral et al., 2002). Hypothalamic amenorrhea is yet another disease associated with leptin deficiency (Bluher and Mantzoros, 2007). Recombinant leptin therapy in these patients has been shown to improve the gonadal function associated with nutritional calorie deficiency (Welt et al., 2004). However, the development of better leptin analogs for long-term treatment is needed because of leptin-related weight loss in those patients, already underweight. Obesity also increases the risk of cardiovascular

disease and the elevated leptin levels in such individuals are found to be correlated with hypertension and atherosclerosis, stroke and inflammation (Beltowski, 2006; Sweeney, 2010).

The above mentioned clinically-related diseases implicated by leptin do not cover by far all potential clinical application of leptin-based therapies. Therefore, understanding the molecular mechanisms of leptin signaling and resistance is crucial to combat not just obesity but all pathways affected by defective leptin signaling in order to develop effective therapeutics.

Part of the work in this thesis is concerned with investigating the leptin/leptin receptor signaling complex and aims to uncover valuable insights of the mechanism of activation and understand better this pleiotropic pharmacological target.

1.7 The Opioid Receptor System

Introduction to opiates and their receptors

For centuries, opium and its derivatives have been utilized in medicine for treatment of chronic pain as well as "recreationally" as euphoriant agents. Opium is an extract of the poppy plant *Papaver Somniferum*. Friedrich Serturner was the first to identify morphine as the active ingredient. However, it was not until over a hundred years later when the actions of morphine were demonstrated at the receptor level (Pert and Snyder, 1973). Opiate receptors are of fundamental physiological importance because they mediate responses for pain, sedation and euphoria (Waldhoer et al., 2004). Opioid drugs such as morphine and codeine are invaluable pain killers and sedatives but their addictive nature limits their clinical usage. The opioid receptors therefore are important structural targets to design new drugs exerting beneficial actions and lacking the side effects (Hughes and Kosterlitz, 1983; Waldhoer et al., 2004).

Opioid receptors can be activated by a variety of ligands either produced by the body (e.g. endorphins), found in nature (e.g. morphine) or synthetically made (e.g. heroin). Various glands throughout the body, such as the pituitary and the adrenal glands as well as the central nervous system (CNS) are responsible for production of endogenous opioid

peptides. Endogenous opioids are secreted as hormones or neurotransmitters in the circulation, travel to target organs and induce responses (Janecka et al., 2004). Endogenous opiate peptides can also serve as neuromodulators when produced by nerve cells and produce responses in the brain and the spinal cord. By mediating their actions on the CNS and in the circulation, endogenous peptides serve a broad range of physiological roles. The opioid receptors are also activated by exogenous non-peptide molecules termed alkaloids or opiate drugs such as morphine (Kieffer, 1995). These drugs can produce not only strong analgesic effects but also very addictive actions by mimicking the actions of the endogenous peptides. In addition, adverse side effects of opiate drugs could be attributed to their interference with the tightly regulated endogenous opioid system.

Classification of opioid receptors

Even before their biochemical identification, the notion of receptor subtypes has been suggested by classical pharmacological studies. To this end, there are four opioid receptors cloned and they are named after the pharmacological profile of the compounds used to identify them - MOR (μ = mu for morphine), KOR (κ = kappa for ketocyclazocine), DOR (δ = delta for deferens) and the NOR (nociceptin-orpharin) receptors (Waldhoer et al., 2004). It is suggested, however, that there may be additional opioid receptor subtypes resulting from posttranslational modification, alternative mRNA splicing, tissue distribution and alternative protein scaffolding (Jordan and Devi, 1999; Pasternak, 2001). Opioid receptors are coupled to pertussis-toxin-sensitive inhibitory G-proteins termed Gi/o (Yaksh, 1997). The opioid signals are efficiently blocked by pertussis toxin (PTX), a bacterial toxin by *Bordetella pertussis* which ADP-rybosylates the α subunit thus inactivating Gi heterotrimer and preventing the receptor from signaling. In general, the Gi action is mediated through blocking the activity of adenylyl cylase which in turn reduces cAMP and leads to multiple actions, including modulation of sodium channel activity (Law et al., 2000). In addition, the G-proteins can also act by stimulating the potassium channels and increasing calcium levels (North et al., 1987) (Jin et al., 1992). Interestingly, G-proteins have also been shown to regulate mitogen-activated protein kinase (MAPK) activity (Standifer and Pasternak, 1997). Understanding

the opioid receptors mediated signal transduction is crucial to understanding the regulatory mechanisms of their effectors. An important class of proteins that serve as GTPase activating proteins by facilitating the hydrolysis of GTP to GDP are regulators of G-proteins (RGS). The nucleotide hydrolysis facilitates the G-protein subunits re-association and signal termination and they have been implicated in opioid tolerance (Garzon et al., 2001). Another mode of regulation of GPCR signaling is through β-arrestins. Upon agonist stimulation of GPCRs, the G-protein receptor kinases (GRKs) phosphorylate the receptor which in turn leads to the recruitment of β-arrestins. These proteins promote the dissociation of G-proteins from the receptor and terminate signaling. In addition, G-proteins are also capable of facilitating the internalization of inactivated receptors to promote recycling or even degradation (Raehal and Bohn, 2005). Interestingly, β-arrestins have been shown to also have signaling roles by associating with additional scaffolding proteins and thus influencing overall receptor responsiveness (Shukla et al., 2011).

The μ-opioid receptor (MOR)

MOR is a subtype of opioid receptors class of GPCRs. MORs are encoded by the MOR-1 gene and they bind morphine most tightly compared to DORs and KORs. Studies in mice have shown that opioid alkaloids target primarily μ-opioid receptors to exert the effects of analgesia, euphoria, sedation, respiratory depression and cough suppression and even constipation as a peripheral effect (Katzung, 2009; Matthes et al., 1996). Because the opioid drugs are highly addictive, their clinical efficacy is limited by the development of tolerance and dependence. Activation of MOR can be attributed to both beneficial and adverse effects likely mediated by different downstream signaling and regulatory pathways.

To signal, μ-OR couples to Gi/Go subunit which is responsible for its analgesic effects (Raffa et al., 1994). Several chimeric and mutagenesis approaches have identified functional residues in the receptor, responsible for ligand-binding on the N-terminus and G-protein (Pan and Pasternak, 2011). As a member of the GPCR family, the MOR also utilizes a GTP/GDP exchange within the heterotrimeric G-protein to catalyze signaling.

Activation of the receptor is through its interaction with G-proteins which induces the release of GDP from the α-subunit of the G-protein. This allows GTP to bind and results in the dissociation of the heterotrimeric G-protein into α and βγ signaling subunits. The α subunit has an inherent GTPase activity, which hydrolyzes the bound GTP to GDP resulting in the recycling of the heterotrimeric G-protein into its inactive state thereby affecting the signal potency and efficacy.

The crystal structure of the MOR has been determined in the presence of bound antagonist, morphinan, but in the absence of associated G-protein (Manglik et al., 2012). Opioid receptors are similar to other GPCRs in their overall helical organization. Further, recent crystal structures have revealed a remarkably deep ligand-binding pocket in GPCRs. In the crystal structure of MOR, however, the bound antagonist is largely exposed to the extracellular surface, suggesting why the half-life of some opioid ligands, such as heroin, is short. Additionally, the receptor is crystallized as a twofold symmetrical dimer with a significantly large contact between individual protomers which suggests that this could serve as stabilization mechanism in vivo (Manglik et al., 2012). Despite the plethora of biochemical and recently structural information about the MORs, their mechanism of activation is still poorly understood.

Insights from recent structural studies

Recently the crystal structures of MOR, DOR and KOR have been reported (Granier et al., 2012; Manglik et al., 2012; Wu et al., 2012). Most likely their crystal structures represent an inactive state because they were crystallized in the presence of antagonist and without a bound G-protein. Nevertheless, these structures provide detailed information about ligand-binding specificity and an insight into an activation mechanism by a conformational rearrangement of the transmembrane helices.

Recent studies of β_2AR in complex with its G-protein have also begun to reveal some insight into its activation mechanism. Specifically, it has been suggested that the conformational changes in the receptor are coupled to conformational changes in the G-protein, resulting in the movement of the N-terminal α-helical domain which in turn opens the nucleotide binding pocket (Chung et al., 2011; Rasmussen et al., 2011b;

Westfield et al., 2011). It is supposedly logical to think that the MOR involves a similar activation mechanism, although, the presence of the characteristically deep and solvent exposed binding pocket could potentially dictate a different mechanism. Thus, the precise structural basis for the MOR activation and specifically, how upon ligand-binding the structural information is transferred to the G-protein and to downstream effectors, remains to be elucidated. Also, the ultimate goal of the opioid research is to determine the optimal ligand-receptor complex profiles that infer maximal clinical efficacy with minimal side effects.

The second part of my thesis work is concerned with analyzing the MOR-Gi complex with negative stain electron microscopy and comparing its overall domain organization to that of the β2AR-Gαs complex. In addition, one of the long-term goals of this work is to discover stabilizing nucleotides and/or nanobodies that will aid in the crystallization of the complex. Ultimately, the EM studies of the MOR-Gi complex would reveal a common mechanism of activation of the intracellularly bound G-proteins by a way of flexing and extending the AH domain of the Gα subunit.

1.8 References

Audet, M., and Bouvier, M. (2012). Restructuring G-protein- coupled receptor activation. Cell *151*, 14-23.

Azzi, M., Charest, P.G., Angers, S., Rousseau, G., Kohout, T., Bouvier, M., and Pineyro, G. (2003). Beta-arrestin-mediated activation of MAPK by inverse agonists reveals distinct active conformations for G protein-coupled receptors. Proceedings of the National Academy of Sciences of the United States of America *100*, 11406-11411.

Baker, S.J., Rane, S.G., and Reddy, E.P. (2007). Hematopoietic cytokine receptor signaling. Oncogene *26*, 6724-6737.

Bandaranayake, R.M., Ungureanu, D., Shan, Y., Shaw, D.E., Silvennoinen, O., and Hubbard, S.R. (2012). Crystal structures of the JAK2 pseudokinase domain and the pathogenic mutant V617F. Nature structural & molecular biology *19*, 754-759.

Banks, A.S., Davis, S.M., Bates, S.H., and Myers, M.G., Jr. (2000). Activation of downstream signals by the long form of the leptin receptor. The Journal of biological chemistry *275*, 14563-14572.

Baumann, H., Morella, K.K., White, D.W., Dembski, M., Bailon, P.S., Kim, H., Lai, C.F., and Tartaglia, L.A. (1996). The full-length leptin receptor has signaling capabilities

of interleukin 6-type cytokine receptors. Proceedings of the National Academy of Sciences of the United States of America *93*, 8374-8378.

Bazan, J.F. (1990a). Haemopoietic receptors and helical cytokines. Immunology today *11*, 350-354.

Bazan, J.F. (1990b). Shared architecture of hormone binding domains in type I and II interferon receptors. Cell *61*, 753-754.

Beltowski, J. (2006). Leptin and atherosclerosis. Atherosclerosis *189*, 47-60.

Berg, J.M., Tymoczko, J.L., Stryer, L., Stryer, L., and National Center for Biotechnology Information (U.S.) (2002). Biochemistry. (New York

[Bethesda, MD], W.H. Freeman ;NCBI).

Bjorbaek, C., El-Haschimi, K., Frantz, J.D., and Flier, J.S. (1999). The role of SOCS-3 in leptin signaling and leptin resistance. The Journal of biological chemistry *274*, 30059-30065.

Bjorbaek, C., Elmquist, J.K., Frantz, J.D., Shoelson, S.E., and Flier, J.S. (1998). Identification of SOCS-3 as a potential mediator of central leptin resistance. Molecular cell *1*, 619-625.

Bluher, S., and Mantzoros, C.S. (2007). Leptin in reproduction. Current opinion in endocrinology, diabetes, and obesity *14*, 458-464.

Boggon, T.J., Li, Y., Manley, P.W., and Eck, M.J. (2005). Crystal structure of the Jak3 kinase domain in complex with a staurosporine analog. Blood *106*, 996-1002.

Bravo, J., and Heath, J.K. (2000). Receptor recognition by gp130 cytokines. The EMBO journal *19*, 2399-2411.

Cantley, L.C. (2002). The phosphoinositide 3-kinase pathway. Science *296*, 1655-1657.

Cheng, L., Zhu, J., Hui, W.H., Zhang, X., Honig, B., Fang, Q., and Zhou, Z.H. (2010). Backbone model of an aquareovirus virion by cryo-electron microscopy and bioinformatics. Journal of molecular biology *397*, 852-863.

Cherezov, V., Rosenbaum, D.M., Hanson, M.A., Rasmussen, S.G., Thian, F.S., Kobilka, T.S., Choi, H.J., Kuhn, P., Weis, W.I., Kobilka, B.K.*, et al.* (2007). High-resolution crystal structure of an engineered human beta2-adrenergic G protein-coupled receptor. Science *318*, 1258-1265.

Chow, D., He, X., Snow, A.L., Rose-John, S., and Garcia, K.C. (2001). Structure of an extracellular gp130 cytokine receptor signaling complex. Science *291*, 2150-2155.

Chung, K.Y., Rasmussen, S.G., Liu, T., Li, S., DeVree, B.T., Chae, P.S., Calinski, D., Kobilka, B.K., Woods, V.L., Jr., and Sunahara, R.K. (2011). Conformational changes in the G protein Gs induced by the beta2 adrenergic receptor. Nature *477*, 611-615.

Clapham, D.E., and Neer, E.J. (1997). G protein beta gamma subunits. Annual review of pharmacology and toxicology *37*, 167-203.

Considine, R.V., Sinha, M.K., Heiman, M.L., Kriauciunas, A., Stephens, T.W., Nyce, M.R., Ohannesian, J.P., Marco, C.C., McKee, L.J., Bauer, T.L.*, et al.* (1996). Serum immunoreactive-leptin concentrations in normal-weight and obese humans. The New England journal of medicine *334*, 292-295.

Couturier, C., and Jockers, R. (2003). Activation of the leptin receptor by a ligand-induced conformational change of constitutive receptor dimers. The Journal of biological chemistry *278*, 26604-26611.

Darnell, J.E., Jr. (1997). STATs and gene regulation. Science *277*, 1630-1635.

Darnell, J.E., Jr., Kerr, I.M., and Stark, G.R. (1994). Jak-STAT pathways and transcriptional activation in response to IFNs and other extracellular signaling proteins. Science *264*, 1415-1421.

de Vos, A.M., Ultsch, M., and Kossiakoff, A.A. (1992). Human growth hormone and extracellular domain of its receptor: crystal structure of the complex. Science *255*, 306-312.

Dong, C., Davis, R.J., and Flavell, R.A. (2002). MAP kinases in the immune response. Annual review of immunology *20*, 55-72.

Duhe, R.J., and Farrar, W.L. (1995). Characterization of active and inactive forms of the JAK2 protein-tyrosine kinase produced via the baculovirus expression vector system. The Journal of biological chemistry *270*, 23084-23089.

Eastell, R., Reid, D.M., Compston, J., Cooper, C., Fogelman, I., Francis, R.M., Hosking, D.J., Purdie, D.W., Ralston, S.H., Reeve, J.*, et al.* (1998). A UK Consensus Group on management of glucocorticoid-induced osteoporosis: an update. Journal of internal medicine *244*, 271-292.

Elmquist, J.K., Bjorbaek, C., Ahima, R.S., Flier, J.S., and Saper, C.B. (1998). Distributions of leptin receptor mRNA isoforms in the rat brain. The Journal of comparative neurology *395*, 535-547.

Exton, J.H. (1996). Regulation of phosphoinositide phospholipases by hormones, neurotransmitters, and other agonists linked to G proteins. Annual review of pharmacology and toxicology *36*, 481-509.

Farooqi, I.S., Matarese, G., Lord, G.M., Keogh, J.M., Lawrence, E., Agwu, C., Sanna, V., Jebb, S.A., Perna, F., Fontana, S.*, et al.* (2002). Beneficial effects of leptin on obesity, T

cell hyporesponsiveness, and neuroendocrine/metabolic dysfunction of human congenital leptin deficiency. The Journal of clinical investigation *110*, 1093-1103.

Feng, J., Witthuhn, B.A., Matsuda, T., Kohlhuber, F., Kerr, I.M., and Ihle, J.N. (1997). Activation of Jak2 catalytic activity requires phosphorylation of Y1007 in the kinase activation loop. Molecular and cellular biology *17*, 2497-2501.

Firmbach-Kraft, I., Byers, M., Shows, T., Dalla-Favera, R., and Krolewski, J.J. (1990). tyk2, prototype of a novel class of non-receptor tyrosine kinase genes. Oncogene *5*, 1329-1336.

Fong, T.M., Huang, R.R., Tota, M.R., Mao, C., Smith, T., Varnerin, J., Karpitskiy, V.V., Krause, J.E., and Van der Ploeg, L.H. (1998). Localization of leptin binding domain in the leptin receptor. Molecular pharmacology *53*, 234-240.

Frank, J. (2006). Three-dimensional electron microscopy of macromolecular assemblies visualization of biological molecules in their native state, 2nd edn (Oxford ; New York: Oxford University Press).

Frank, J., Radermacher, M., Penczek, P., Zhu, J., Li, Y., Ladjadj, M., and Leith, A. (1996). SPIDER and WEB: processing and visualization of images in 3D electron microscopy and related fields. Journal of structural biology *116*, 190-199.

Frank, S.J., Yi, W., Zhao, Y., Goldsmith, J.F., Gilliland, G., Jiang, J., Sakai, I., and Kraft, A.S. (1995). Regions of the JAK2 tyrosine kinase required for coupling to the growth hormone receptor. The Journal of biological chemistry *270*, 14776-14785.

Fredriksson, R., Lagerstrom, M.C., Lundin, L.G., and Schioth, H.B. (2003). The G-protein-coupled receptors in the human genome form five main families. Phylogenetic analysis, paralogon groups, and fingerprints. Molecular pharmacology *63*, 1256-1272.

Freissmuth, M., and Gilman, A.G. (1989). Mutations of GS alpha designed to alter the reactivity of the protein with bacterial toxins. Substitutions at ARG187 result in loss of GTPase activity. The Journal of biological chemistry *264*, 21907-21914.

Friedman, J.M. (1998). Leptin, leptin receptors, and the control of body weight. Nutrition reviews *56*, s38-46; discussion s54-75.

Fuller, S.D., Butcher, S.J., Cheng, R.H., and Baker, T.S. (1996). Three-dimensional reconstruction of icosahedral particles--the uncommon line. Journal of structural biology *116*, 48-55.

Gabriel, S.E., Brigman, K.N., Koller, B.H., Boucher, R.C., and Stutts, M.J. (1994). Cystic fibrosis heterozygote resistance to cholera toxin in the cystic fibrosis mouse model. Science *266*, 107-109.

Garg, A. (2000). Lipodystrophies. The American journal of medicine *108*, 143-152.

Garzon, J., Rodriguez-Diaz, M., Lopez-Fando, A., and Sanchez-Blazquez, P. (2001). RGS9 proteins facilitate acute tolerance to mu-opioid effects. The European journal of neuroscience *13*, 801-811.

Granier, S., Manglik, A., Kruse, A.C., Kobilka, T.S., Thian, F.S., Weis, W.I., and Kobilka, B.K. (2012). Structure of the delta-opioid receptor bound to naltrindole. Nature *485*, 400-404.

Haan, C., Behrmann, I., and Haan, S. (2010). Perspectives for the use of structural information and chemical genetics to develop inhibitors of Janus kinases. Journal of cellular and molecular medicine *14*, 504-527.

Hanson, M.A., Roth, C.B., Jo, E., Griffith, M.T., Scott, F.L., Reinhart, G., Desale, H., Clemons, B., Cahalan, S.M., Schuerer, S.C.*, et al.* (2012). Crystal structure of a lipid G protein-coupled receptor. Science *335*, 851-855.

Harpur, A.G., Andres, A.C., Ziemiecki, A., Aston, R.R., and Wilks, A.F. (1992). JAK2, a third member of the JAK family of protein tyrosine kinases. Oncogene *7*, 1347-1353.

Hill, C.P., Johnston, N.L., and Cohen, R.E. (1993). Crystal structure of a ubiquitin-dependent degradation substrate: a three-disulfide form of lysozyme. Proceedings of the National Academy of Sciences of the United States of America *90*, 4136-4140.

Huang, L.J., Constantinescu, S.N., and Lodish, H.F. (2001). The N-terminal domain of Janus kinase 2 is required for Golgi processing and cell surface expression of erythropoietin receptor. Molecular cell *8*, 1327-1338.

Hughes, J., and Kosterlitz, H.W. (1983). Opioid Peptides: introduction. British medical bulletin *39*, 1-3.

Huyton, T., Zhang, J.G., Luo, C.S., Lou, M.Z., Hilton, D.J., Nicola, N.A., and Garrett, T.P. (2007). An unusual cytokine:Ig-domain interaction revealed in the crystal structure of leukemia inhibitory factor (LIF) in complex with the LIF receptor. Proceedings of the National Academy of Sciences of the United States of America *104*, 12737-12742.

Ihle, J.N. (2001). The Stat family in cytokine signaling. Current opinion in cell biology *13*, 211-217.

Ingalls, A.M., Dickie, M.M., and Snell, G.D. (1950). Obese, a new mutation in the house mouse. The Journal of heredity *41*, 317-318.

Iserentant, H., Peelman, F., Defeau, D., Vandekerckhove, J., Zabeau, L., and Tavernier, J. (2005). Mapping of the interface between leptin and the leptin receptor CRH2 domain. Journal of cell science *118*, 2519-2527.

James, C., Ugo, V., Le Couedic, J.P., Staerk, J., Delhommeau, F., Lacout, C., Garcon, L., Raslova, H., Berger, R., Bennaceur-Griscelli, A.*, et al.* (2005). A unique clonal JAK2

mutation leading to constitutive signalling causes polycythaemia vera. Nature *434*, 1144-1148.

Janecka, A., Fichna, J., and Janecki, T. (2004). Opioid receptors and their ligands. Current topics in medicinal chemistry *4*, 1-17.

Jatiani, S.S., Baker, S.J., Silverman, L.R., and Reddy, E.P. (2010). Jak/STAT pathways in cytokine signaling and myeloproliferative disorders: approaches for targeted therapies. Genes & cancer *1*, 979-993.

Jin, W., Lee, N.M., Loh, H.H., and Thayer, S.A. (1992). Dual excitatory and inhibitory effects of opioids on intracellular calcium in neuroblastoma x glioma hybrid NG108-15 cells. Molecular pharmacology *42*, 1083-1089.

Jordan, B.A., and Devi, L.A. (1999). G-protein-coupled receptor heterodimerization modulates receptor function. Nature *399*, 697-700.

Katzung, B.G. (2009). Basic & clinical pharmacology. (New York, Lange Medical Books/McGraw Hill).

Khwaja, A. (2006). The role of Janus kinases in haemopoiesis and haematological malignancy. British journal of haematology *134*, 366-384.

Kieffer, B.L. (1995). Recent advances in molecular recognition and signal transduction of active peptides: receptors for opioid peptides. Cellular and molecular neurobiology *15*, 615-635.

Kisseleva, T., Bhattacharya, S., Braunstein, J., and Schindler, C.W. (2002). Signaling through the JAK/STAT pathway, recent advances and future challenges. Gene *285*, 1-24.

Kloek, C., Haq, A.K., Dunn, S.L., Lavery, H.J., Banks, A.S., and Myers, M.G., Jr. (2002). Regulation of Jak kinases by intracellular leptin receptor sequences. The Journal of biological chemistry *277*, 41547-41555.

Kobilka, B.K. (2007). G protein coupled receptor structure and activation. Biochimica et biophysica acta *1768*, 794-807.

Kotenko, S.V., Izotova, L.S., Pollack, B.P., Muthukumaran, G., Paukku, K., Silvennoinen, O., Ihle, J.N., and Pestka, S. (1996). Other kinases can substitute for Jak2 in signal transduction by interferon-gamma. The Journal of biological chemistry *271*, 17174-17182.

Landau, E.M., and Rosenbusch, J.P. (1996). Lipidic cubic phases: a novel concept for the crystallization of membrane proteins. Proceedings of the National Academy of Sciences of the United States of America *93*, 14532-14535.

Law, P.Y., Wong, Y.H., and Loh, H.H. (2000). Molecular mechanisms and regulation of opioid receptor signaling. Annual review of pharmacology and toxicology *40*, 389-430.

Lee, A.G. (2003). Lipid-protein interactions in biological membranes: a structural perspective. Biochimica et biophysica acta *1612*, 1-40.

Lee, A.G. (2004). How lipids affect the activities of integral membrane proteins. Biochimica et biophysica acta *1666*, 62-87.

Lee, G.H., Proenca, R., Montez, J.M., Carroll, K.M., Darvishzadeh, J.G., Lee, J.I., and Friedman, J.M. (1996). Abnormal splicing of the leptin receptor in diabetic mice. Nature *379*, 632-635.

Lefkowitz, R.J., and Shenoy, S.K. (2005). Transduction of receptor signals by beta-arrestins. Science *308*, 512-517.

Leonard, W.J., and O'Shea, J.J. (1998). Jaks and STATs: biological implications. Annual review of immunology *16*, 293-322.

Llorca, O. (2005). Introduction to 3D reconstruction of macromolecules using single particle electron microscopy. Acta pharmacologica Sinica *26*, 1153-1164.

Lodish, H., Berk, A., Zipursky, S.L., Matsudaira, P., Baltimore, D., Darnell, J., and others (2000). Protein structure and function.

Ludtke, S.J., Baldwin, P.R., and Chiu, W. (1999). EMAN: semiautomated software for high-resolution single-particle reconstructions. Journal of structural biology *128*, 82-97.

Manglik, A., Kruse, A.C., Kobilka, T.S., Thian, F.S., Mathiesen, J.M., Sunahara, R.K., Pardo, L., Weis, W.I., Kobilka, B.K., and Granier, S. (2012). Crystal structure of the micro-opioid receptor bound to a morphinan antagonist. Nature *485*, 321-326.

Mantzoros, C.S., and Flier, J.S. (2000). Editorial: leptin as a therapeutic agent--trials and tribulations. The Journal of clinical endocrinology and metabolism *85*, 4000-4002.

Margetic, S., Gazzola, C., Pegg, G.G., and Hill, R.A. (2002). Leptin: a review of its peripheral actions and interactions. International journal of obesity and related metabolic disorders : journal of the International Association for the Study of Obesity *26*, 1407-1433.

Matthes, H.W., Maldonado, R., Simonin, F., Valverde, O., Slowe, S., Kitchen, I., Befort, K., Dierich, A., Le Meur, M., Dolle, P.*, et al.* (1996). Loss of morphine-induced analgesia, reward effect and withdrawal symptoms in mice lacking the mu-opioid-receptor gene. Nature *383*, 819-823.

Mertens, C., Zhong, M., Krishnaraj, R., Zou, W., Chen, X., and Darnell, J.E., Jr. (2006). Dephosphorylation of phosphotyrosine on STAT1 dimers requires extensive spatial reorientation of the monomers facilitated by the N-terminal domain. Genes & development *20*, 3372-3381.

Minokoshi, Y., Kim, Y.B., Peroni, O.D., Fryer, L.G., Muller, C., Carling, D., and Kahn, B.B. (2002). Leptin stimulates fatty-acid oxidation by activating AMP-activated protein kinase. Nature *415*, 339-343.

Mistrik, P., Moreau, F., and Allen, J.M. (2004). BiaCore analysis of leptin-leptin receptor interaction: evidence for 1:1 stoichiometry. Analytical biochemistry *327*, 271-277.

Montaville, P., and Jamin, N. (2010). Determination of membrane protein structures using solution and solid-state NMR. Methods in molecular biology *654*, 261-282.

Murray, P.J. (2007). The JAK-STAT signaling pathway: input and output integration. Journal of immunology *178*, 2623-2629.

Neculai, D., Neculai, A.M., Verrier, S., Straub, K., Klumpp, K., Pfitzner, E., and Becker, S. (2005). Structure of the unphosphorylated STAT5a dimer. The Journal of biological chemistry *280*, 40782-40787.

North, R.A., Williams, J.T., Surprenant, A., and Christie, M.J. (1987). Mu and delta receptors belong to a family of receptors that are coupled to potassium channels. Proceedings of the National Academy of Sciences of the United States of America *84*, 5487-5491.

Ohi, M., Li, Y., Cheng, Y., and Walz, T. (2004). Negative Staining and Image Classification - Powerful Tools in Modern Electron Microscopy. Biological procedures online *6*, 23-34.

Oldham, W.M., and Hamm, H.E. (2008). Heterotrimeric G protein activation by G-protein-coupled receptors. Nature reviews. Molecular cell biology *9*, 60-71.

Oral, E.A., Simha, V., Ruiz, E., Andewelt, A., Premkumar, A., Snell, P., Wagner, A.J., DePaoli, A.M., Reitman, M.L., Taylor, S.I*., et al.* (2002). Leptin-replacement therapy for lipodystrophy. The New England journal of medicine *346*, 570-578.

Pallen, C.J., Tan, Y.H., and Guy, G.R. (1992). Protein phosphatases in cell signalling. Current opinion in cell biology *4*, 1000-1007.

Pan, Y.X., and Pasternak, G.W. (2011). Molecular Biology of Mu Opioid Receptors. Recept Ser, 121-160.

Pasternak, G.W. (2001). Insights into mu opioid pharmacology the role of mu opioid receptor subtypes. Life sciences *68*, 2213-2219.

Peelman, F., Iserentant, H., De Smet, A.S., Vandekerckhove, J., Zabeau, L., and Tavernier, J. (2006). Mapping of binding site III in the leptin receptor and modeling of a hexameric leptin.leptin receptor complex. The Journal of biological chemistry *281*, 15496-15504.

Peelman, F., Van Beneden, K., Zabeau, L., Iserentant, H., Ulrichts, P., Defeau, D., Verhee, A., Catteeuw, D., Elewaut, D., and Tavernier, J. (2004). Mapping of the leptin binding sites and design of a leptin antagonist. The Journal of biological chemistry *279*, 41038-41046.

Pert, C.B., and Snyder, S.H. (1973). Opiate receptor: demonstration in nervous tissue. Science *179*, 1011-1014.

Radermacher, M., and Ruiz, T. (2006). Three-dimensional reconstruction of single particles in electron microscopy image processing. Methods in molecular biology *319*, 427-461.

Radermacher, M., Wagenknecht, T., Verschoor, A., and Frank, J. (1987). Three-dimensional reconstruction from a single-exposure, random conical tilt series applied to the 50S ribosomal subunit of Escherichia coli. Journal of microscopy *146*, 113-136.

Raehal, K.M., and Bohn, L.M. (2005). Mu opioid receptor regulation and opiate responsiveness. The AAPS journal *7*, E587-591.

Raffa, R.B., Martinez, R.P., and Connelly, C.D. (1994). G-protein antisense oligodeoxyribonucleotides and mu-opioid supraspinal antinociception. European journal of pharmacology *258*, R5-7.

Rane, S.G., and Reddy, E.P. (1994). JAK3: a novel JAK kinase associated with terminal differentiation of hematopoietic cells. Oncogene *9*, 2415-2423.

Rasmussen, S.G., Choi, H.J., Fung, J.J., Pardon, E., Casarosa, P., Chae, P.S., Devree, B.T., Rosenbaum, D.M., Thian, F.S., Kobilka, T.S.*, et al.* (2011a). Structure of a nanobody-stabilized active state of the beta(2) adrenoceptor. Nature *469*, 175-180.

Rasmussen, S.G., DeVree, B.T., Zou, Y., Kruse, A.C., Chung, K.Y., Kobilka, T.S., Thian, F.S., Chae, P.S., Pardon, E., Calinski, D.*, et al.* (2011b). Crystal structure of the beta2 adrenergic receptor-Gs protein complex. Nature *477*, 549-555.

Raunser, S., and Walz, T. (2009). Electron crystallography as a technique to study the structure on membrane proteins in a lipidic environment. Annual review of biophysics *38*, 89-105.

Reddy, E.P., Korapati, A., Chaturvedi, P., and Rane, S. (2000). IL-3 signaling and the role of Src kinases, JAKs and STATs: a covert liaison unveiled. Oncogene *19*, 2532-2547.

Remy, I., Wilson, I.A., and Michnick, S.W. (1999). Erythropoietin receptor activation by a ligand-induced conformation change. Science *283*, 990-993.

Richter, M.F., Dumenil, G., Uze, G., Fellous, M., and Pellegrini, S. (1998). Specific contribution of Tyk2 JH regions to the binding and the expression of the interferon

alpha/beta receptor component IFNAR1. The Journal of biological chemistry *273*, 24723-24729.

Robinson, R.C., Grey, L.M., Staunton, D., Vankelecom, H., Vernallis, A.B., Moreau, J.F., Stuart, D.I., Heath, J.K., and Jones, E.Y. (1994). The crystal structure and biological function of leukemia inhibitory factor: implications for receptor binding. Cell *77*, 1101-1116.

Rosenbaum, D.M., Cherezov, V., Hanson, M.A., Rasmussen, S.G., Thian, F.S., Kobilka, T.S., Choi, H.J., Yao, X.J., Weis, W.I., Stevens, R.C.*, et al.* (2007). GPCR engineering yields high-resolution structural insights into beta2-adrenergic receptor function. Science *318*, 1266-1273.

Saharinen, P., and Silvennoinen, O. (2002). The pseudokinase domain is required for suppression of basal activity of Jak2 and Jak3 tyrosine kinases and for cytokine-inducible activation of signal transduction. The Journal of biological chemistry *277*, 47954-47963.

Saltiel, A.R., and Kahn, C.R. (2001). Insulin signalling and the regulation of glucose and lipid metabolism. Nature *414*, 799-806.

Saxena, N.K., Sharma, D., Ding, X., Lin, S., Marra, F., Merlin, D., and Anania, F.A. (2007). Concomitant activation of the JAK/STAT, PI3K/AKT, and ERK signaling is involved in leptin-mediated promotion of invasion and migration of hepatocellular carcinoma cells. Cancer research *67*, 2497-2507.

Schindler, C., Levy, D.E., and Decker, T. (2007). JAK-STAT signaling: from interferons to cytokines. The Journal of biological chemistry *282*, 20059-20063.

Seki, Y., Hayashi, K., Matsumoto, A., Seki, N., Tsukada, J., Ransom, J., Naka, T., Kishimoto, T., Yoshimura, A., and Kubo, M. (2002). Expression of the suppressor of cytokine signaling-5 (SOCS5) negatively regulates IL-4-dependent STAT6 activation and Th2 differentiation. Proceedings of the National Academy of Sciences of the United States of America *99*, 13003-13008.

Shukla, A.K., Xiao, K., and Lefkowitz, R.J. (2011). Emerging paradigms of beta-arrestin-dependent seven transmembrane receptor signaling. Trends in biochemical sciences *36*, 457-469.

Sprecher, C.A., Grant, F.J., Baumgartner, J.W., Presnell, S.R., Schrader, S.K., Yamagiwa, T., Whitmore, T.E., O'Hara, P.J., and Foster, D.F. (1998). Cloning and characterization of a novel class I cytokine receptor. Biochemical and biophysical research communications *246*, 82-90.

Standifer, K.M., and Pasternak, G.W. (1997). G proteins and opioid receptor-mediated signalling. Cellular signalling *9*, 237-248.

Strader, C.D., Fong, T.M., Tota, M.R., Underwood, D., and Dixon, R.A. (1994). Structure and function of G protein-coupled receptors. Annual review of biochemistry *63*, 101-132.

Stryer, L., and Bourne, H.R. (1986). G proteins: a family of signal transducers. Annual review of cell biology *2*, 391-419.

Sunahara, R.K., Dessauer, C.W., and Gilman, A.G. (1996). Complexity and diversity of mammalian adenylyl cyclases. Annual review of pharmacology and toxicology *36*, 461-480.

Sweeney, G. (2010). Cardiovascular effects of leptin. Nature reviews. Cardiology *7*, 22-29.

Tamada, T., Honjo, E., Maeda, Y., Okamoto, T., Ishibashi, M., Tokunaga, M., and Kuroki, R. (2006). Homodimeric cross-over structure of the human granulocyte colony-stimulating factor (GCSF) receptor signaling complex. Proceedings of the National Academy of Sciences of the United States of America *103*, 3135-3140.

Tanner, J.W., Chen, W., Young, R.L., Longmore, G.D., and Shaw, A.S. (1995). The conserved box 1 motif of cytokine receptors is required for association with JAK kinases. The Journal of biological chemistry *270*, 6523-6530.

Tartaglia, L.A., Dembski, M., Weng, X., Deng, N., Culpepper, J., Devos, R., Richards, G.J., Campfield, L.A., Clark, F.T., Deeds, J.*, et al.* (1995). Identification and expression cloning of a leptin receptor, OB-R. Cell *83*, 1263-1271.

Thomson, A.W., and Lotze, M.T. (2003). The cytokine handbook, 4th edn (Amsterdam ; Boston: Academic Press).

Tuteja, N. (2009). Signaling through G protein coupled receptors. Plant signaling & behavior *4*, 942-947.

Unwin, P.N., and Henderson, R. (1975). Molecular structure determination by electron microscopy of unstained crystalline specimens. Journal of molecular biology *94*, 425-440.

Usacheva, A., Sandoval, R., Domanski, P., Kotenko, S.V., Nelms, K., Goldsmith, M.A., and Colamonici, O.R. (2002). Contribution of the Box 1 and Box 2 motifs of cytokine receptors to Jak1 association and activation. The Journal of biological chemistry *277*, 48220-48226.

Vahedi-Faridi, A., Jastrzebska, B., Palczewski, K., and Engel, A. (2012). 3D imaging and quantitative analysis of small solubilized membrane proteins and their complexes by transmission electron microscopy. Journal of electron microscopy.

Vainchenker, W., Delhommeau, F., Constantinescu, S.N., and Bernard, O.A. (2011). New mutations and pathogenesis of myeloproliferative neoplasms. Blood *118*, 1723-1735.

van Heel, M., Harauz, G., Orlova, E.V., Schmidt, R., and Schatz, M. (1996). A new generation of the IMAGIC image processing system. Journal of structural biology *116*, 17-24.

Vanhaesebroeck, B., Leevers, S.J., Ahmadi, K., Timms, J., Katso, R., Driscoll, P.C., Woscholski, R., Parker, P.J., and Waterfield, M.D. (2001). Synthesis and function of 3-phosphorylated inositol lipids. Annual review of biochemistry *70*, 535-602.

Villanueva, E.C., and Myers, M.G., Jr. (2008). Leptin receptor signaling and the regulation of mammalian physiology. International journal of obesity *32 Suppl 7*, S8-12.

Wade, R.H. (1992). A Brief Look at Imaging and Contrast Transfer. Ultramicroscopy *46*, 145-156.

Waldhoer, M., Bartlett, S.E., and Whistler, J.L. (2004). Opioid receptors. Annual review of biochemistry *73*, 953-990.

Wall, M.A., Coleman, D.E., Lee, E., Iniguez-Lluhi, J.A., Posner, B.A., Gilman, A.G., and Sprang, S.R. (1995). The structure of the G protein heterotrimer Gi alpha 1 beta 1 gamma 2. Cell *83*, 1047-1058.

Wang, X., Lupardus, P., Laporte, S.L., and Garcia, K.C. (2009). Structural biology of shared cytokine receptors. Annual review of immunology *27*, 29-60.

Ward, A.C., Touw, I., and Yoshimura, A. (2000). The Jak-Stat pathway in normal and perturbed hematopoiesis. Blood *95*, 19-29.

Welt, C.K., Chan, J.L., Bullen, J., Murphy, R., Smith, P., DePaoli, A.M., Karalis, A., and Mantzoros, C.S. (2004). Recombinant human leptin in women with hypothalamic amenorrhea. The New England journal of medicine *351*, 987-997.

Westfield, G.H., Rasmussen, S.G., Su, M., Dutta, S., DeVree, B.T., Chung, K.Y., Calinski, D., Velez-Ruiz, G., Oleskie, A.N., Pardon, E.*, et al.* (2011). Structural flexibility of the G alpha s alpha-helical domain in the beta2-adrenoceptor Gs complex. Proceedings of the National Academy of Sciences of the United States of America *108*, 16086-16091.

Wettschureck, N., and Offermanns, S. (2005). Mammalian G proteins and their cell type specific functions. Physiological reviews *85*, 1159-1204.

Wilks, A.F., Harpur, A.G., Kurban, R.R., Ralph, S.J., Zurcher, G., and Ziemiecki, A. (1991). Two novel protein-tyrosine kinases, each with a second phosphotransferase-related catalytic domain, define a new class of protein kinase. Molecular and cellular biology *11*, 2057-2065.

Williams, D.B., and Carter, C.B. (1996). Transmission Electron Microscopy A Textbook for Materials Science. Plenum Press Ney York and London.

Wu, H., Wacker, D., Mileni, M., Katritch, V., Han, G.W., Vardy, E., Liu, W., Thompson, A.A., Huang, X.P., Carroll, F.I.*, et al.* (2012). Structure of the human kappa-opioid receptor in complex with JDTic. Nature *485*, 327-332.

Yaksh, T.L. (1997). Pharmacology and mechanisms of opioid analgesic activity. Acta anaesthesiologica Scandinavica *41*, 94-111.

Yeh, T.C., and Pellegrini, S. (1999). The Janus kinase family of protein tyrosine kinases and their role in signaling. Cellular and molecular life sciences : CMLS *55*, 1523-1534.

Zabeau, L., Defeau, D., Iserentant, H., Vandekerckhove, J., Peelman, F., and Tavernier, J. (2005). Leptin receptor activation depends on critical cysteine residues in its fibronectin type III subdomains. The Journal of biological chemistry *280*, 22632-22640.

Zabeau, L., Defeau, D., Van der Heyden, J., Iserentant, H., Vandekerckhove, J., and Tavernier, J. (2004). Functional analysis of leptin receptor activation using a Janus kinase/signal transducer and activator of transcription complementation assay. Molecular endocrinology *18*, 150-161.

Zhang, F., Basinski, M.B., Beals, J.M., Briggs, S.L., Churgay, L.M., Clawson, D.K., DiMarchi, R.D., Furman, T.C., Hale, J.E., Hsiung, H.M.*, et al.* (1997). Crystal structure of the obese protein leptin-E100. Nature *387*, 206-209.

Zhang, F., Chen, Y., Heiman, M., and Dimarchi, R. (2005). Leptin: structure, function and biology. Vitamins and hormones *71*, 345-372.

Zhang, F.L., and Casey, P.J. (1996). Protein prenylation: molecular mechanisms and functional consequences. Annual review of biochemistry *65*, 241-269.

Zhang, X., Jin, L., Fang, Q., Hui, W.H., and Zhou, Z.H. (2010). 3.3 A cryo-EM structure of a nonenveloped virus reveals a priming mechanism for cell entry. Cell *141*, 472-482.

Zhang, Y., Proenca, R., Maffei, M., Barone, M., Leopold, L., and Friedman, J.M. (1994). Positional cloning of the mouse obese gene and its human homologue. Nature *372*, 425-432.

Zhao, Y., Wagner, F., Frank, S.J., and Kraft, A.S. (1995). The amino-terminal portion of the JAK2 protein kinase is necessary for binding and phosphorylation of the granulocyte-macrophage colony-stimulating factor receptor beta c chain. The Journal of biological chemistry *270*, 13814-13818.

Zhou, Z.H. (2011). Atomic resolution cryo electron microscopy of macromolecular complexes. Advances in protein chemistry and structural biology *82*, 1-35.

Zhu, J., Penczek, P.A., Schroder, R., and Frank, J. (1997). Three-dimensional reconstruction with contrast transfer function correction from energy-filtered cryoelectron micrographs: procedure and application to the 70S Escherichia coli ribosome. Journal of structural biology *118*, 197-219.

Zou, Y., Weis, W.I., and Kobilka, B.K. (2012). N-terminal T4 lysozyme fusion facilitates crystallization of a G protein coupled receptor. PloS one *7*, e46039.

Chapter 2 Ligand induced architecture of the leptin receptor signaling complex

2.1 Abstract

Despite the crucial impact of leptin signaling on metabolism and body weight, little is known about the structure of the primary transducer in this pathway, the liganded leptin receptor (LEP-R) complex. Here we applied single-particle electron microscopy (EM) to characterize the architecture of the extracellular region of LEP-R alone and in complex with leptin. We show that unliganded LEP-R displays significant flexibility in a hinge region within the cytokine homology region 2 (CHR2) that is connected to rigid membrane-proximal FnIII domains. Examination of liganded LEP-R complexes reveals that leptin binds to CHR2 in order to restrict the flexible hinge and the disposition of the FnIII 'legs'. Through a separate interaction, leptin engages the Ig-like domain of a second liganded LEP-R, resulting in the formation of a quaternary signaling complex. We propose that the membrane proximal domain rigidification in the context of a liganded cytokine receptor dimer is a key mechanism for the transactivation of dimeric Janus kinases (Jaks) bound at the intracellular receptor region.

2.2 Introduction

Cytokines are secreted signaling molecules that mediate crucial cellular responses through binding to their respective cell surface receptors (Gainsford et al., 1996; Hirahara et al., 2010; Li et al., 2008). Leptin, a class I cytokine, plays a key role in the regulation of energy homeostasis and body weight. Leptin is secreted from adipose tissue at levels that are proportional to body fat content (Considine et al., 1996), and after crossing the blood-brain barrier it engages the leptin receptor (LEP-R) in the central nervous system in order to modulate both food intake and energy expenditure (Bates et al., 2003; Halaas et al., 1995; Morton et al., 2005). Based on controlling homeostasis and growth, leptin signaling also regulates the endocrine and immune systems, affecting diverse processes

such as glucose level regulation, reproduction, bone formation and wound healing (Ahima et al., 1996; Lord et al., 1998; Peelman et al., 2006a).

Leptin adopts a four-helix bundle structure, sharing structural homology to several helical cytokines of the hematopoietin family, such as interleukin-6 (IL-6), leukemia inhibitory factor (LIF), and ciliary neurotrophic factor (CNTF) (Zhang et al., 1997). Based on structural analyses and comparisons with homologous cytokines, leptin possesses three binding epitopes (sites I, II and III) that can be potentially employed for receptor engagement and activation (Bravo and Heath, 2000; Iserentant et al., 2005). Earlier biochemical studies suggested that epitope II constitutes the primary binding site of leptin to LEP-R (Peelman et al., 2004). However, the roles of the remaining epitopes in forming the leptin/LEP-R complex have been a matter of debate, leading to different models for the signaling assembly (Couturier and Jockers, 2003; Mistrik et al., 2004; Peelman et al., 2006b).

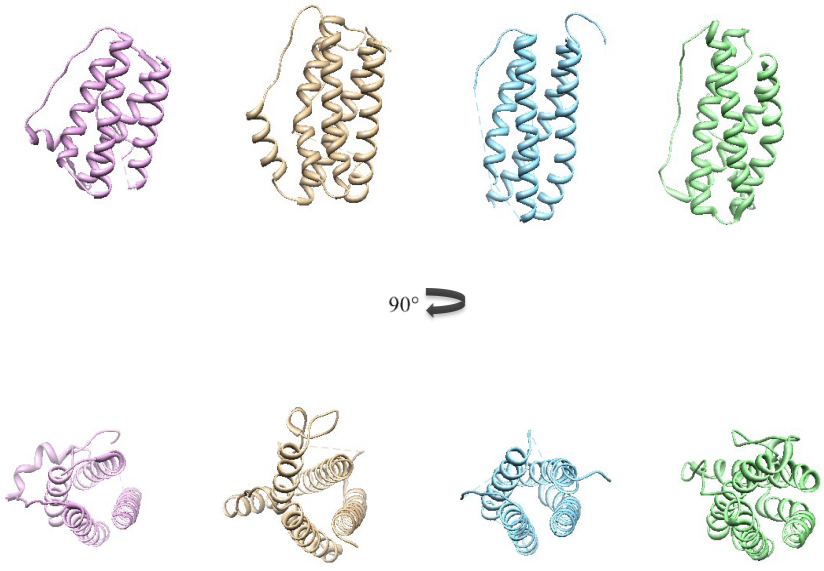

Figure 2-1 Crystal structure of some class I cytokines
Top row, left to right – side views crystal structures of leptin, IL-6, CNTF and LIF; bottom row, left to right – top views of leptin, IL-6, CNTF,LIF;

The leptin receptor exists in at least five isoforms (LEP-R*a-e*) differing in the length of their C-terminal tails, but only the long isoform *b* has demonstrated full intracellular signaling capabilities (Friedman, 1998; Lee et al., 1996). LEP-R belongs to the class I cytokine receptor family, which includes glycoprotein 130 (gp130), the LIF receptor (LIF-R), the CNTF receptor (CNTF-R), the granulocyte colony stimulating factor receptor (GCSF-R), and others (Baumann et al., 1996; Tartaglia et al., 1995; Wang et al., 2009). Class I cytokine receptors do not possess intrinsic kinase activity, but rely on activating Janus kinases (Jaks) that are constitutively bound to the receptor intracellular domains (ICDs). The ICD of LEP-R, which consists of approximately 300 amino acid residues (*b*-isoform), includes two highly conserved membrane-proximal motifs, termed box1 and box2, that are critical for Jak2 binding and activation (Kloek et al., 2002). As has been proposed with other cytokine receptors, leptin binding on the extracellular portion of LEP-R presumably stabilizes the trans-membrane receptor α-helices in a conformation that favors Jak2 trans-phosphorylation and subsequent instigation of downstream signaling (Couturier and Jockers, 2003; Murray, 2007).

The signature module of class I cytokine receptors is the so-called cytokine homology region (CHR) in the extracellular portion. The CHR consists of two domains with a characteristic fibronectin type III (FnIII) fold that contain the classical motif for cytokine binding (Wang et al., 2009). Along with oncostatin M receptor (OSM-R) and LIF-R, LEP-R is an unusual class I receptor since it contains not one, but two CHR modules. The N-terminal CHR1 and the C-terminal CHR2 are membrane-distal and separated by an immunoglobulin-like domain (IgD). Both CHR modules represent potential ligand binding sites, however, only CHR2 has been shown to be required for leptin binding (Fong et al., 1998; Iserentant et al., 2005; Peelman et al., 2004). Furthermore, unlike LIF-R and gp130, LEP-R possesses two, rather than three, FnIII membrane-proximal domains. Although the IgD (D3) and the two membrane-proximal FnIII domains are not prerequisites for high-affinity leptin binding, they have been shown to be essential for LEP-R activation (Figure 2-2) (Zabeau et al., 2005; Zabeau et al., 2004).

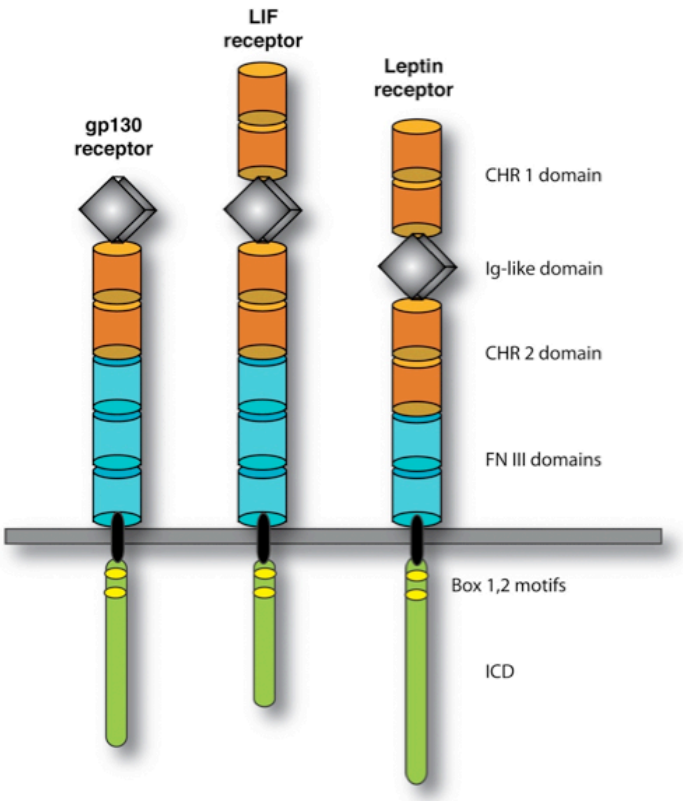

Figure 2-2 Domain organization in class I cytokine receptors.
Members of class I cytokine receptors have similar domain organization at their extracellular regions. The domains consist of an array of fibronectin II fold structures, grouped into modules. Cytokine homology region (CHR) and Immunoglobulin (Ig) domain play role in ligand binding. Intracellular short tails contain conserved motifs Box 1 and 2 that are required to Janus kinase binding.

Earlier studies on cytokine receptor complexes, such as gp130/IL-6/IL6-Rα (Boulanger et al., 2003a; Skiniotis et al., 2005), gp130/LIF-R/CNTF/CNTF-Rα (Skiniotis et al., 2008), and the granulocyte colony-stimulating factor (GSCF) with its receptor GSCF-R (Tamada et al., 2006), have provided a wealth of information on the structural organization of these important signaling assemblies, shedding light on common principles of complex formation. Very recently, the crystal structure of human LEP-R CHR2 in complex with a Fab fragment from a leptin blocking monoclonal antibody provided insights into the mechanism of antagonism and potential modes of leptin binding to this region (Carpenter et al., 2012). However, owing to the existence of the three conserved epitopes on leptin, the structure of the activated signaling leptin/LEP-R complex has been a matter of debate, with the two main models proposing either a 2:2 or

a 2:4 stoichiometry between leptin and LEP-R (Figure 2-3) (Couturier and Jockers, 2003; Mistrik et al., 2004; Peelman et al., 2006b).

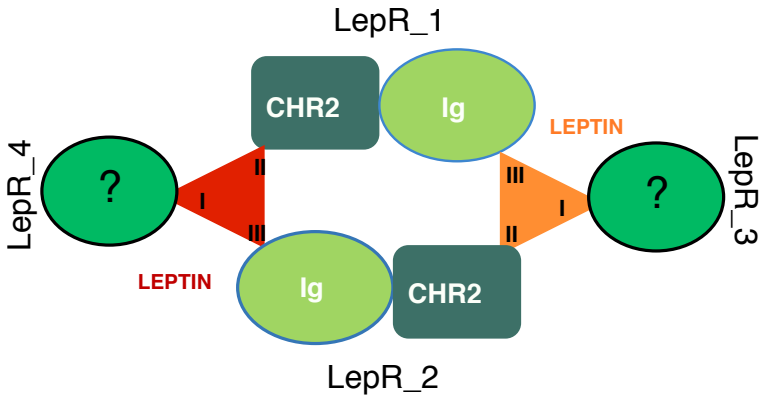

Figure 2-3 Hexameric homology model of the leptin/LEP-R complex.
The model is based on the 3 leptin binding epitopes (from Peelman et al.,2006b). the CHR2 domain form one receptor chain engages epitope II of one leptin molecule which the Ig domain of another LepR engages epitope III of the same leptin molecule. Epitope I of leptin is potentially involved in interaction with an additional LepR chain, forming a 4:2 signaling complex.

Given the lack of structural information on LEP-R and the controversy regarding its arrangement when bound to leptin, we used single-particle electron microscopy (EM) to visualize the extracellular portion of LEP-R alone and in complex with the cytokine. This approach allowed us to elucidate the architecture the leptin/LEP-R complex, and to obtain valuable insights into the mechanism of signal transduction.

2.3 Experimental procedures

Protein Expression & Purification

LEP-R[D1-D7], LEP-R[D1-D5], LEP-R[D1-D7]-GCN4, and LEP-R[D3-D5] constructs were subcloned into the baculovirus FastBac pH7pFB LIC expression vector including a secretion signal sequence. Recombinant viruses were used to infect Sf9 cells and the protein constructs were purified from the supernatant using Ni-NTA Agarose affinity beads (Qiagen, USA). The samples were further purified by size exclusion chromatography (SEC) in 20 mM HEPES, 50 mM NaCl, pH 7.2 (Figure 2.9). For

complex formation, purified LEP-R proteins constructs were incubated with excess recombinant mouse leptin (R&D Systems, Inc., USA). The liganded complexes were subsequently purified by SEC to remove excess leptin, and the purity of the samples was determined by SDS-PAGE stained with Coomassie Blue dye (Figure 1). LEP-R[D1-D7] L503S;L504S and LEP-R[D1-D7] L370A mutants were generated with Quick Change Mutagenesis® (Stratagene), subcloned into FastBac pH7pFB LIC expression vector, and purified as described above (Figure 2.18)

Effect of different reducing reagents on leptin

Leptin may form both intra and inter disulfide bonds making its existence as a dimer and monomer a dynamic process. In order to assess the effect of different reducing agents on leptin dimer formation, the commercially acquired leptin was incubated with different concentrations of dithiothreitol (DTT), tris (2-carboxyethyl)phosphine (TCEP) and β-mercaptoethanol (βME), samples were boiled, ran on SDS-PAGE gels and silver stained. Interestingly, DTT and TCEP were effective to reduce the dimer to monomer at both low and high concentrations. On the other hand, β-ME was only effective at concentration of over 100mM.

Isothermal Titration Calorimetry

Titrations were performed on a NanoITC$_{TM}$ – Low Volume calorimeter (TA Instruments) at 25 °C. Data were processed with the NanoAnalyze software. Briefly, both LEP-R[D1-D7] (11.4 M) and LEP-R[D1-D5] (13 M) were titrated with leptin (75 M) (Figure 2.11 a, c). The titrations showed ~1:1 complex formation for both constructs and indicated high affinity leptin binding (K_D=17.0 nM and K_D=15.4 nM, respectively). The experiment was performed in 20mM HEPES, pH 8.0, 50mM NaCl at 25°C, 2µl/injection, 300 sec/inj., 250 rpm stirring, high feedback, 0.190 ml cell volume.

Analytical Ultracentrifugation (AUC)

Sedimentation velocity experiments were carried out using a ProteomeLab XL-I (Beckman Coulter). Sample triplets were loaded into sector-shaped double channel centerpieces and sedimentation was carried out at 20,000 rpm, 22°C using an AN50TI

rotor. Intensity scans were collected continuously at a wavelength of 235 nm at a radial resolution of 30 μm. Data analysis was with the enhanced van Holde-Weischet analysis module and 2-dimensional sedimentation spectrum analysis (2-DSA) using the finite element modeling module provided with the Ultrascan3 software (http:/www.ultrascan.uthscsa.edu). Sedimentation profiles were analyzed at a grid resolution of 60 using 20 grid repetitions fitting time- and radial invariant noise. Confidence levels were derived from 2-DSA data refinement using genetic algorithm followed by 30 Monte Carlo simulations. Calculations were performed on the UltraScan LIMS cluster at the Bioinformatics Core Facility at the University of Texas Health Science Center at San Antonio and the Lonestar cluster at the Texas Advanced Computing Center supported by NSF Teragrid Grant #MCB070038 (to Borries Demeler).

Electron Microscopy

Protein samples were prepared for electron microscopy using the conventional negative staining protocol (Ohi et al., 2004), and imaged at room temperature with a Tecnai T12 electron microscope operated at 120 kV using low-dose procedures. Images were recorded at a magnification of 71,139x and a defocus value of ~1.6 μm on a Gatan US4000 CCD camera. All images were binned (2 x 2 pixels) to obtain a pixel size of 4.16 Å on the specimen level. Particle projections were manually excised using Boxer [part of the EMAN 1.9 software suite] (Ludtke et al., 1999) apart from tilt-pair images, where particles were selected using WEB (Frank et al., 1996).

Image Processing

Reference-free alignment and classification for the projection analysis of LEP-R and leptin/LEP-R complexes were carried out using the SPIDER image processing suite (Frank et al., 1996). For LEP-R[D1-D7], 23,933 particle projections were classified into 100 classes (Figure 2.14a). For LEP-R[D1-D5], 8,352 particle projections were classified into 80 classes (Figure 2.14b). For the leptin/LEP-R[D1-D5] complex, 5,215 particle images were classified into 100 classes (Figure 2.16c,d). For the LEP-R[D1-D7] L503S;L504S mutant, 6,189 particle images were classified into 50 classes (Figure 2.18

c). For the leptin/LEP-R[D1-D7] L370A mutant complex, 4,964 particle images were classified into 50 classes (Figure 2.18 f).

For the leptin/LEP-R[D1-D7] complex, 20,065 tilt-pair particle projections were interactively selected from 0º and 60º tilted images. To analyze the challenging projection variability of the entire extracellular liganded receptor chains and calculate 3D reconstructions we employed a three-step process: In the first step, the untilted particle images were subjected to 10 cycles of reference-free alignment and classification into 300 classes (Figure 2.16a). In the second step, particles belonging to class averages with poor features and misaligned projections were removed from the dataset, and the remaining 13,616 projections were subjected to another round of iterative classification and alignment into 150 classes (Figure 2.16b). In the third step, we created separate particle sub-groups including projections displaying a specific type of conformation or composition. Thus, we created subgroups for the binary leptin/LEP-R[D1-D7] complex (liganded single chains), and for the side and top views of the leptin/LEP-R[D1-D7] quaternary complexes (Figure 2.16 b, d and 2-17a). This approach allowed us to probe the fine variability within each type of projection, and also select well-defined class averages for 3D reconstructions. The random conical tilt technique (Radermacher et al., 1987) was used to calculate a first back projection map from individual classes using the images of the tilted specimen. After angular refinement, the corresponding particles from the images of the untilted specimens were added, and the images were subjected to another cycle of refinement. Using the resulting maps as reference models, we used FREALIGN (Grigorieff, 2007) for further refinement of the orientation parameters. The 3D maps of the binary leptin/LEP-R[D1-D7], and of the side and top views of the leptin/LEP-R[D1-D7] quaternary complexes were based on 2,374, 1,194, and 772 0º and 60º projections, with indicated resolutions of 40Å, 40Å and 45Å, respectively.

Molecular Modeling and Docking

The model of LEP-R[D1-D7] was built from the first five domains of the crystal structure of LIF-R (Huyton et al., 2007; Skiniotis et al., 2008) and the last two membrane proximal

FnIII domains from the crystal structure of gp130 (Xu et al., 2010) (Figure 2-15c). The binary and quaternary leptin/LEP-R[D1-D7] models were built by aligning the homologous domains from crystal structures of gp130/IL-6 (Boulanger et al., 2003b), GCSF/GCSF-R (Tamada et al., 2006), LIF-R (Huyton et al., 2007; Skiniotis et al., 2008), and leptin (Zhang et al., 1997). Due to the limited resolution of the 3D maps, all docking operations in the EM densities were performed manually with visual inspection of the best fit. The binary leptin/LEP-R[D1-D7] model and the gp130/IL-6 crystal structure were fit as rigid bodies into the 3D maps of the binary complex and the top view of the quaternary complex, respectively (Figures 2-15 f, 2-19e). For the 3D map from side views of the quaternary complex, two liganded leptin/LEP-R[D1-D7] models were flexibly fit into the EM densities (Figure 2-19b).

2.4 Results

Purification trials for LEP-R

The $CaCl_2$/$NiCl_2$ precipitation method

Expressing and purifying secreted proteins from insect cells can be very challenging due to the large volume of media to be handled. There are components in the insect cell media that will strip a Ni resin and that is why the media cannot be applied directly to the Ni-NTA. Therefore, one-way to adapt the media for passage though the Nickel is to precipitate out the interfering components by $CaCl_2$/$NiCl_2$ precipitation. All steps are carried out at a room temperature. Cells are spun and the media is filtered through a 0.2um filter. To each liter of cell the following mixture is added:

1 ml of 1M Nickel Chloride

1ml of 5M Calcium Chloride

50ml of 1M Tris pH 8

Once the precipitation mixture is added, a heavy white precipitate will form immediately. The cells are spun again at least 6000rpm for 15 minutes. After filtration through a 0.2um filter the media is poured into a beaker with a stir bar and 2ml of Nickel slurry is added to

each liter of cells. Incubation is carried out for at least 3 hours at room temperature. The resin is then collected into a polyprep column and washed with 1x HBS and then eluted with 250mM imidazole. It is extremely important to keep the media at room temperature otherwise the Ni resin will be lost in the heavy white precipitate again which will form if the temperature is decreased.

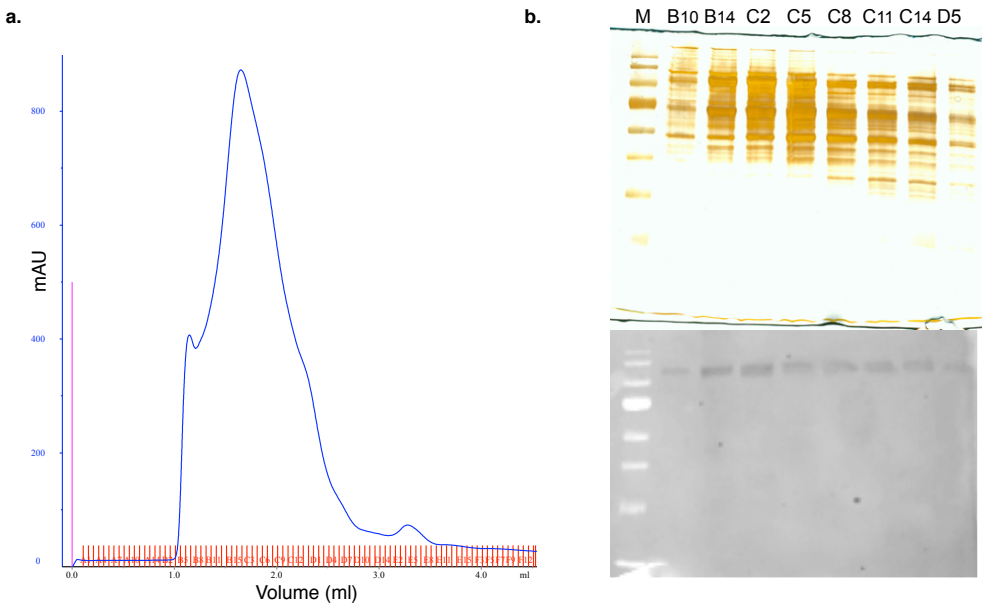

Figure 2-4 Analysis of protein purified with the precipitation method
a. SEC of FL LEP-R b., SDS silver stained gel of SEC fractions and bottom anti-His Western blot of SEC fractions.

In this method the results are difficult to reproduce and usually the proteins are very hard to separate from other contaminants even after affinity and size exclusion steps (Figure 2-4). In addition, adding any components to the media prior or during the Ni incubation step also leads to precipitation. Therefore, this method is not the ideal way to purify secreted proteins.

Buffer exchange method

Another way to strip the media from its interfering components before the Ni application is to exchange buffer for HBS overnight. This method also requires handling very large volumes and is unpractical to carry out for expression volumes over 1.5L. The reason is

that the need to have at least 10X the amount of buffer in the beaker with the media to be exchanged. Therefore, for high protein concentration this method is unsuitable. However, for small volume protein purifications, buffer exchange overnight yields media that could be passed through the Ni-NTA resin without stripping it.

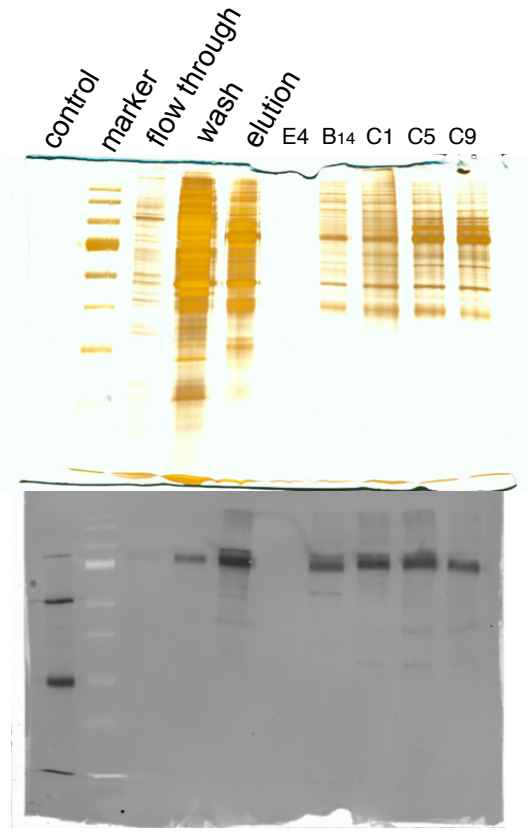

Figure 2-5 SDS-PAGE silver stain (top) and anti-His Western (bottom).
Different purification fractions from full length extracellular LEP-R purified by buffer exchange method.

Moreover, proteins purified with this method may be subject to degradation as illustrated from the Western blot in Figure 2-5 above. Also, the contaminants are difficult to separate from the target protein even after a gel filtration step.

DEAE ion exchange purification method

The diethylaminoethyl (DEAE) cellulose is an ion exchange resin that was tested against the insect media as a buffer exchange step. The ion exchange relies on the reversible

exchange of ions in solution with ions that are bound electrostatically to the resin. Whether or not the protein interacts with the resin and binds or flows through depends on its net charge, which depends on the isoelectric point of the protein and the buffer pH.. Thus, making the protein more negatively charged could be accomplished by raising the pH or more positively charged by lowering the pH and this will ultimately dictate its binding to the ion exchange resin. DEAE cellulose is a positively charged resin that is capable of locking negatively charged proteins. Therefore, when LEP-R in insect cell media is passed through the DEAE it flows through while all media interfering components are retained. This method is not very effective because of the unspecific binding of LEP-R to the DEAE.

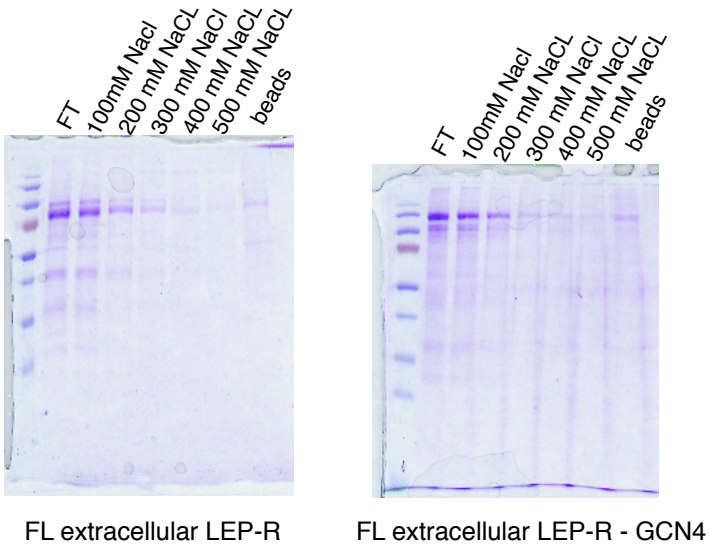

Figure 2-6 DEAE cellulose purification of full length extracellular LEP-R and LEP-R-GCN4.
SDS-PAGE analysis of different purification fractions for LEP-R constructs.

As the figure above illustrates most of the protein flows through the DEAE but more importantly about 50% remains on the resin (Figure 2-6). Although, most of it could be eluted with competing sodium chloride, the amount lost in the process that subsequently could not be directly applied on the Ni is significant. Additionally, the cleaning of the

DEAE is very laborious and time consuming. Therefore, this method is not practical for efficient and clean purification of secreted proteins.

The Millipore concentrator method

This method is the most successful one in dealing with large volumes of media. Here, after the cells have been collected, spun and filtered, the media is applied through the concentrator and the media volume is brought down to 10X. For example, if the starting expression volume is 5L, the concentrator allows for concentrating down to 500ml. Then, the final volume is buffer-exchanged overnight and the purification protocol is carried as usual in the following day. In addition to allowing a large-scale purification of secreted proteins, this method also provides a faster and less error prone methodology in handling sensitive secreted proteins. This method provides a fast and reliably reproducible approach for purification of secreted proteins and is therefore the preferred one for purification of the LEP-R constructs in this thesis.

Effect of vector type, infection time and insect cell line on protein expression

The Baculovirus protein expression has many advantages for producing recombinant mammalian proteins because it permits post-translational modifications such as phosphorylation, disulfide bond formation, proper protein folding, glycosylation and even signal peptide cleavage. Baculoviruses are well known in their ability to infect insects. They contain a double stranded, supercoiled DNA inside of a rod-shape capsid (Summers and Anderson, 1972). One of the most prominent isolate used in foreign gene expression is the *Autographa californica* multiple nuclear polyhedrosis virus (AcMNPV) and the *Orgyia pseudotsugata* muticapsid nuclear polyhedrosisvirus (OpMNPV), used for expression of the LEP-R constructs (Brown et al., 2011). The disadvantages of this system are that the process is quite lengthy (about 2 months from cloning to protein expression), contains multiple steps, many variables, few control check points and can get expensive for large scale protein production. Nevertheless, the Baculovirus expression usually works where E. coli fails to produce the target protein with all the needed post-translational modifications.

Depending on the target protein either *Spodoptera frugipedra* (Sf9) or *Trichoplusia ni* (Hi5) insect cells can lead to better expression. In addition, the allowed time post infection as well as the type of vector used can also influence expression.

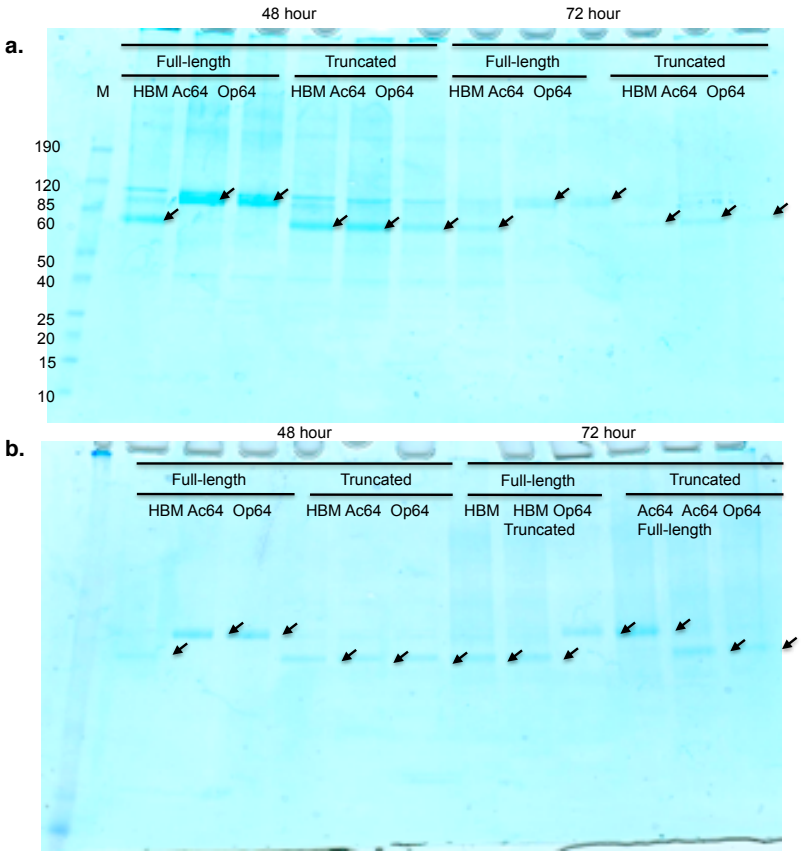

Figure 2-7 Effect of cell type, vector and time of post-infection on protein expression.
a., Expresion in Sf9 cells for different constructs and times. Arrows point to overexpressed protein. b., Expression in Hi5 cells for different constructs, vectors and time. Arrows point to overexpressed proteins. (Courtesy of Clay Brown)

The expression of LEP-R constructs gave best yield in Sf9 cell, at 48 hours post-infection and in vectors containing the Ac64 and Op64 signal sequences (Figure 2-7).

Effect of different reducing reagents on leptin

Leptin may form both intra and inter disulfide bonds making its existence as a dimer and monomer a dynamic process. In order to assess the effect of different reducing agents on leptin dimer formation, commercial leptin was incubated with different concentrations of

dithiothreitol (DTT), tris (2-carboxyethyl)phosphine (TCEP) and β-mercaptoethanol (βME), samples were boiled, ran on SDS-PAGE gels and silver stained. Interestingly, DTT and TCEP were effective to reduce the dimer to monomer at both low and high concentrations which β-ME was only effective at concentration of over 100mM (Figure 2-8).

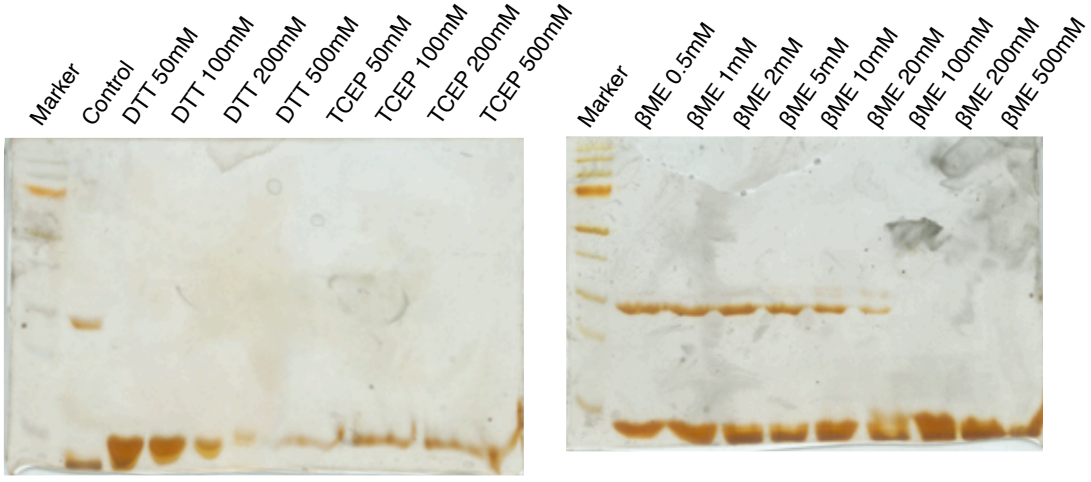

Figure 2-8 Effect of different reducing agents on leptin.
Commercially available leptin was mixed with different reducing agents and samples were analyzed with SDS-PAGE. The gels were silver stained and clearly reveal the leptin dimeric and monomeric species.

Assembly of the Extracellular Leptin/LEP-R complex

For the present study we used a baculovirus system to express the entire extracellular region (domains D1-D7) of murine LEP-R and a truncated construct of the same protein lacking the two membrane-proximal FnIII domains (D1-D5). Both protein constructs were engineered with an N-terminal His-tag facilitating nickel affinity purification, and were further purified to homogeneity by size exclusion chromatography (Figure 2-9).

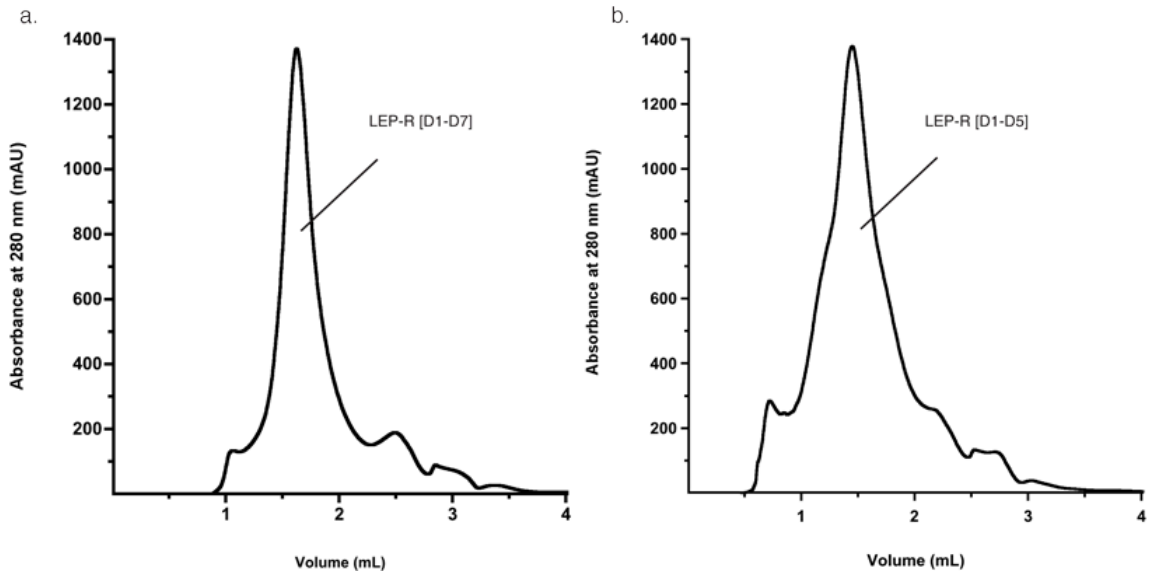

Figure 2-9 Size exclusion chromatography of LEP-R[D1-D7] and LEP-R[D1-D5]. After Ni-affinity purification of LepR constructs, the elution fractions were concentrated and applied to size exclusion chromatography separation. Only fractions under the highest peak were used for subsequent EM analysis.

To evaluate the leptin/LEP-R complex formation and the binding stoichiometry, we employed analytical ultracentrifugation (AUC) and isothermal titration calorimetry (ITC) to measure the thermodynamics of the interaction. Both methods suggested 1:1 stoichiometry of the complex although the ITC provided smaller error.

The sedimentation velocities of both LEP-R[D1-D7] and LEP-R[D1-D5] constructs were measured at room temperature and the AUC species are represented in Figure 2-10.

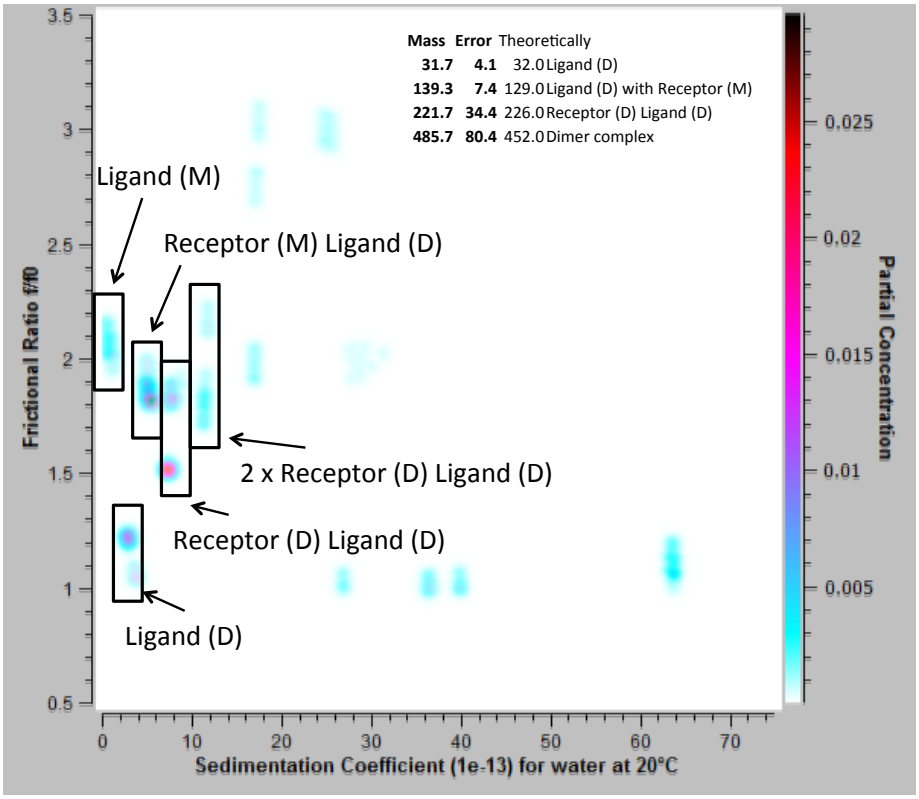

Figure 2-10 Analytical Ultracentrifugation of LEP-R[D1-D7] and LEP-R[D1-D5] in the presence of excess leptin.
Densitometry graph representing relative concentration of different species related to their sedimentation coefficient and relative mass. Data is generated by Titus Franzmann.

The results from the AUC show multiple populations in the mixture after the sedimentation was carried. In fact, the concentration of dimerized leptin was higher than the monomeric species. This in turn increased the bias of whether complex formation was due to ligand dimerization or a dimerization of receptor and ligand. The major species in the mixture consisted of two receptors and two ligands. However, there was also a small population of monomeric receptor chains bound to leptin and some higher order species.

For both the D1-D7 and D1-D5 constructs, the ITC measurements suggested that leptin engages LEP-R with high affinity interaction with K_D value of ~17 nM, providing a first indication for stoichiometric complex formation in a 1:1 ratio (Figure 2-11 a, c). We thus incubated purified LEP-R[D1-D7] and LEP-R[D1-D5] with excess recombinant

murine leptin and used size exclusion chromatography to isolate liganded receptor complexes for subsequent analysis (Figure 2-11 b, d).

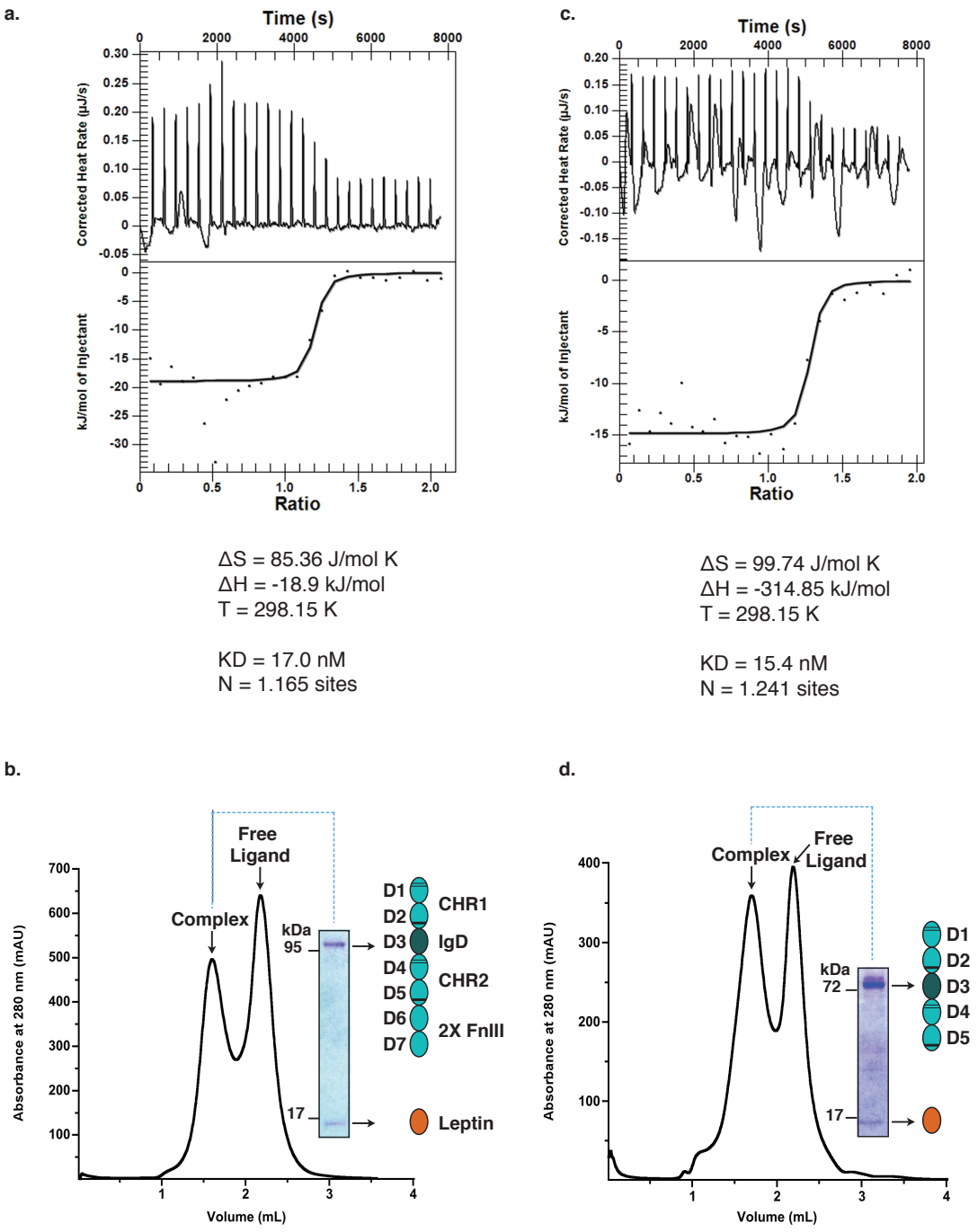

Figure 2-11 Thermodynamic Analysis and Purification of the leptin/LEP-R[D1-D7] and leptin/LEP-R[D1-D5] complex (Mancour et al., 2012)

a, Isothermal titration calorimetry for the assembly of leptin and LEP-R[D1-D7] complex. **b,** Size exclusion chromatography profile and SDS-PAGE analysis of purified liganded LEP-R[D1-D7]. **c,** Isothermal titration calorimetry for the assembly of leptin and LEP-R[D1-D5] complex. **d,** Size exclusion chromatography profile and SDS-PAGE analysis of purified liganded LEP-R[D1-D5].

Rigid Membrane-Proximal Domains Connected to a Flexible CHR2

As a first step in our structural analysis we examined unliganded LEP-R[D1-D7] and LEP-R[D1-D5] preparations by negative stain EM. Both samples revealed monodisperse particle projections embedded in the negative stain (Figure 2-12 and).

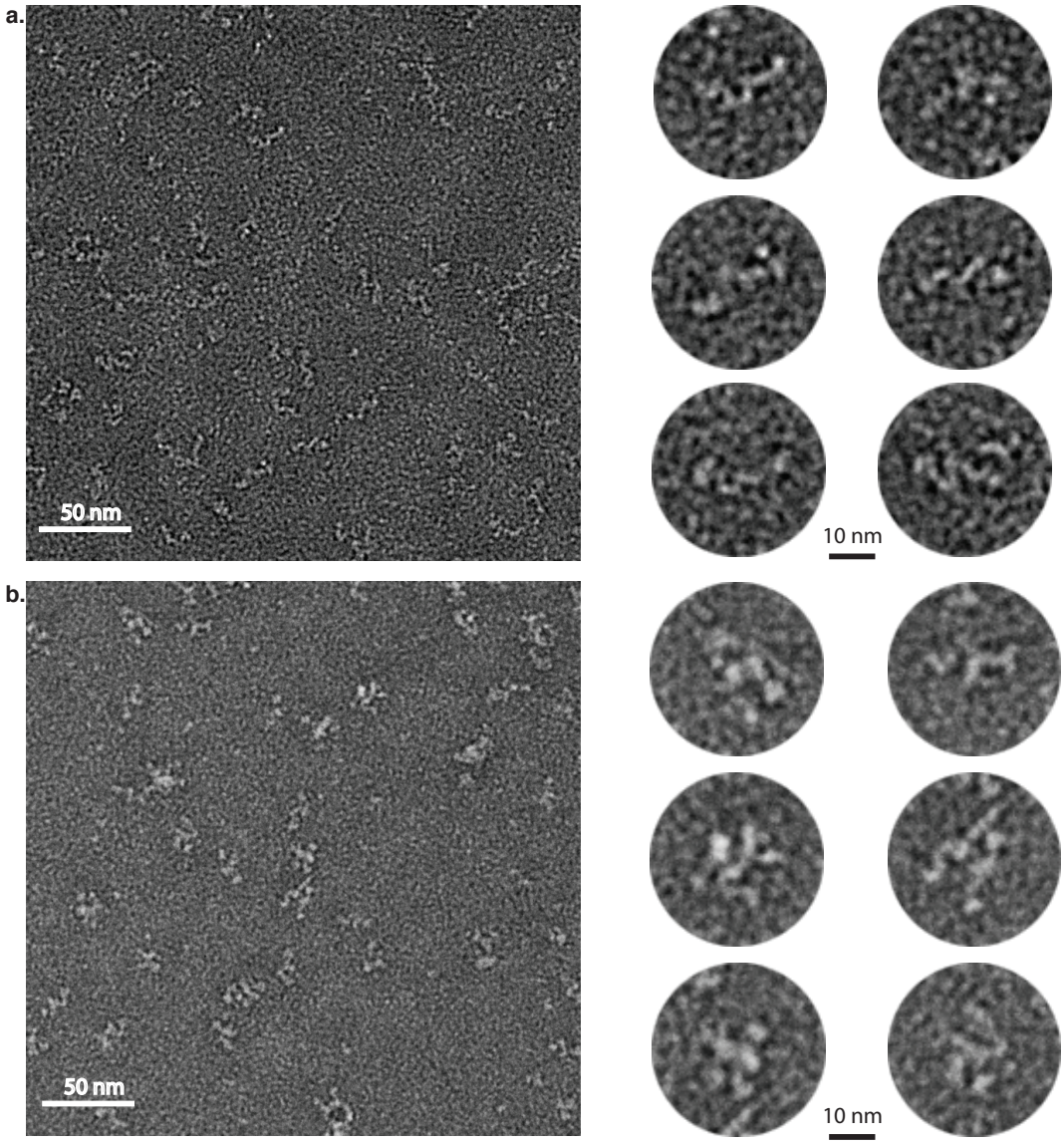

Figure 2-12 Raw EM images of LEP-R[D1-D7] and leptin/LEP-R[D1-D7] complex.
a, raw micrograph of negatively stained LEP-R[D1-D7], individual particles to the right. b, raw micrograph of leptin/LEP-R[D1-D7] complex, individual particles to the right (Mancour et al., 2012).

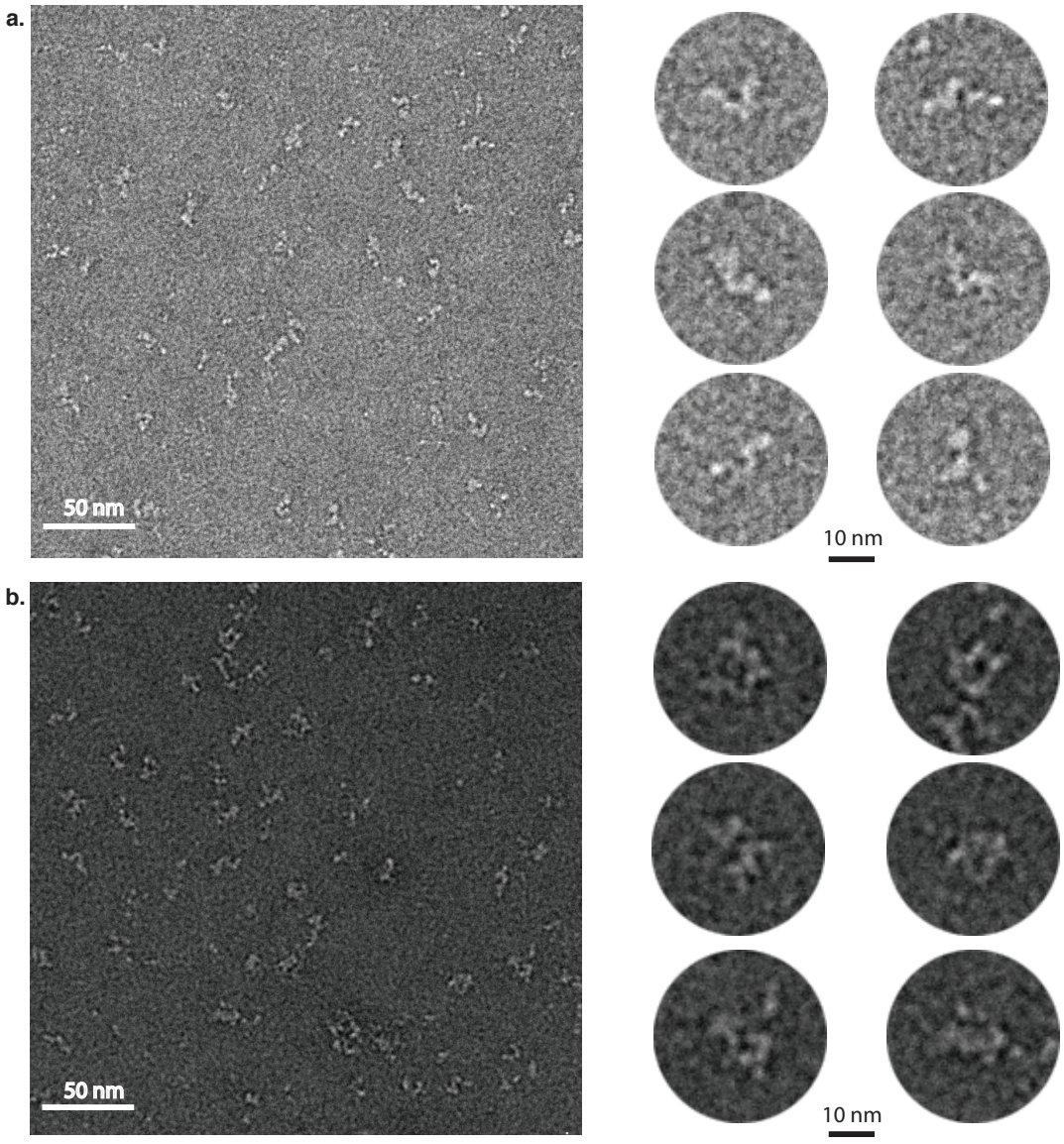

Figure 2-13 Raw EM images of LEP-R[D1-D5] and leptin LEP-R[D1-D5] complex
a, raw micrograph of negatively stained LEP-R[D1-D5], individual particles**.** b, raw micrograph of leptin/LEP-R[D1-D5] complex, individual particles (Mancour et al., 2012).

The samples were analyzed and classified according to the reference-free protocol. Class averages of the D1-D7 construct revealed a single preferred orientation of distinct rod-

like structure of approximately 21 nm in length, which displays a characteristic 'V' shape closer to one end (Figure 2-14a, Figure 2-15 a).

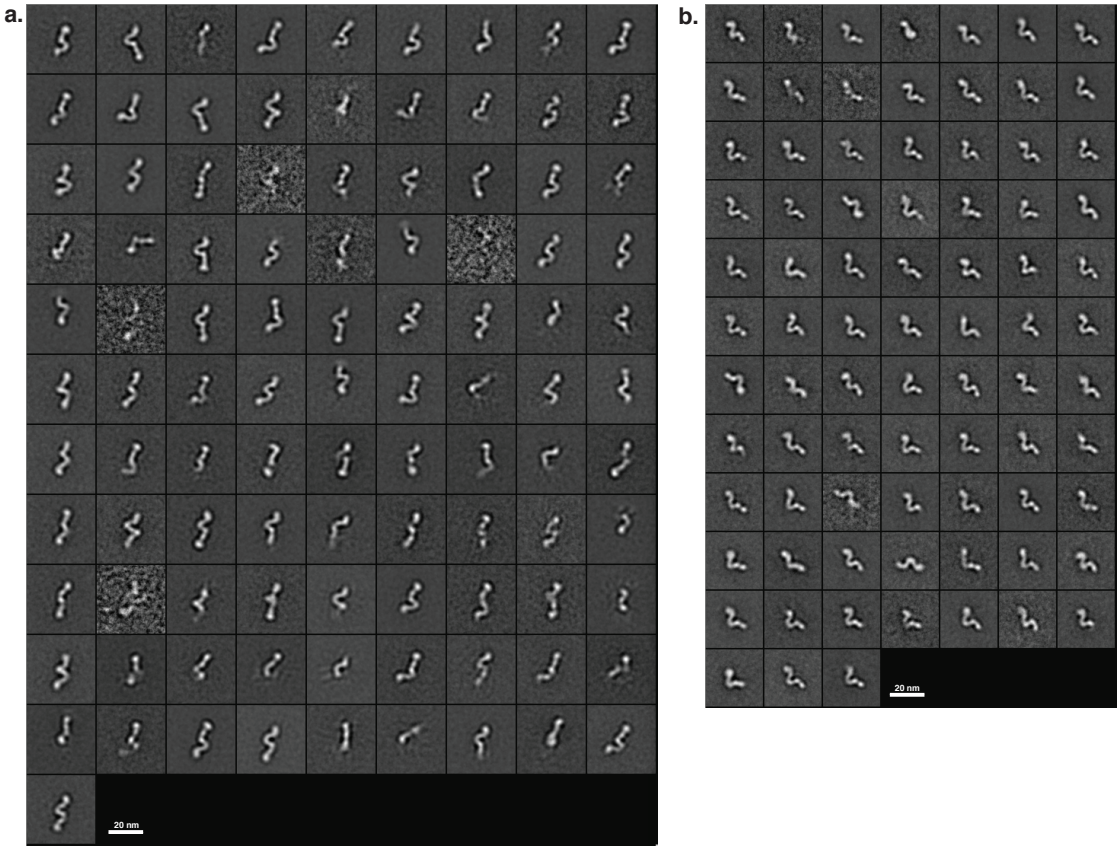

Figure 2-14 Final 2D classifications of LEP-R[D1-D7] and LEP-R[D1-D5]
a., 23,933 particle projections classified into 100 classes. b., 8,352 particle projections classified into 80 classes (Mancour et al., 2012).

Comparison of EM averages from the D1-D7 construct and the shorter D1-D5 construct (~16.5 nm) reveals the orientation of the LEP-R termini with the 'V' shape being closer to the N-terminus (Figure 2-15a, b). A higher density lobe at the C-terminus of the D1-D7 construct suggests that the two membrane-proximal FnIII domains likely assume a sharp bend, similar to what has been observed in the crystal structure of the gp130 ectodomain (Xu et al., 2010). Beyond the membrane-proximal domains, the observed structure is highly reminiscent to the extended "flying V" architecture observed in the crystal structures of murine and human LIF-R (Huyton et al., 2007; Skiniotis et al., 2008) (Figure 2-15c). In this configuration, the D1-D2 and D4-D5 CHR modules adopt the

canonical bent elbow shape commonly seen in other cytokine receptors, while the IgD (D3) is centrally positioned at the base of the 'V'. Given the highly similar extracellular domain architecture of LIF-R[D1-D5] and gp130[D1-D6], and also the similarities with the recently solved structure of LEP-R CHR2 region (Carpenter et al., 2012), we aligned and merged their available crystal structures to produce a homology model for the entire extracellular region of LEP-R (Figure 2-15c). This model is in striking agreement with the projection averages of LEP-R, indicating the common domain organization of the tall cytokine receptor family.

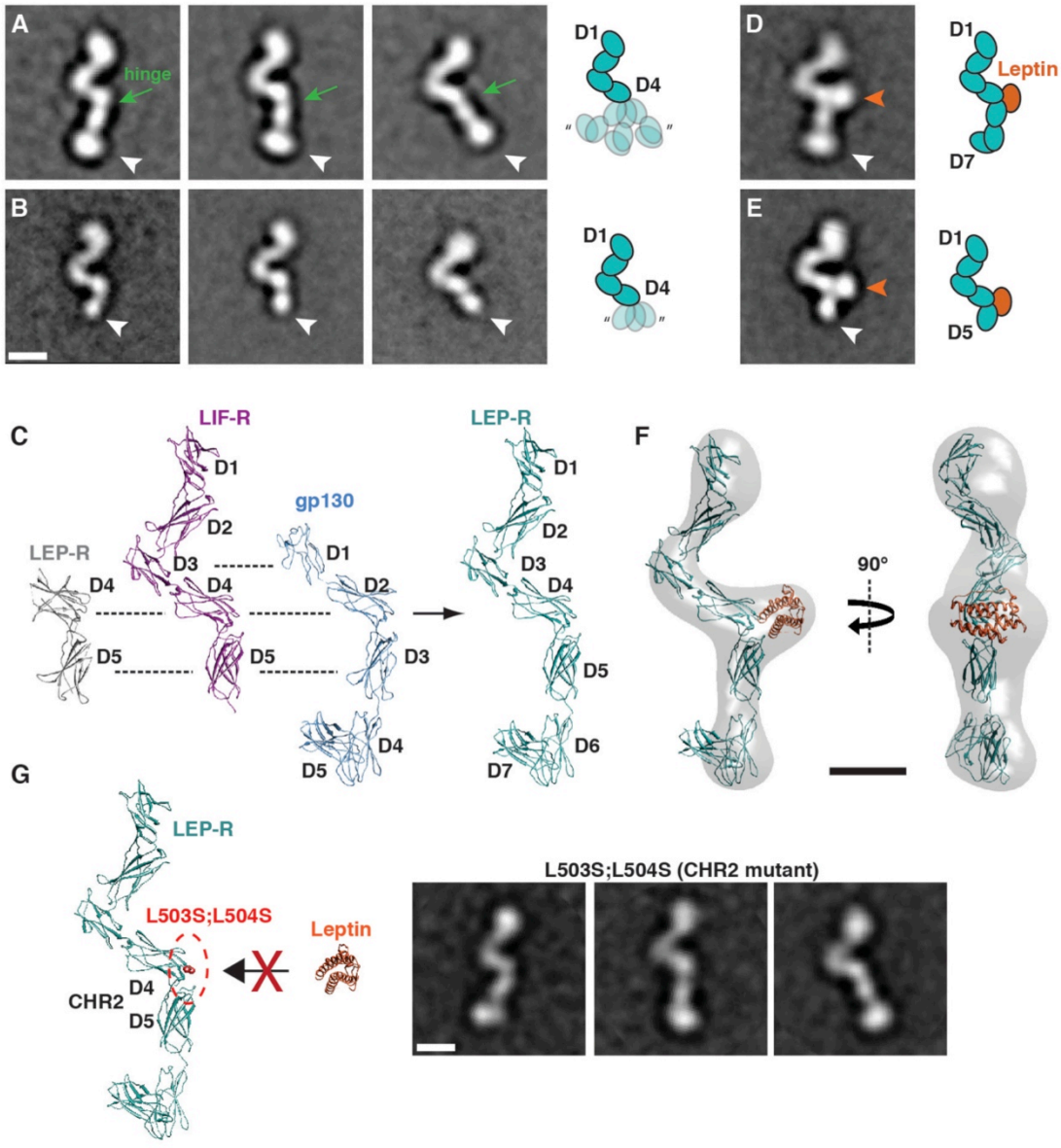

Figure 2-15 Conformational dynamics of LEP-R in unliganded and liganded states
a., representative two-dimensional class averages of unliganded LEP-R[D1-D7] reveal significant flexibility in the hinge between D4 and the rigid D5-D7 module (white arrow heads). **b.,** two dimensional class averages of unliganded LEP-R[D1-D5] confirm the domain assignments and the variable deposition of D5 (white arrowheads) in regards to D4. **c.,** Comparison of the crystal strucutres from LEP-R, gp130 and LIF-R extracellular domain and homology model for LEP-R[D1-D7 **d.,** Representative two-dimensional class average of the binary leptin/LEP-R[D1-D7] complex. The cytokine binds to CHR2 resulting in the stabilization of the rigid D5-D7 module in a single conformation. **e.,** Representative two-dimensional class average the binary leptin/LEP-R[D1-D5] complex. The orange and white arrowheads point to the leptin density and the LEP-R C terminus, respectively. **f.,** Three-dimensional reconstruction of the binary leptin/LEP-R[D1-D7] complex with docked leptin/LEP-R homology model. **g.,** The double mutation L503S/L504S on D4 of Lep-R abolishes leptin binding via epitope II. EM class averages of this mutant after incubation with leptin reveal only monomeric receptor chains with no ligand bound at CHR2 (compare to **a** and **d**). All scale bars correspond to 5 nm (Mancour et al., 2012).

Interestingly, D5 of CHR2 and the two membrane-proximal FnIII domains (D6-D7) are well defined and assume the same angle, suggesting that they behave as a rigid body (Figure 2-15a). However, the orientation of the D5-D7 module in respect to the central 'V' is highly variable and assumes a continuum of angles with a range of ~40° in the plane of the carbon support of the EM grid. This observation suggests that the linker connecting the two domains composing CHR2 (D4-D5) is highly flexible and allows for variability in the relative configuration of the connected domains. Indeed, examination of class averages of the truncated construct lacking the FnIII 'legs' (D6-D7) clearly reveals that D5 assumes variable positions around D4 with the same angular range observed in the full-length extracellular construct (Figure 2-15 a, b).

Leptin Engages CHR2 to Stabilize the Membrane-Proximal Domains

In a next step we examined leptin/LEP-R complexes by negative stain EM. Raw images of this preparation revealed monodisperse particles with variable shapes (Figure 2-12 b, Figure 2-13 b), which represent different orientations or configurations adopted by individual complexes when adsorbed on the carbon support of the EM grid. This characteristic projection variability has been previously observed in our earlier studies involving gp130 (Skiniotis et al., 2005), gp130/LIF-R (Skiniotis et al., 2008), and vascular endothelial growth factor receptor (VEGF-R) (Ruch et al., 2007) liganded

complexes. Similarly to those studies, we applied a three-step strategy of reference-free alignment and classification, enabling us to analyze the projection variability of the receptor chains and calculate 3D reconstructions (for a detailed description see materials and methods section and Figure 2-15, Figure 2-17 and Figure 2-19).

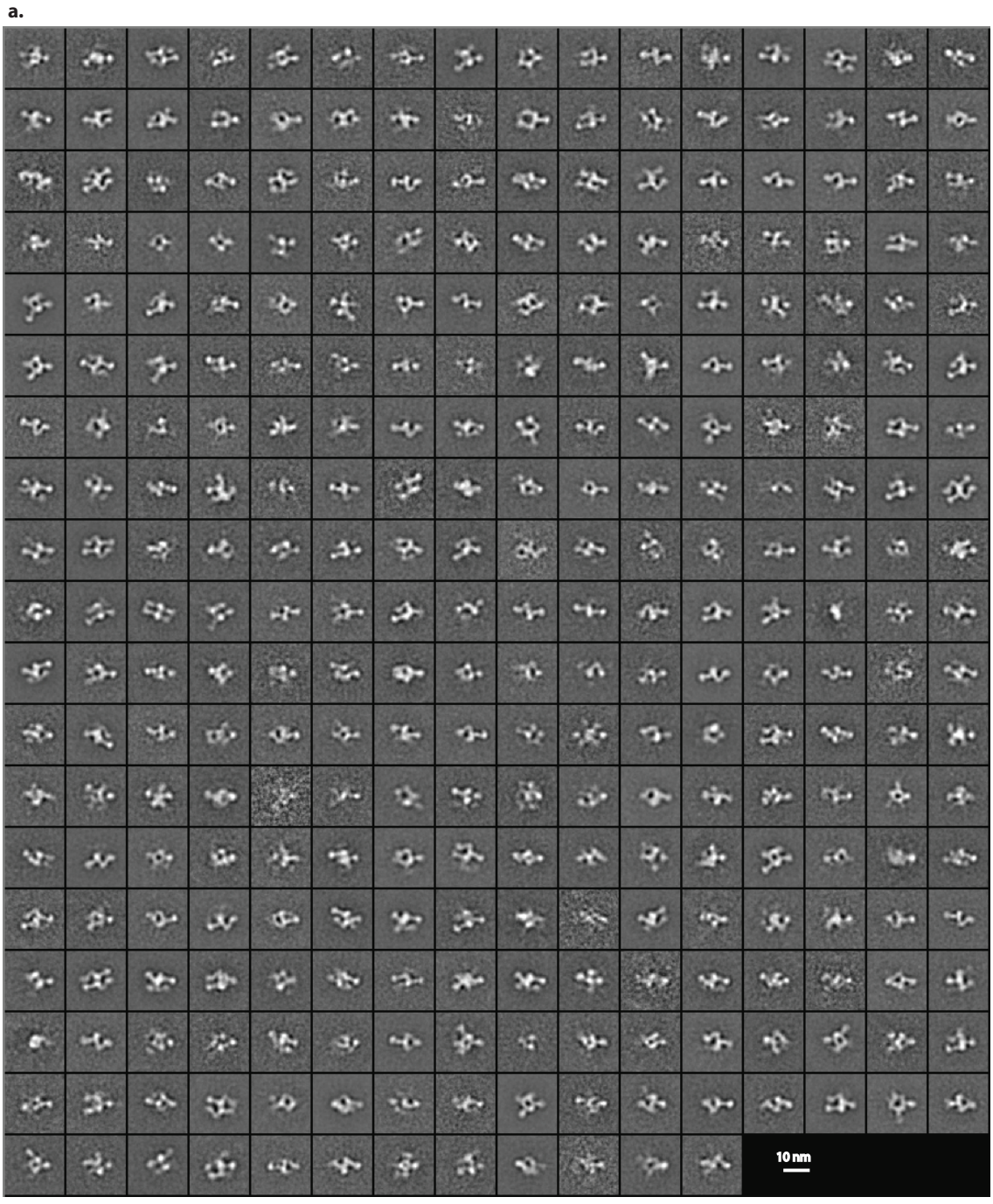

b.

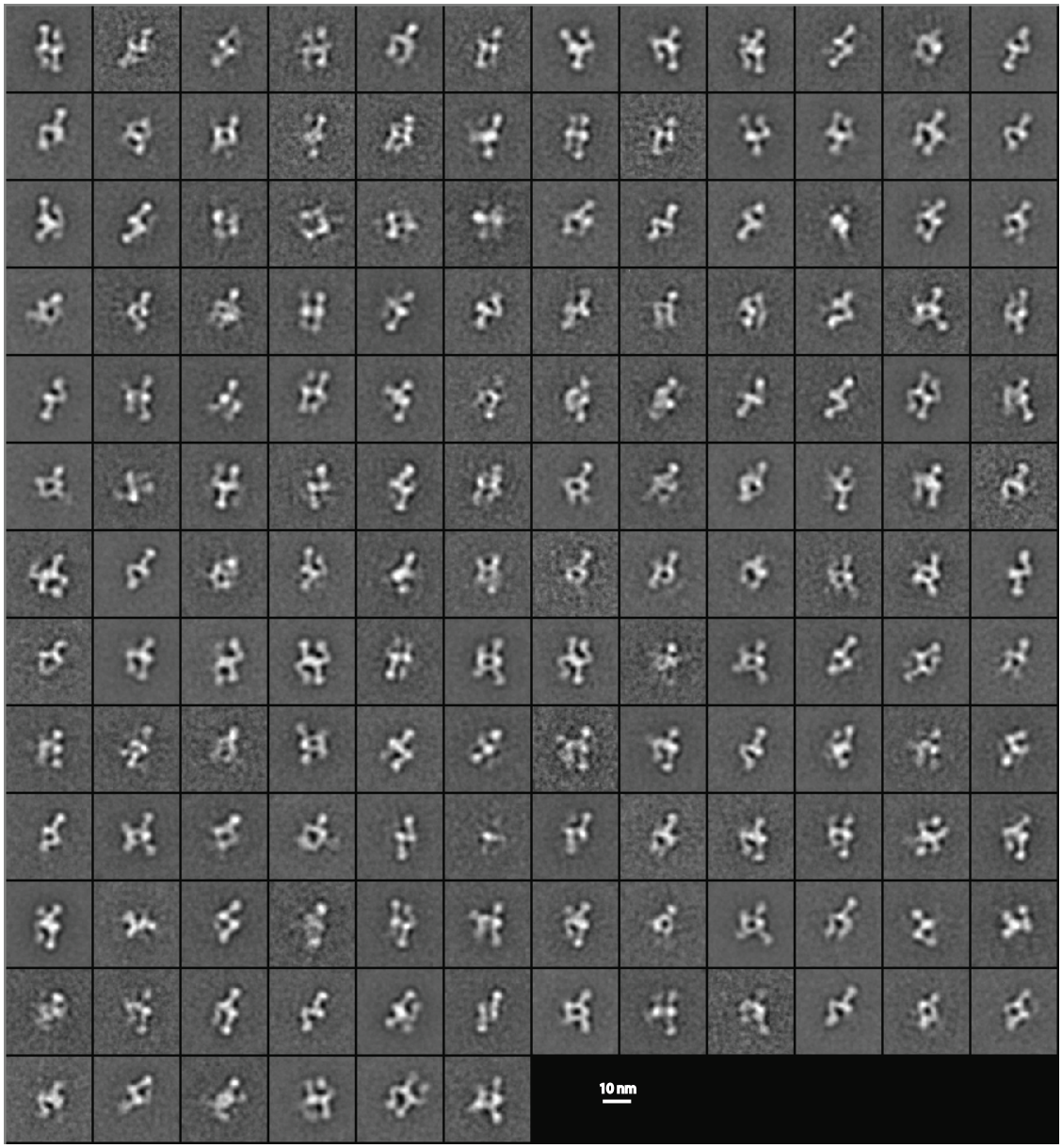

c.

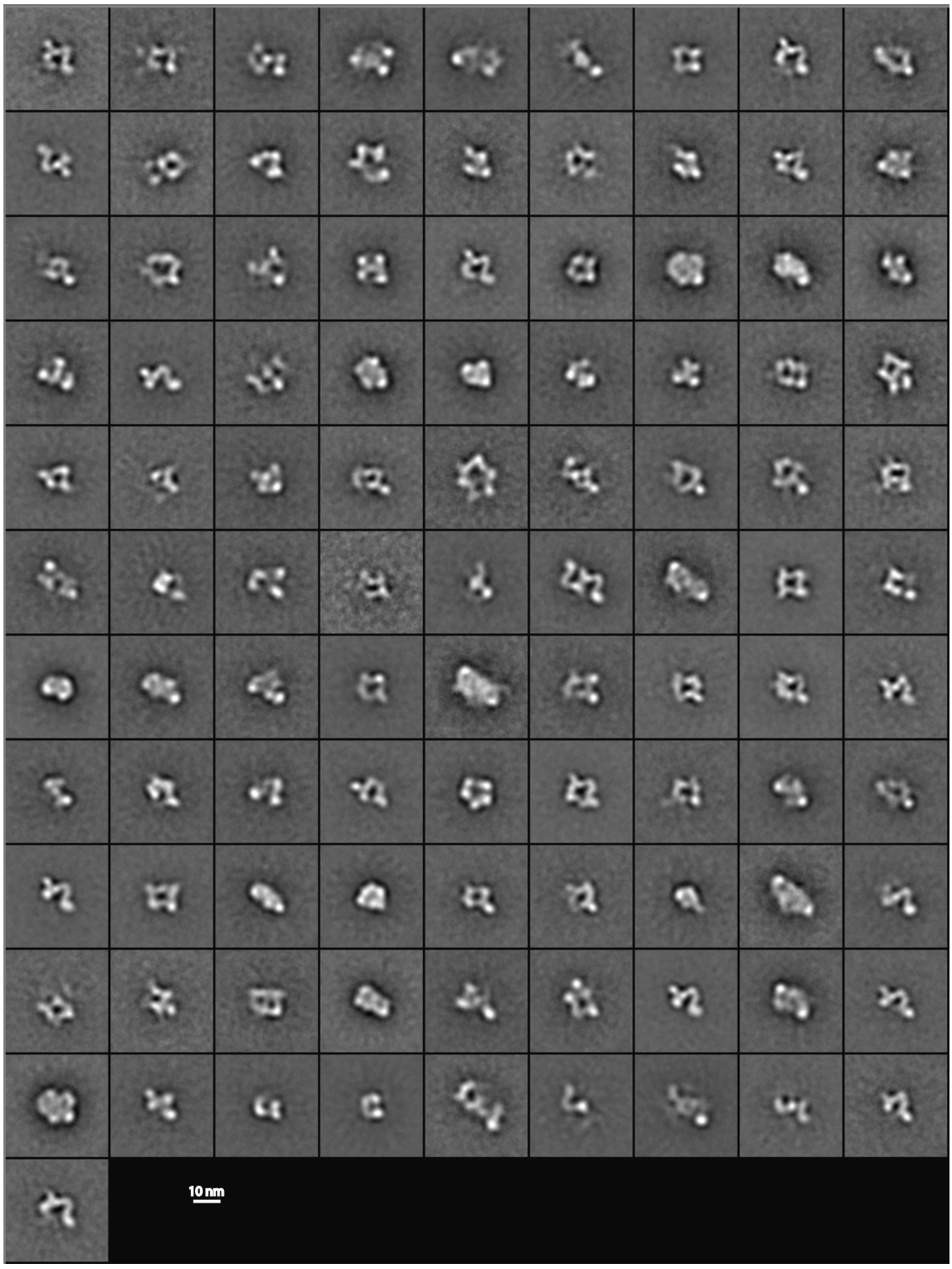

d.

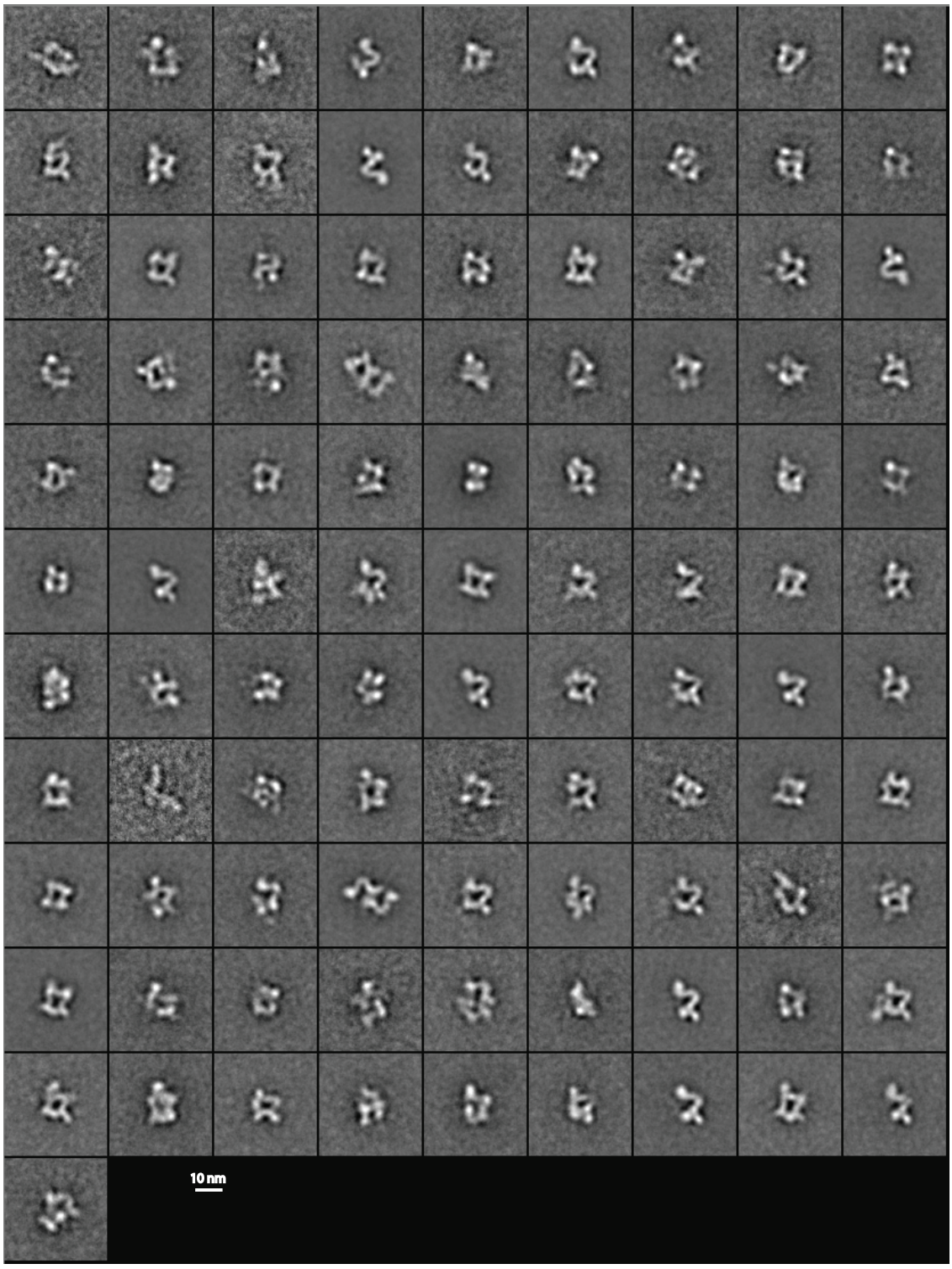

Figure 2-16 Steps in analyzing the challenging projection variability.
a, 20,065 particle projections of the leptin/LEP-R[D1-D7] complex classified into 300 classes. **b,** 13,616 projections of the leptin-LEP-R[D1-D7] complex classified into 150

classes after removing the misaligned projections as well the ones with poor features. **c,** 17,106 particle projection of the leptin/LEP-R[D1-D5] complex into 200 classes. **d,** 5,215 particle projections of the leptin/LEP-R[D1-D5] complex into 100 classes (Mancour et al., 2012).

A fraction of the particles from the liganded LEP-R[D1-D7] and LEP-R[D1-D5] complexes reveal a single preferred orientation of monomeric chains with an additional distinct globular density towards the middle of the receptor, at the junction between domains D4 and D5 (Figure 2-15 d, e; approximately 15% and 25% of particles, respectively). The extra density can only be attributed to a leptin molecule bound to CHR2. This type of interaction has been previously observed in the signaling complexes of IL-6 with gp130 (Boulanger et al., 2003b; Skiniotis et al., 2005) and GCSF with GCSF-R (Tamada et al., 2006), where the cytokines use epitope II to interact with the elbow of the CHR module, and is in agreement with earlier mutagenesis studies (Iserentant et al., 2005). To support this interpretation, we calculated a 3D reconstruction of the liganded monomeric LEP-R chain and compared it to our homology model including a site II interaction of leptin (Figure 2-15 f and Figure 2-17).

a.

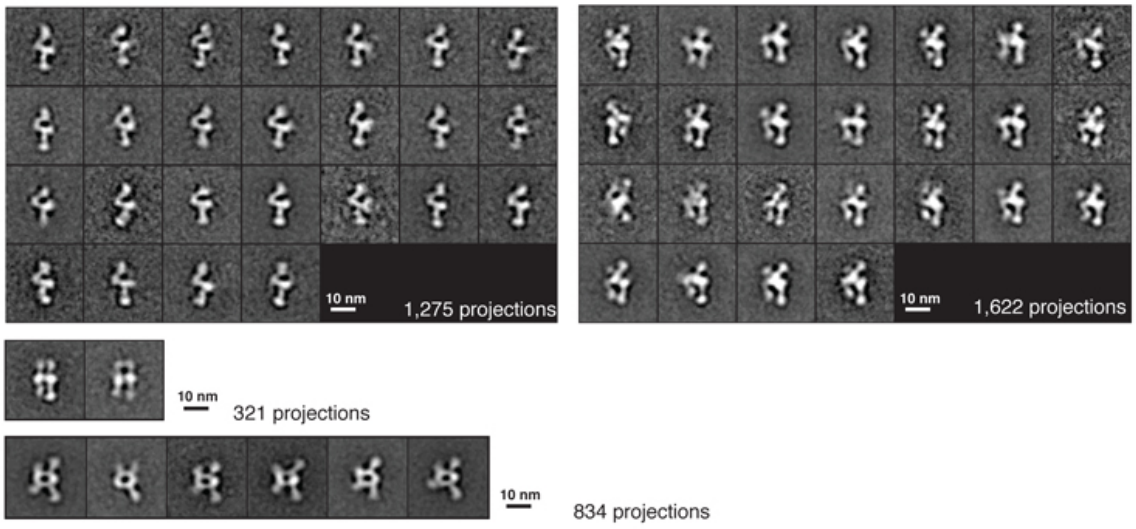

b.

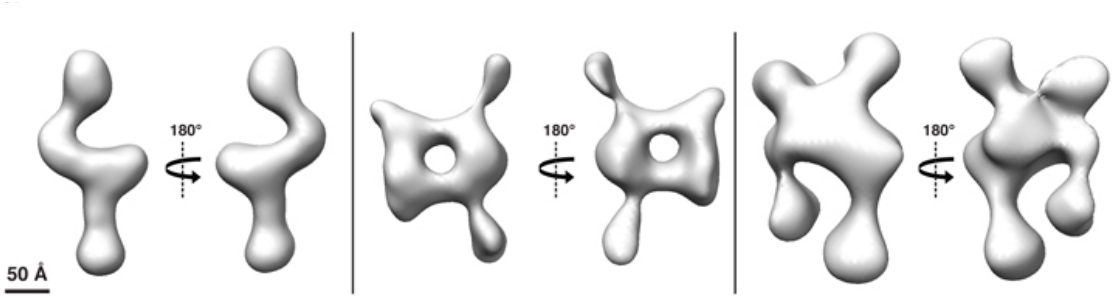

Figure 2-17 2D classification and 3D reconstructions of leptin/LEP-R[D1-D7] projection sub-groups.
a, Sub-group 0° projections from 'STEP 3' (see methods) were individually classified to fine-tune the alignment and facilitate 3D reconstruction by the random conical tilt approach. **b**, 3D reconstructions of binary and quaternary leptin/LEP-R[D1-D7] complexes (Mancour et al., 2012).

Docking of the model in the 3D map shows a very good fit, reinforcing our analysis on the leptin/LEP-R interaction. Furthermore, we produced and analyzed a LEP-R[D1-D7] construct bearing the mutations L503S;L504S at the CHR2, as originally described by Tavernier and colleagues (Iserentant et al., 2005). As expected, incubation of this mutant with leptin did not result in a binary complex formation, and EM analysis showed that there was no additional distinct globular density attached to the region that we attributed to CHR2 (Figure 2-15 g and Figure 2-18). Interestingly, none of the averages from monomeric receptor chains display leptin density at the level of the IgD (D3), located at the base of the flying 'V' architecture (Figure 2-15 d, e). These observations suggest that the CHR2 of LEP-R represents the primary site for leptin binding via a high-affinity interaction, as also supported by our binding thermodynamics data (**Figure 2-10** and Figure 2-11 a, c). Importantly, the liganded monomeric LEP-R chains from both extracellular constructs do not display any variability in the relative disposition of the D4 and D5 domains of CHR2. Class averages from this population reveal a distinct single conformation of the D5-(D6-D7) module with a fixed angle in relation to the membrane-distal domains (Figure 2-17). Thus, leptin binding on CHR2 constrains D5 and the rigidly attached membrane-proximal FnIII domains (D6-D7) in a fixed orientation towards the plane of the membrane.

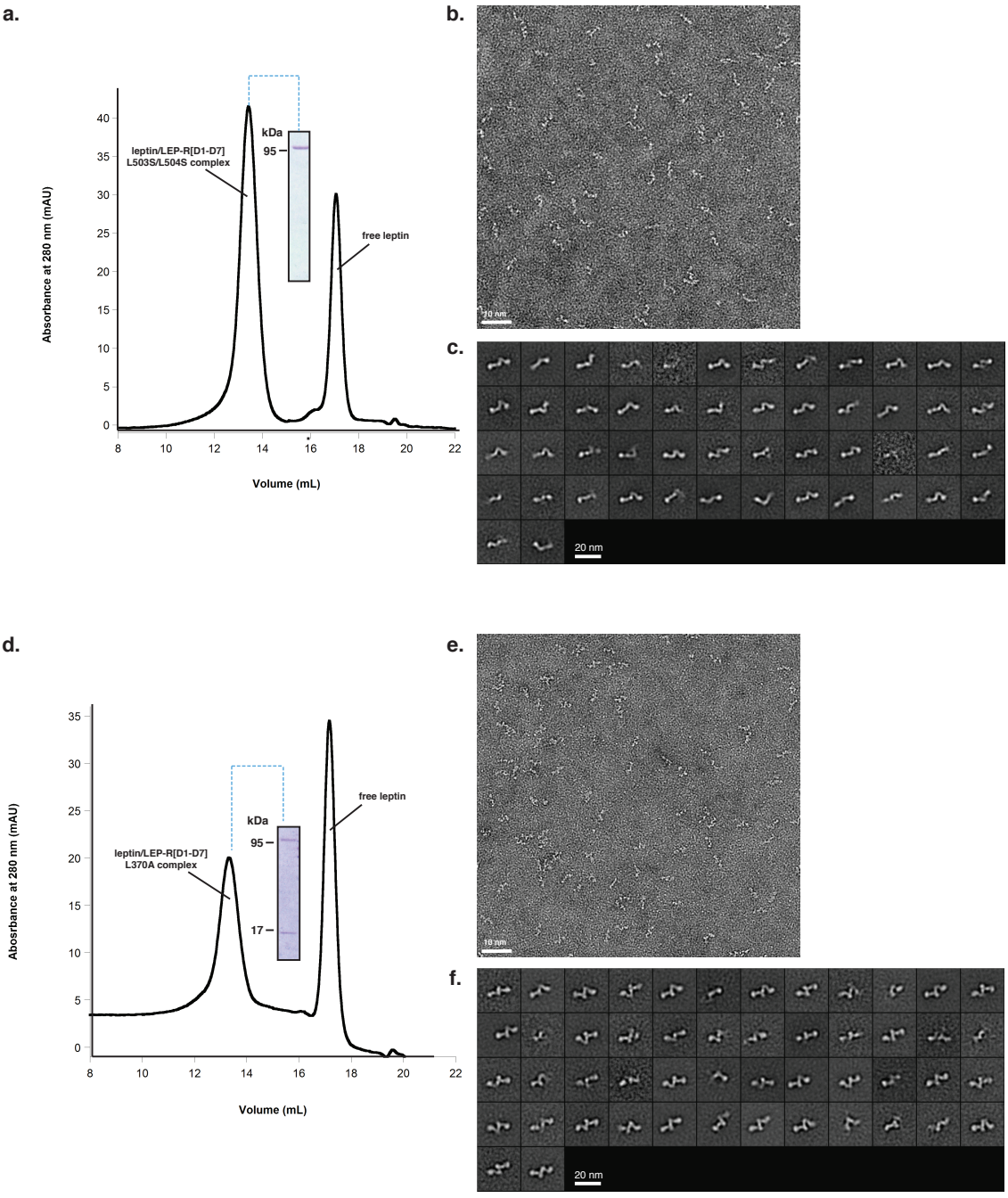

Figure 2-18 Purification and 2D classification of LEP-R[D1-D7] L503S/L504S and L370A mutants after incubation with leptin.

a, SEC of LEP-R[D1-D7]L503S/L504S after incubation with leptin. **b,** Raw image of negative stained sample from the fraction shown in (a). **c,** 6,189 particle projections classified into 50 classes. **d,** SEC of LEP-R[D1-D7]L370A after incubation with leptin. **e,** Raw image of negative stained sample from the fraction shown in (d). **f,** 4,964 particle projections classified into 50 classes (Mancour et al., 2012).

Liganded LEP-R Assembles into 2:2 Quaternary Complex

The majority of leptin/LEP-R complexes in our classification display variable views of dimeric LEP-R chains. A prominent set of class averages reveals a characteristic side view of the complex, where the two LEP-R chains appear to be crossing at the level of the CHR2 module, while both the CHR1 and the membrane-proximal modules remain unengaged (Figure 2-19 a). This interpretation was confirmed by 3D reconstructions and molecular docking, showing that the LEP-R chains cross over to opposite sides at the level of CHR2 and IgD (Figure 2-19 b). In most class averages the two LEP-R chains appear asymmetric, presumably due to the projection angle and distortion of the receptor chains on the carbon support of the EM grid, as was also the case with our study on the gp130/IL6/IL6-R complex (Skiniotis et al., 2005). In support of this notion, averages of relatively few particles in our population show a perfectly symmetric dimeric complex formation (Figure 2-16 and Figure 2-17). Nevertheless, in all projection averages where the two LEP-R chains are clearly distinguished the membrane-proximal domains appear to be constrained and point towards each other (Figure 2-19 a). This conformation reflects the same fixed geometry observed in the liganded monomeric LEP-R chains (Figure 2-19 d-f). In the context of the signaling LEP-R dimer, leptin induced stabilization of CHR2 appears to result in fixing the two membrane-proximal domains towards each other and in close proximity at their C-terminal tips.

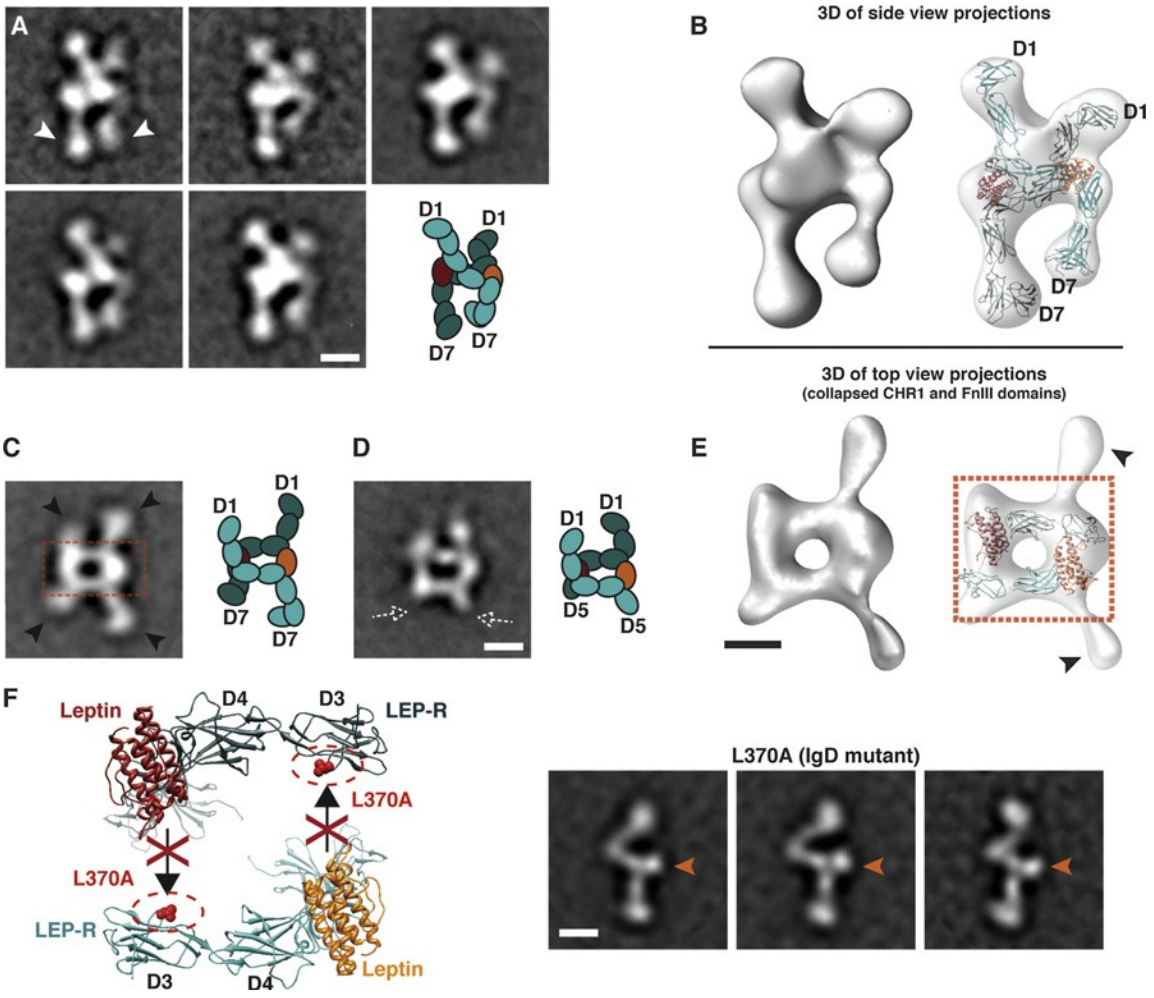

Figure 2-19 Architecture of the Quaternary Leptin/LEP-R Signaling Complex.
a, Two-dimensional class averages of side-view projections reveal the crossover configuration of two LEP-R extracellular chains. The two chains connect at the CHR2 level, while the membrane proximal domains (white arrowheads) point toward each other and arrive in close proximity at their C-terminal tips. **b,** Three-dimensional reconstruction of the leptin/LEP-R side-view projections shown in **(a)**. Flexible docking of two liganded LEP-R chains into the three-dimensional density map shows the complex configuration (right). **c,** Representative two-dimensional class average of a top view of the quaternary leptin/LEP-R [D1-D7] complex. In this type of projections the N-terminal CHR1 and C-terminal FnIII domains are collapsed on the carbon support (black arrowheads). The boxed area shows the rectangular formation that is reminiscent of the anti-parallel gp130/IL-6 or GCSF/GCSF-R interaction. **d,** Representative two-dimensional class average of a top view of the quaternary leptin/LEP-R[D1- D5] complex, as in (**c**). The dashed white arrowheads point to missing densities from the omitted C-terminal domains of the truncated construct, as compared to (c). **e,** Three-dimensional reconstruction from topview leptin/LEP-R[D1-D7] projections shown in (**c**), and docked gp130/IL-6 crystal structure into the central rectangular density of the three-dimensional map (right). **f,** Mutation L370A on the IgD (D3) of LEP-R abolishes leptin binding via epitope III. EM

class averages of this mutant after incubation with leptin reveal only monomeric receptor chains with ligand bound at CHR2 (orange arrows). All scale bars correspond to 5 nm (Mancour et al., 2012).

The 3D reconstruction from the side view particle projections has limited resolution in the plane perpendicular to the electron beam, and thus does not provide adequate detail for elucidating the arrangement between leptin and LEP-R in the context of the dimeric receptor complex. However, an abundant series of class averages reveals a top view of the complex (Figure 2-19c), reminiscent to the top views we characterized in our earlier study of the gp130/IL6/IL6-R complex (Skiniotis et al., 2005). Here, we also recognize a central rectangular formation with a distinct stain accumulation region in the center, suggesting a hole or cavity in this position. Emanating from the rectangle in the LEP-R top view are the projections from membrane-proximal FnIII and N-terminal CHR1 domains that collapse in a distinct fashion on the carbon support (pointed by arrows in Figure 2-19c). The rectangular cap architecture represents the top view of the tetrameric arrangement between leptin and LEP-R that follows the identical topological blueprint of the gp130/IL-6 (Skiniotis et al., 2005) or GCSF/GCSF-R interaction (Tamada et al., 2006). In this arrangement, while epitope II of leptin interacts with the CHR2 (D4-D5) of LEP-R, epitope III engages the IgD (D3) of the second, opposing receptor. This set of interactions, which was also observed in class averages of complexes formed by the truncated LEP-R chains (Figure 2-19d), results in the formation of a closed tetrameric cap with antiparallel subunits of leptin and LEP-R. This organization is further supported by the good fit of the gp130/IL-6 structure (Boulanger et al., 2003b) in the 3D EM reconstruction of the collapsed top view of the leptin/LEP-R complex (Figure 2-19e), and also by the good match between our 2D projections and reprojections of a quaternary 3D model in this arrangement (Figure 2-20).

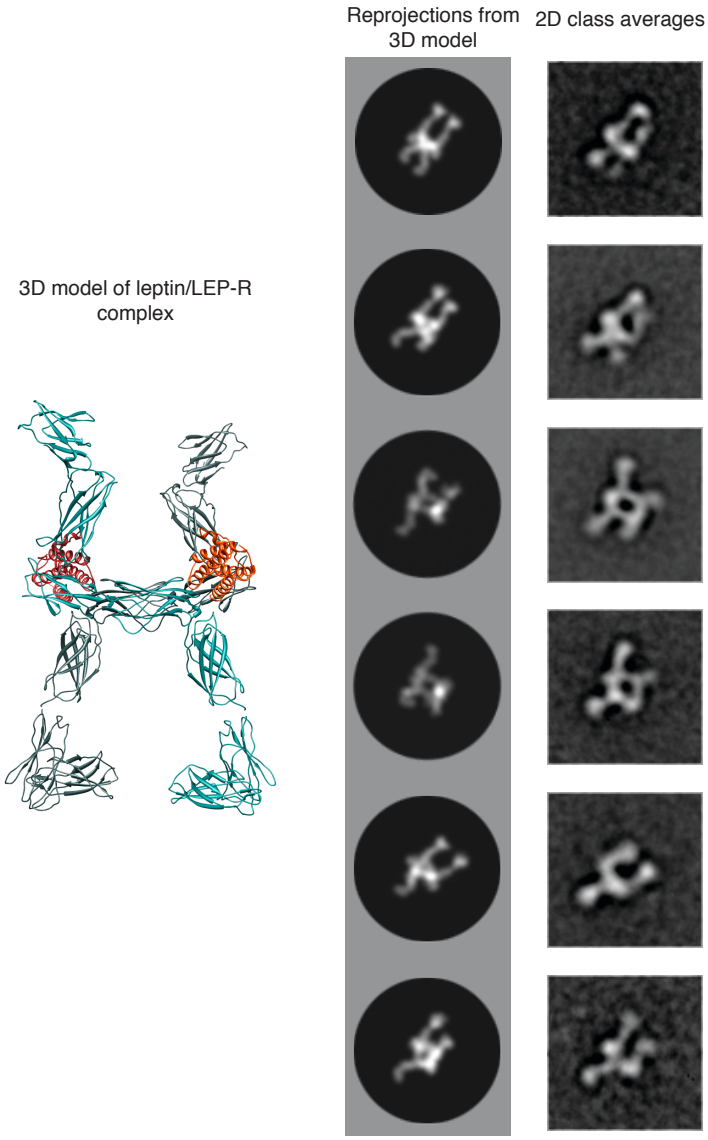

Figure 2-20 Projection comparison.
Comparison between reprojections of the 3D homology model of the quaternary leptin/LEP-R[D1-D7] complex (left) and experimental 2D class averages (right) (Mancour et al., 2012).

To fully confirm this interpretation, we produced and analyzed a LEP-R[D1-D7] construct bearing the IgD mutation L370A, which has been previously shown to abolish leptin signaling (Peelman et al., 2006b). EM analysis of this IgD mutant LEP-R reveals that while it forms the binary complex with leptin through CHR2, it is unable to form the signaling quaternary complex that is based on the interaction of the IgD with epitope III of leptin (Figures 2-19f and 2-18d-f). Thus, the quaternary signaling leptin/LEP-R

complex forms in a 2:2 stoichiometry by following the same organizing principles as gp130/IL6 and GCSF/GCSF-R complexes (Figure 2-21).

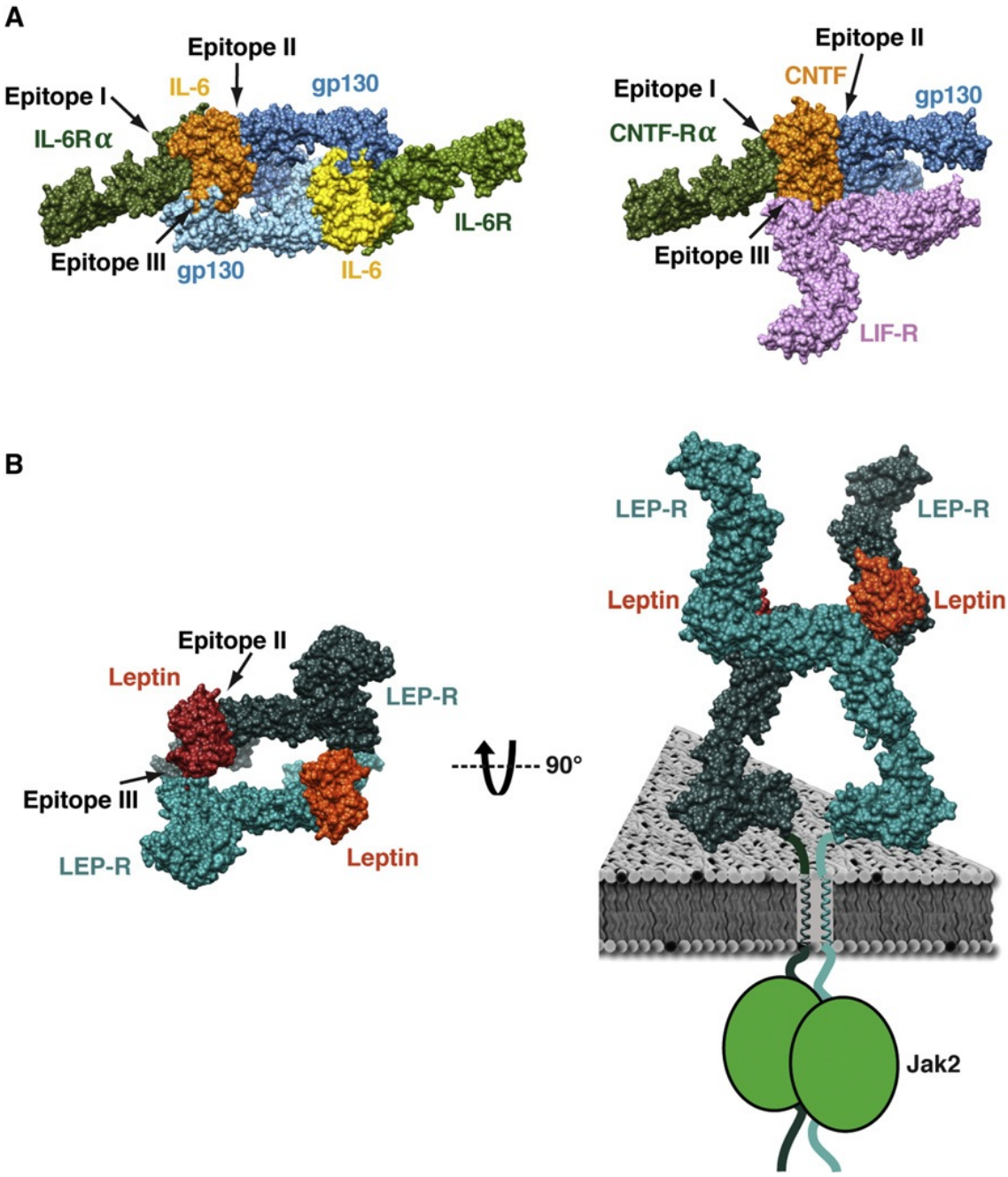

Figure 2-21 Signaling Architecture of Tall Cytokine Receptors.
Receptor organization and ligand epitope usage in the signaling complexes of gp130/IL-6/IL-6Ra (**a, left**), gp130/LIF-R/CNTF/ CNTF-Ra (**a; right**), and leptin/LEP-R (**b, left**). Leptin employs only epitopes II and III to engage the CHR2 and IgD of LEP-R, respectively. Leptin-induced stabilization of each CHR2 in the quaternary complex

results in the constrained and close disposition of the membrane-proximal domains, which likely favors intracellular Jak2 transphosphorylation (**b, right**) (Mancour et al., 2012).

2.5 Discussion

Reduced or deficient leptin signaling causes hyperphagia and morbid obesity in both animals and humans (Zhang et al., 1994), while administration of leptin has been shown to reduce food intake and body weight (Pelleymounter et al., 1995). Paradoxically, most obese patients display elevated levels of leptin, which underlines the so-called "leptin resistance", a term used to describe the failure of high levels of leptin to prevent obesity (Considine et al., 1996; Frederich et al., 1995; Myers et al., 2008). One of the main causes of leptin resistance is the impairment of leptin receptor function and signaling that also results in obesity and associated metabolic diseases (Munzberg et al., 2005; Oswal and Yeo, 2010; Prosnak, 1976; White et al., 1997). For example, the originally described *db/db* obese mice lack the leptin receptor, and they resemble the leptin-deficient *ob/ob* mice (Clement et al., 1998; Friedman and Halaas, 1998; Hummel et al., 1966; Ingalls et al., 1950; Montague et al., 1997). Therefore, the elucidation of the molecular mechanism of leptin receptor activation is a key issue for the design of appropriate therapeutic strategies. Considering the diverse signaling events and significant physiological responses exerted by leptin, both stimulation and inhibition of the leptin receptor have pharmacological applications in disease treatment (Peelman et al., 2006a).

For the present study we employed single-particle EM to characterize the architecture of the entire extracellular LEP-R alone and in complex with leptin. The unliganded extracellular receptor appears highly similar to the crystallographic structures of extracellular regions from gp130 (Xu et al., 2010), LIF-R (Huyton et al., 2007; Skiniotis et al., 2008), and GCSF-R (Tamada et al., 2006) (Figure 2-15). This result is perhaps not unexpected, considering the high sequence similarity and common domain organization of tall cytokine receptors. Nevertheless, this finding reinforces the notion that the overall architecture of tall cytokine receptors is relatively constrained, although the extracellular chains are composed of an array of linker-connected FnIII and Ig-like domains. A puzzling issue however is that crystal structures of gp130 and LIF-R show the same

receptor conformation in the presence and absence of the ligand, with a CHR2 configuration that is similar to the one observed in the recently determined crystal structure of LEP-R CHR2 in complex with a Fab fragment (Carpenter et al., 2012). Here we show that LEP-R displays significant flexibility in the hinge region connecting the D4 and D5 domains composing CHR2, which presumably allows the membrane-proximal domains to assume variable configurations in the absence of ligand. In contrast, leptin binding on CHR2 of LEP-R rigidifies the position of D5, thereby stabilizing the membrane-proximal FnIII domains (D6-D7) in a single conformation (Figure 2-15 d-f). The obtained LEP-R homology model, based on gp130 and LIF-R unliganded crystal structures, fits well in the 3D reconstruction of monomeric LEP-R in complex with leptin (Figure 2-15 c, f). This observation suggests that crystallization conditions may have induced the unliganded receptors to assume the same conformation as in the presence of ligand.

The 2D projection analysis reveals that all monomeric LEP-R chains in the presence of ligand display stable leptin binding on CHR2. This finding indicates that CHR2 is the primary site for leptin binding with a high-affinity interaction, as supported by our ITC experiments and earlier biochemical studies (Fong et al., 1998; Iserentant et al., 2005). Based on the homologous interactions observed for gp130 (Boulanger et al., 2003b) and GCSF-R (Tamada et al., 2006), the LEP-R CHR2 interaction must be maintained through epitope II of leptin, as also supported by mutagenesis studies (Iserentant et al., 2005) (Figure 2-21a).

Similar to the other hematopoietic cytokines, leptin possesses two additional conserved epitopes with the potential to be engaged in receptor binding. 3D reconstructions and modeling suggest that conserved epitope III of leptin is used for engaging the IgD (D3) of the second receptor chain that is juxtaposed in an antiparallel fashion. In the case of gp130 homodimers and heterodimers (e.g., gp130/LIF-R), epitope I is used to engage the CHR of a non-signaling α-receptor (e.g., IL6-Rα or CNTF-Rα) that is required for signaling complex formation (Boulanger et al., 2003b; Skiniotis et al., 2008) (Figure 2-21a). However, the leptin/LEP-R signaling complex does not include a non-signaling α-receptor. This omission has led to the proposal that four LEP-R chains participate in the

signaling complex through the additional engagement of epitope I. This is clearly not the case, as we show here that the signaling complex between leptin and LEP-R forms at a 2:2 stoichiometry, by engaging only leptin epitopes II and III (Figure 2-21 a,b). Curiously, the N-terminal CHR1 of LEP-R does not appear to participate in any interactions, as has also been the case with the CHR1 of LIF-R in the gp130/LIF-R/CNTF/CNTF-Rα complex (Skiniotis et al., 2008). It will thus be interesting to examine whether these regions have a different type of functionality that is independent of signaling.

It is also worth noting that our results explain the absence of observed leptin density interacting with the IgD (D3) in monomeric LEP-R chains. Similarly to the gp130/IL6 system (Boulanger et al., 2003b), the epitope III interaction has undetectably low affinity for LEP-R IgD alone, and is only stabilized by the avidity afforded by the "two-point attachment" between preformed and antiparallel leptin/LEP-R dimeric complexes. In this context, the mode of complex formation is likely cooperative, with leptin binding first to the CHR2 of one LEP-R with a 1:1 stoichiometry, followed by two liganded LEP-Rs engaging at the membrane distal regions (Figure 2-21b).

Earlier work on gp130 and gp130/LIF-R signaling complexes has shown that the membrane-proximal FnIII domains of two juxtaposed receptors bend towards each other to reach the same position at the membrane level (Skiniotis et al., 2005; Skiniotis et al., 2008). Within this family of receptors, LEP-R is the only member possessing two, rather than three, FnIII domains connecting the distal cytokine binding regions to the cell membrane. Perhaps this "handicap" is utilized to differentiate LEP-R in the types of intracellular signaling exerted by the liganded receptor. Nevertheless, we show here that the FnIII 'legs' in the leptin/LEP-R quaternary signaling complex also point towards each other and come in close proximity at their C-terminal tips. For the tall class of cytokine receptor liganded complexes the present study shows that this configuration of the FnIII 'legs' is induced and stabilized by the binding of the cytokine on the flexible CHR. In the absence of ligand, the membrane proximal FnIII domains and the preceding C-terminal domain of CHR appear to behave like rigid rods that assume variable relative orientations in regards to the membrane plane (Figure 2-15a,b). Ligand binding on the CHR fixes the

membrane-proximal domains in a single configuration that facilitates precise and close juxtaposition at the membrane level (Figures 2-15d-e, 2-19a,b, 2-21b).

Our EM studies with full-length gp130 and LIF-R constructs have suggested that the dimeric arrangement of the extracellular membrane-proximal domains was significantly stabilized by the presence of the receptor trans-membrane regions. As has been shown for the erythropoietin receptor, this is likely facilitated by dimerization properties of the receptor single-pass α-helices spanning the membrane (Constantinescu et al., 2001b). It is thus reasonable to assume that LEP-R and most cytokine receptors are preformed non-signaling dimers at the cell membrane. Elegant mutagenesis experiments by Constantinescu et al. (2001) on the erythropoietin receptor have revealed that the exact disposition and pitch of the TM helices is crucial for intracellular signaling (Constantinescu et al., 2001a). Given the leptin-induced stabilization and precise disposition of the membrane-proximal LEP-R regions observed here, we postulate that ligand binding on the membrane-distal regions of receptor dimers is rigidly transmitted towards the receptor trans-membrane helices. This likely represents a common mechanism for cytokine and hormone receptors to stabilize an intracellular conformation that favors Jak trans-phosphorylation.

2.6 Acknowledgements

Data from this chapter is contained in the manuscript “Ligand-Induced Architecture of the Leptin Receptor Signaling Complex” which was published in the *Molecular Cell Journal,* October, 2012. Min Su ensured the proper alignment and instrument running. Hikmat Daghestani co-wrote the paper and co-produced figures. Gerwin Westfield ran the 3D reconstructions and helped with image collection of the D1-D7 complex as well as particle picking. Somnath Dutta helped with collecting images for the D1-D7 construct and picked particles. Steven Chou produced the homology model. Austin Oleskie helped with particle picking of the D1-D7 complex. The LIC vectors were provided by Dr. Clay Brown (LSI) and Krishnapriya Chinnaswamy (LSI) ran the ITC experiments.

2.7 References

Ahima, R.S., Prabakaran, D., Mantzoros, C., Qu, D., Lowell, B., Maratos-Flier, E., and Flier, J.S. (1996). Role of leptin in the neuroendocrine response to fasting. Nature *382*, 250-252.

Bates, S.H., Stearns, W.H., Dundon, T.A., Schubert, M., Tso, A.W., Wang, Y., Banks, A.S., Lavery, H.J., Haq, A.K., Maratos-Flier, E*., et al.* (2003). STAT3 signalling is required for leptin regulation of energy balance but not reproduction. Nature *421*, 856-859.

Baumann, H., Morella, K.K., White, D.W., Dembski, M., Bailon, P.S., Kim, H., Lai, C.F., and Tartaglia, L.A. (1996). The full-length leptin receptor has signaling capabilities of interleukin 6-type cytokine receptors. Proceedings of the National Academy of Sciences of the United States of America *93*, 8374-8378.

Boulanger, M.J., Bankovich, A.J., Kortemme, T., Baker, D., and Garcia, K.C. (2003a). Convergent mechanisms for recognition of divergent cytokines by the shared signaling receptor gp130. Mol Cell *12*, 577-589.

Boulanger, M.J., Chow, D.C., Brevnova, E.E., and Garcia, K.C. (2003b). Hexameric structure and assembly of the interleukin-6/IL-6 alpha-receptor/gp130 complex. Science *300*, 2101-2104.

Bravo, J., and Heath, J.K. (2000). Receptor recognition by gp130 cytokines. The EMBO journal *19*, 2399-2411.

Brown, W.C., DelProposto, J., Rubin, J.R., Lamiman, K., Carless, J., and Smith, J.L. (2011). New ligation-independent cloning vectors compatible with a high-throughput platform for parallel construct expression evaluation using baculovirus-infected insect cells. Protein expression and purification *77*, 34-45.

Carpenter, B., Hemsworth, G.R., Wu, Z., Maamra, M., Strasburger, C.J., Ross, R.J., and Artymiuk, P.J. (2012). Structure of the human obesity receptor leptin-binding domain reveals the mechanism of leptin antagonism by a monoclonal antibody. Structure *20*, 487-497.

Clement, K., Vaisse, C., Lahlou, N., Cabrol, S., Pelloux, V., Cassuto, D., Gourmelen, M., Dina, C., Chambaz, J., Lacorte, J.M*., et al.* (1998). A mutation in the human leptin receptor gene causes obesity and pituitary dysfunction. Nature *392*, 398-401.

Considine, R.V., Sinha, M.K., Heiman, M.L., Kriauciunas, A., Stephens, T.W., Nyce, M.R., Ohannesian, J.P., Marco, C.C., McKee, L.J., Bauer, T.L*., et al.* (1996). Serum immunoreactive-leptin concentrations in normal-weight and obese humans. The New England journal of medicine *334*, 292-295.

Constantinescu, S.N., Huang, L.J., Nam, H., and Lodish, H.F. (2001a). The erythropoietin receptor cytosolic juxtamembrane domain contains an essential, precisely oriented, hydrophobic motif. Mol Cell *7*, 377-385.

Constantinescu, S.N., Keren, T., Socolovsky, M., Nam, H., Henis, Y.I., and Lodish, H.F. (2001b). Ligand-independent oligomerization of cell-surface erythropoietin receptor is mediated by the transmembrane domain. Proc Natl Acad Sci U S A *98*, 4379-4384.

Couturier, C., and Jockers, R. (2003). Activation of the leptin receptor by a ligand-induced conformational change of constitutive receptor dimers. The Journal of biological chemistry *278*, 26604-26611.

Fong, T.M., Huang, R.R., Tota, M.R., Mao, C., Smith, T., Varnerin, J., Karpitskiy, V.V., Krause, J.E., and Van der Ploeg, L.H. (1998). Localization of leptin binding domain in the leptin receptor. Molecular pharmacology *53*, 234-240.

Frank, J., Radermacher, M., Penczek, P., Zhu, J., Li, Y., Ladjadj, M., and Leith, A. (1996). SPIDER and WEB: processing and visualization of images in 3D electron microscopy and related fields. Journal of structural biology *116*, 190-199.

Frederich, R.C., Hamann, A., Anderson, S., Lollmann, B., Lowell, B.B., and Flier, J.S. (1995). Leptin levels reflect body lipid content in mice: evidence for diet-induced resistance to leptin action. Nat Med *1*, 1311-1314.

Friedman, J.M. (1998). Leptin, leptin receptors, and the control of body weight. Nutrition reviews *56*, s38-46; discussion s54-75.

Friedman, J.M., and Halaas, J.L. (1998). Leptin and the regulation of body weight in mammals. Nature *395*, 763-770.

Gainsford, T., Willson, T.A., Metcalf, D., Handman, E., McFarlane, C., Ng, A., Nicola, N.A., Alexander, W.S., and Hilton, D.J. (1996). Leptin can induce proliferation, differentiation, and functional activation of hemopoietic cells. Proc Natl Acad Sci U S A *93*, 14564-14568.

Grigorieff, N. (2007). FREALIGN: high-resolution refinement of single particle structures. J Struct Biol *157*, 117-125.

Halaas, J.L., Gajiwala, K.S., Maffei, M., Cohen, S.L., Chait, B.T., Rabinowitz, D., Lallone, R.L., Burley, S.K., and Friedman, J.M. (1995). Weight-reducing effects of the plasma protein encoded by the obese gene. Science *269*, 543-546.

Hirahara, K., Ghoreschi, K., Laurence, A., Yang, X.P., Kanno, Y., and O'Shea, J.J. (2010). Signal transduction pathways and transcriptional regulation in Th17 cell differentiation. Cytokine Growth Factor Rev *21*, 425-434.

Hummel, K.P., Dickie, M.M., and Coleman, D.L. (1966). Diabetes, a new mutation in the mouse. Science *153*, 1127-1128.

Huyton, T., Zhang, J.G., Luo, C.S., Lou, M.Z., Hilton, D.J., Nicola, N.A., and Garrett, T.P. (2007). An unusual cytokine:Ig-domain interaction revealed in the crystal structure of leukemia inhibitory factor (LIF) in complex with the LIF receptor. Proceedings of the National Academy of Sciences of the United States of America *104*, 12737-12742.

Ingalls, A.M., Dickie, M.M., and Snell, G.D. (1950). Obese, a new mutation in the house mouse. J Hered *41*, 317-318.

Iserentant, H., Peelman, F., Defeau, D., Vandekerckhove, J., Zabeau, L., and Tavernier, J. (2005). Mapping of the interface between leptin and the leptin receptor CRH2 domain. Journal of cell science *118*, 2519-2527.

Kloek, C., Haq, A.K., Dunn, S.L., Lavery, H.J., Banks, A.S., and Myers, M.G., Jr. (2002). Regulation of Jak kinases by intracellular leptin receptor sequences. The Journal of biological chemistry *277*, 41547-41555.

Lee, G.H., Proenca, R., Montez, J.M., Carroll, K.M., Darvishzadeh, J.G., Lee, J.I., and Friedman, J.M. (1996). Abnormal splicing of the leptin receptor in diabetic mice. Nature *379*, 632-635.

Li, W., Lewis-Antes, A., Huang, J., Balan, M., and Kotenko, S.V. (2008). Regulation of apoptosis by type III interferons. Cell Prolif *41*, 960-979.

Lord, G.M., Matarese, G., Howard, J.K., Baker, R.J., Bloom, S.R., and Lechler, R.I. (1998). Leptin modulates the T-cell immune response and reverses starvation-induced immunosuppression. Nature *394*, 897-901.

Ludtke, S.J., Baldwin, P.R., and Chiu, W. (1999). EMAN: semiautomated software for high-resolution single-particle reconstructions. Journal of structural biology *128*, 82-97.

Mistrik, P., Moreau, F., and Allen, J.M. (2004). BiaCore analysis of leptin-leptin receptor interaction: evidence for 1:1 stoichiometry. Analytical biochemistry *327*, 271-277.

Montague, C.T., Farooqi, I.S., Whitehead, J.P., Soos, M.A., Rau, H., Wareham, N.J., Sewter, C.P., Digby, J.E., Mohammed, S.N., Hurst, J.A*., et al.* (1997). Congenital leptin deficiency is associated with severe early-onset obesity in humans. Nature *387*, 903-908.

Morton, G.J., Blevins, J.E., Williams, D.L., Niswender, K.D., Gelling, R.W., Rhodes, C.J., Baskin, D.G., and Schwartz, M.W. (2005). Leptin action in the forebrain regulates the hindbrain response to satiety signals. J Clin Invest *115*, 703-710.

Munzberg, H., Bjornholm, M., Bates, S.H., and Myers, M.G., Jr. (2005). Leptin receptor action and mechanisms of leptin resistance. Cell Mol Life Sci *62*, 642-652.

Murray, P.J. (2007). The JAK-STAT signaling pathway: input and output integration. J Immunol *178*, 2623-2629.

Myers, M.G., Cowley, M.A., and Munzberg, H. (2008). Mechanisms of leptin action and leptin resistance. Annu Rev Physiol *70*, 537-556.

Ohi, M., Li, Y., Cheng, Y., and Walz, T. (2004). Negative Staining and Image Classification - Powerful Tools in Modern Electron Microscopy. Biological procedures online *6*, 23-34.

Oswal, A., and Yeo, G. (2010). Leptin and the control of body weight: a review of its diverse central targets, signaling mechanisms, and role in the pathogenesis of obesity. Obesity (Silver Spring) *18*, 221-229.

Peelman, F., Couturier, C., Dam, J., Zabeau, L., Tavernier, J., and Jockers, R. (2006a). Techniques: new pharmacological perspectives for the leptin receptor. Trends Pharmacol Sci *27*, 218-225.

Peelman, F., Iserentant, H., De Smet, A.S., Vandekerckhove, J., Zabeau, L., and Tavernier, J. (2006b). Mapping of binding site III in the leptin receptor and modeling of a hexameric leptin.leptin receptor complex. The Journal of biological chemistry *281*, 15496-15504.

Peelman, F., Van Beneden, K., Zabeau, L., Iserentant, H., Ulrichts, P., Defeau, D., Verhee, A., Catteeuw, D., Elewaut, D., and Tavernier, J. (2004). Mapping of the leptin binding sites and design of a leptin antagonist. The Journal of biological chemistry *279*, 41038-41046.

Pelleymounter, M.A., Cullen, M.J., Baker, M.B., Hecht, R., Winters, D., Boone, T., and Collins, F. (1995). Effects of the obese gene product on body weight regulation in ob/ob mice. Science *269*, 540-543.

Prosnak, M. (1976). [External gel-filled prosthesis of the breast]. Polski przeglad chirurgiczny *48*, 81-85.

Radermacher, M., Wagenknecht, T., Verschoor, A., and Frank, J. (1987). Three-dimensional reconstruction from a single-exposure, random conical tilt series applied to the 50S ribosomal subunit of Escherichia coli. Journal of microscopy *146*, 113-136.

Ruch, C., Skiniotis, G., Steinmetz, M.O., Walz, T., and Ballmer-Hofer, K. (2007). Structure of a VEGF-VEGF receptor complex determined by electron microscopy. Nat Struct Mol Biol *14*, 249-250.

Skiniotis, G., Boulanger, M.J., Garcia, K.C., and Walz, T. (2005). Signaling conformations of the tall cytokine receptor gp130 when in complex with IL-6 and IL-6 receptor. Nat Struct Mol Biol *12*, 545-551.

Skiniotis, G., Lupardus, P.J., Martick, M., Walz, T., and Garcia, K.C. (2008). Structural organization of a full-length gp130/LIF-R cytokine receptor transmembrane complex. Mol Cell *31*, 737-748.

Summers, M.D., and Anderson, D.L. (1972). Granulosis virus deoxyribonucleic acid: a closed, double-stranded molecule. Journal of virology *9*, 710-713.

Tamada, T., Honjo, E., Maeda, Y., Okamoto, T., Ishibashi, M., Tokunaga, M., and Kuroki, R. (2006). Homodimeric cross-over structure of the human granulocyte colony-stimulating factor (GCSF) receptor signaling complex. Proc Natl Acad Sci U S A *103*, 3135-3140.

Tartaglia, L.A., Dembski, M., Weng, X., Deng, N., Culpepper, J., Devos, R., Richards, G.J., Campfield, L.A., Clark, F.T., Deeds, J.*, et al.* (1995). Identification and expression cloning of a leptin receptor, OB-R. Cell *83*, 1263-1271.

Wang, X., Lupardus, P., Laporte, S.L., and Garcia, K.C. (2009). Structural biology of shared cytokine receptors. Annu Rev Immunol *27*, 29-60.

White, D.W., Wang, D.W., Chua, S.C., Jr., Morgenstern, J.P., Leibel, R.L., Baumann, H., and Tartaglia, L.A. (1997). Constitutive and impaired signaling of leptin receptors containing the Gln --> Pro extracellular domain fatty mutation. Proc Natl Acad Sci U S A *94*, 10657-10662.

Xu, Y., Kershaw, N.J., Luo, C.S., Soo, P., Pocock, M.J., Czabotar, P.E., Hilton, D.J., Nicola, N.A., Garrett, T.P., and Zhang, J.G. (2010). Crystal structure of the entire ectodomain of gp130: insights into the molecular assembly of the tall cytokine receptor complexes. The Journal of biological chemistry *285*, 21214-21218.

Zabeau, L., Defeau, D., Iserentant, H., Vandekerckhove, J., Peelman, F., and Tavernier, J. (2005). Leptin receptor activation depends on critical cysteine residues in its fibronectin type III subdomains. The Journal of biological chemistry *280*, 22632-22640.

Zabeau, L., Defeau, D., Van der Heyden, J., Iserentant, H., Vandekerckhove, J., and Tavernier, J. (2004). Functional analysis of leptin receptor activation using a Janus kinase/signal transducer and activator of transcription complementation assay. Mol Endocrinol *18*, 150-161.

Zhang, F., Basinski, M.B., Beals, J.M., Briggs, S.L., Churgay, L.M., Clawson, D.K., DiMarchi, R.D., Furman, T.C., Hale, J.E., Hsiung, H.M.*, et al.* (1997). Crystal structure of the obese protein leptin-E100. Nature *387*, 206-209.

Zhang, Y., Proenca, R., Maffei, M., Barone, M., Leopold, L., and Friedman, J.M. (1994). Positional cloning of the mouse obese gene and its human homologue. Nature *372*, 425-432.

Chapter 3 Structural Flexibility of the Gi α-helical domain in the μ Opioid Receptor - Gi Complex

3.1 Abstract

The G-protein-coupled receptors (GPCRs) are the largest group of signaling proteins that respond to hormones and neurotransmitters. The fundamental event in GPCR signal transduction is the formation of an active, agonist-bound receptor and G-protein complex. Here, we apply electron microscopy (EM) in order to elucidate the architecture of the μ-opioid receptor (MOR) in complex with its inhibitory G-protein partner, the Gi (Gαiβγ). In comparison with the recent EM study of the β_2AR-Gαs complex, MOR-Gi overall domain organization as well as AH domain conformational flexibility are in striking agreement. We hypothesize that as is the case with β_2AR-Gαs complex, the MOR-Gi α-helical domain will be stabilized in the presence of specific nucleotides such as the pyrophosphate mimic foscarnet (phosphonoformate). 2D averages and 3D reconstructions of the MOR complex are compared to the β_2AR-Gαs complex. The data from these studies reveals structural similarities of two GPCRs-G-protein complexes, signaling through different Gα subunits: β_2AR-Gα through the activating Gαs and μOR through the inhibiting Gαi.

3.2 Introduction

Proteins embedded in the cell membrane, serve as the interface between the extracellular and the intracellular environment of the cell. GPCRs are amongst the largest and most diverse family of proteins that are able to detect extracellular signals such as photons, ions, small organic molecules and protein-ligands (Fredriksson et al., 2003). GPCRs are activated upon ligand binding on their extracellular portion. This results in conformational changes in the receptor's transmembrane region, resulting in the activation of complex intracellular networks and initiating cellular response. Recent advances in obtaining detailed structural information of receptors from this family have

begun to unravel the complicated mechanisms of activation of these transmembrane machineries. In addition, the availability of structures from several GPCRs allows for comparative analysis not only on their three dimensional fold but also in their functional relationship.

Opioid receptors are GPCRs that exert a wide range of actions in the central nervous system such as regulation of pain, euphoria, sedation, and cough suppression, making them important pharmacological targets (Katzung, 2009). Based on their pharmacology and tissue distribution the opioid receptors are grouped into 3 classes, the morphine (μ), vas deferens (δ) and ketocyclazocine (κ) classes (Satoh and Minami, 1995).

MORs can be activated by endogenous peptides such as endorphins and enkephalins (Waldhoer et al., 2004). On the other hand, opioid alkaloids, such as morphine and codeine, and their derivatives bind on MORs and are the most effective in relieving acute and chronic pain. Unfortunately, these medically effective drugs are also highly addictive, contributing to the illicit drug market worldwide and are major contributors to death by intravenous overdose. Therefore, tolerance and dependence are the limiting factors in their clinical efficacy and developing new drugs is of crucial importance to improve human health. MORs can activate a diverse set of downstream signaling and regulatory pathways to mediate both their beneficial and adverse effects (Waldhoer et al., 2004). To initiate intracellular signaling, MORs require the activation of their G-protein counterparts. G-proteins are guanine nucleotide binding proteins that are capable of hydrolyzing the guanosine triphosphate (GTP) to guanine diphosphate (GDP), thus shuffling between active and inactive states, respectively (Coleman and Sprang, 1996). Heterotrimeric G-proteins are composed of 3 types of subunits, the α subunit (39-52kDa), the β subunit (37kDa), and the γ subunit (8kDa), each made by either a different gene or as a result of alternative mRNA splicing. G-proteins are classified based on the identity of the α subunit which is localized to the membrane by a cysteine-linked palmitoyl group (Coleman and Sprang, 1996). The Gα subunits consists of a Ras domain,with a GTP-binding pocket, and a small α-helical bundle domain. The structural characteristics of the Ras domain include a glycine-rich ‘P loop” that surrounds the di- and triphosphate of the guanine nucleotide and two segments termed switch I and switch II. Switch I contains a

conserved arginine and switch II a conserved glutamine and they both change conformation upon GTP hydrolysis (Sprang, 1997). In its inactive state, the α subunit is GDP-bound and has a high affinity for the βγ dimer. When the ligand binds to the receptor, the heterotrimeric G-protein associates with the receptor, GDP is exchanged for GTP within the Gα subunit and heterotrimer dissociates into Gα-GTP and Gβγ. The activated Gα subunit is then able to bind downstream effector proteins and exert its functions (Figure 3-1) (Van Eps et al., 2011). The β subunit and the γ subunit are tightly associated where the γ subunit makes farnesyl or geranylgeranyl contacts to the membrane lipids, localizing the βγ dimer to the membrane (Sprang, 1997). Structural differences between the 5 isoforms of Gβ and the 11 isoforms of Gγ found in mammals could provide selectivity for different GPCRs. Furthermore, the βγ dimer can also have signaling capabilities. For example Gβγ is shown to activate adenylyl cyclase, potassium channels and certain isoform of phospholipase C (Sprang, 1997).

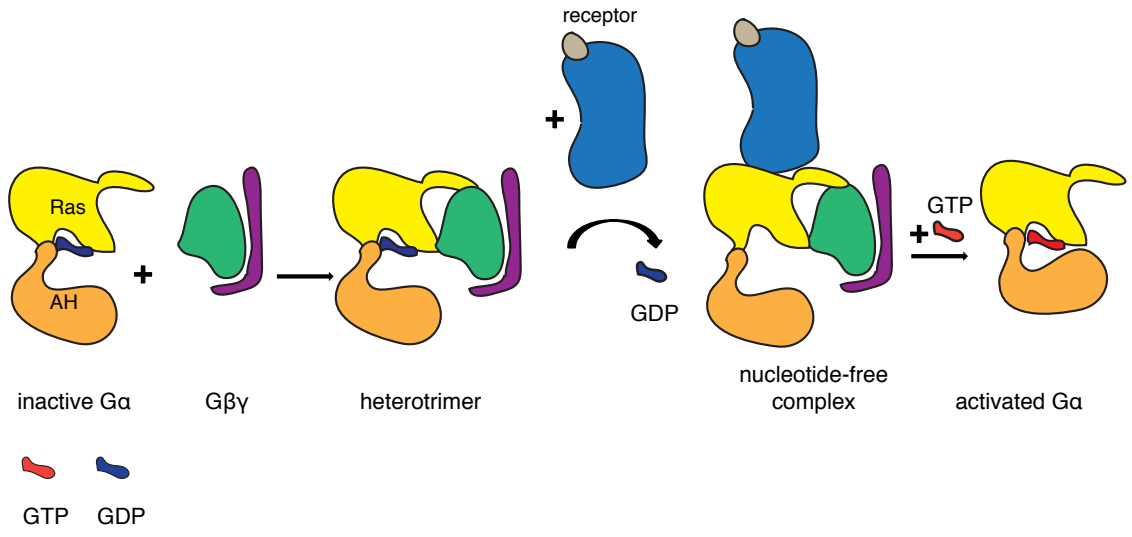

Figure 3-1 The activating cycle of the G-protein accompanied by exchange of GDP for GTP.
The G-protein heterotrimer in its inactive state is composed of Gα and Gβγ and is in GDP bound state. Upon association with the receptor the nucleptide leaves the G-protein and the nucleotide-free receptor-G-protein complex is formed. Gα is activated upon GTP association in place of GDP.

The μ-opioid receptor couples to Gi, the inhibitory subunit of adenylyl cyclase (AC) which is also responsible for exerting its analgesic effect (Raffa et al., 1994). The Gi family of proteins exhibit the most diverse functionalities and can be further subdivided into 5 groups (Gi, o, t, g and z). The α subunit of the G protein undergoes a cycle of nucleotide exchange and hydrolysis when activated by the receptor (Linder, 2004). In addition, members of the Gi family, except Gαz, can be ADP-ribosylated by pertussis toxin at a cysteine residue, near the carboxy terminus, which inhibits their interaction with the receptor (Sprang, 1997). Interestingly, after activation, the receptor is phosphorylated which allows for its coupling to a class of proteins termed arrestins, which can exhibit both signaling and regulatory functions (Shukla et al., 2011).

The structure of MOR in complex with a morphinan antagonist, in its inactive state, was recently solved (Manglik et al., 2012).

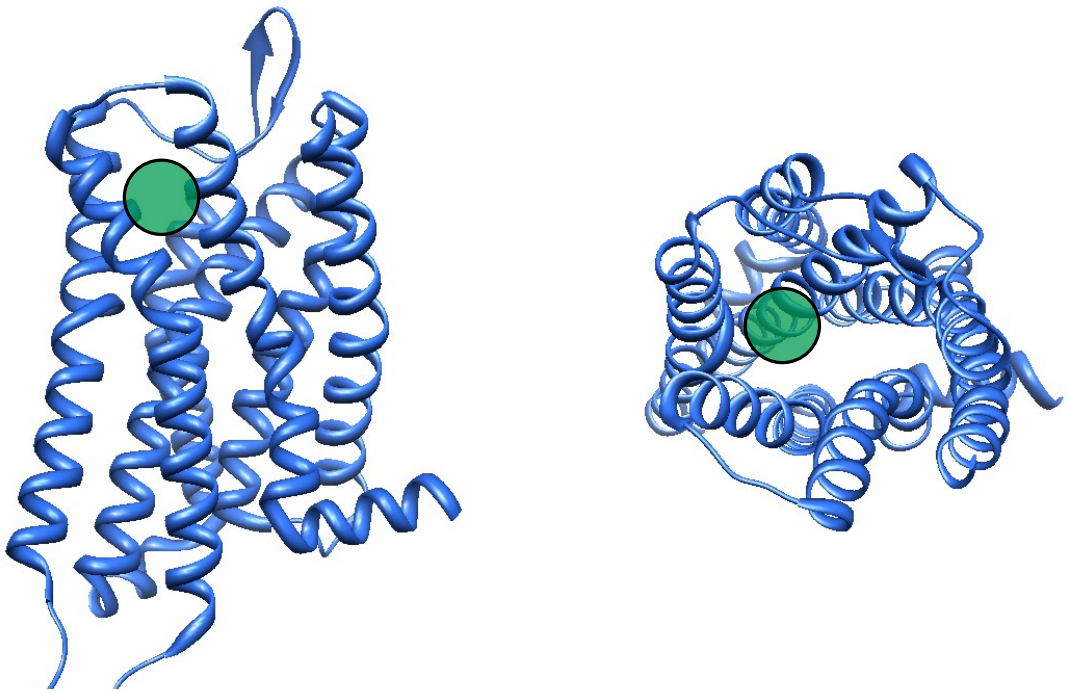

Figure 3-2 Crystal structure of μ-OR bound to morphinan antagonist.
Left – crystal structure of MOR, side view; green circle – bound morphinan antagonist. Right – top view, crystal structure of MOR with bound morphinan antagonist (green circle) (Manglik et al., 2012).

The crystal structures of other opioid receptors have also been determined in their inactive conformations, bound to antagonists (Granier et al., 2012; Wu et al., 2012). In addition, the crystal structure of other GPCRs in their active state have also been determined (Choe et al., 2011; Palczewski et al., 2000; Rasmussen et al., 2011a). Furthermore, a landmark in the field of GPCRs was the successful crystallization of β_2AR in complex with its Gαsβγ-heterotrimer (Rasmussen et al., 2011b). These structural studies have provided important information regarding the association of an activated receptor with its G-protein in the process of signaling

We employed single particle electron microscopy to study the μ-OR-Gi complex aiming to understand overall architecture and dynamics of the mechanism of activation of MORs and facilitate the crystallization of the MOR-Gi signaling complex.

3.3 Experimental procedures

Specimen Preparation and EM Imaging of Negative-stained Samples

T4L-μ-OR-Gi complex was prepared by Aashish Manglik from the lab of Brian Kobilka . All samples were prepared for EM using the conventional negative staining protocol (Ohi et al., 2004). Specimens were imaged at room temperature with Tecnai T12 electron microscope operated at 120kV using low-dose procedures. Images were recorded at magnification of 71,138X and a defocus value of ~1.5 μm on a Gatan US4000 CCD camera. All images were binned (2X2 pixels) to obtain a pixel size of 4.16 å on the specimen level. Tilt-pair particles from 60° and 0° images were selected using WEB (Frank et al., 1996). Particles for only 2D classification of 0° projections were excised using Boxer (part of EMAN 1.9 software suite) (Ludtke et al., 1999).

Two Dimensional Classifications and 3D Reconstructions of T4L-μ-OR-Gi complex.

The 2D reference-free alignment and classification of particle projections were performed using SPIDER (Frank et al., 1996). For all conditions, the 0° particle projections were iteratively classified into multiple classes for 10 cycles. For the 3D reconstructions, in a first step we used the random conical tilt technique (Radermacher and Ruiz, 2006) to determine the initial 3D maps by back-projection of tilted particle images belonging to

individual classes. After a first round of angular refinement, corresponding particles from the untilted images were added, and the images were subjected to another cycle of refinement. Finally, we used FREALIGN for the further refinement of the orientation parameters and reconstruction.

Molecular Modeling

The crystal structure of the T4L-μ-OR (Figure 3-2) was fit into the EM density as a rigid body. Because of the presence of a detergent micelle, which accounted for a significant density surrounding the μ-OR, all docking operations were performed manually with visual inspection of the best fit.

3.4 Results

Overall Architecture of the T4L-μ-OR-Gi complex

In the first part of the analysis we aimed to define the overall architectural organization of the T4L-μ-OR-Gi complex by comparing it to the T4L-β2AR-Gs complex. Initially, the homogeneity of the protein preparation was assessed by visualizing the T4L-MOR-Gi complex by negative stain EM. The negatively stained micrographs revealed a monodisperse particle population (Figure 3-3)

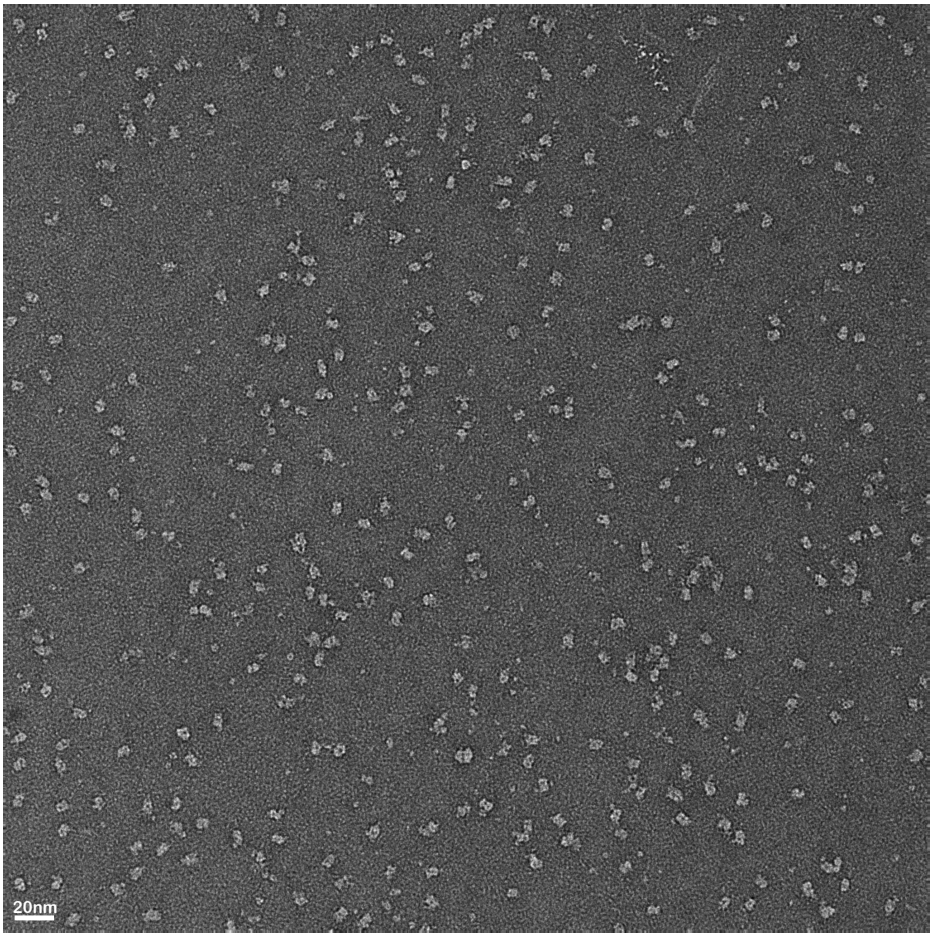

Figure 3-3 Raw image of the T4L-MOR-Gi complex.
The micrograph reveals monodisperse particle projections of the T4L-MOR-Gi complex.

After boxing the particle projections we performed a reference-free 2D classification. Initially, the ~26,000 particle projections were classified into 200 classes (Figure 3-4 a). In a second step, we removed particles from the misaligned classes, and performed a second round of classification with the remaining 19,200 particle projections (Figure 3-4b,c). We divided the particles into both 100 and 50 classes in order to see if number of different populations increases with more classes. Since the 100 and the 50 classes contained similar averages, we decided to use the 50 classes classification for our subsequent analysis where the particle number per class would be higher. The 2D classification revealed characteristic class averages with an overall density displaying striking similarities to the β_2AR-Gαs complex (Westfield et al., 2011).

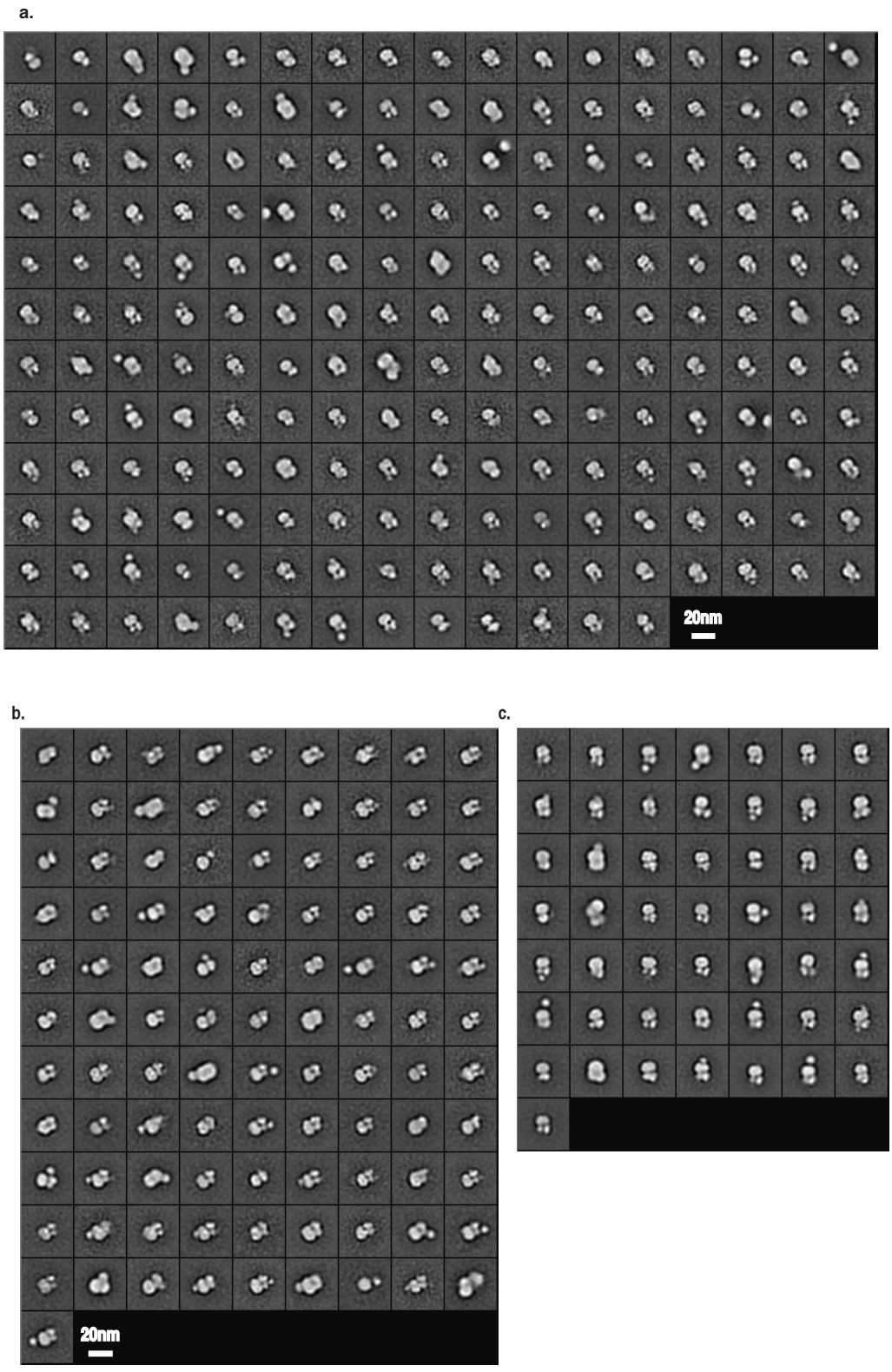

Figure 3-4 2D reference-free alignment and classifications of particle projections of the MOR-Gi complex, using SPIDER.

a, Initial 2D classification of ~26,000 particle projections divided into 200 classes.b, Secondary 2D classification of the remaining ~19,200 particle projections divided into 100 classes. c, Secondary 2D classification of the remaining ~19,200 particle projections divided into 50 classes.

In our initial analysis, we wanted to compare the 2D class averages from the β2AR-Gαs to the 2D class averages of the MOR-Gαi complex side-by-side. Similarly to the β_2AR-Gαs complex, the MOR-Gαi complex also assumed a preferred orientation on the carbon support. This allowed for the side-by-side comparison of the two complexes and aided tremendously in the domain assignment within the MOR-Gi complex (Figure 3-5). Both complexes were similar in size and showed distinct densities that could be easily compared and contrasted, while the domain assignment of β_2AR-Gαs complex served as guidance (Figure 3-5). The distinct features of the class averages in these preferred orientations allowed us to assign the specific features of the complex in its negative stain profile, directly compared to the β2AR-Gαs complex.

As in β_2AR-Gαs complex, the central oval density was attributed to the MOR within the detergent micelle (Figure 3-5a,b- left). In addition, some of the class averages also revealed a small protruding density at one end, which was attributed to the T4 lysozyme (T4L) (Figure 3-4 and 3-5). The engineered T4L served to replace the unstructured extracellular N terminus of the receptor and also helped with the particle alignment. Interestingly, in few of the class averages, the density for the t4L was missing. The reason for the absence of T4L was attributed to the sensitivity of the particles to the out-of-plane tilting, the so-called “rock” and “roll”, unevenness of the carbon support and/or the relative flexibility of the linker between T4L and the receptor. These effects have been well documented in the earlier EM study of the β_2AR-Gs complex (Westfield et al., 2011). Although, the crystal structure of the μ-opioid receptor suggested the existence of a parallel dimer species (Manglik et al., 2012), the overall architecture of the MOR-Gi complex in solution suggests otherwise. Here, the 2D EM class averages reveal only a single T4L density per MOR, conveying only one receptor per complex.

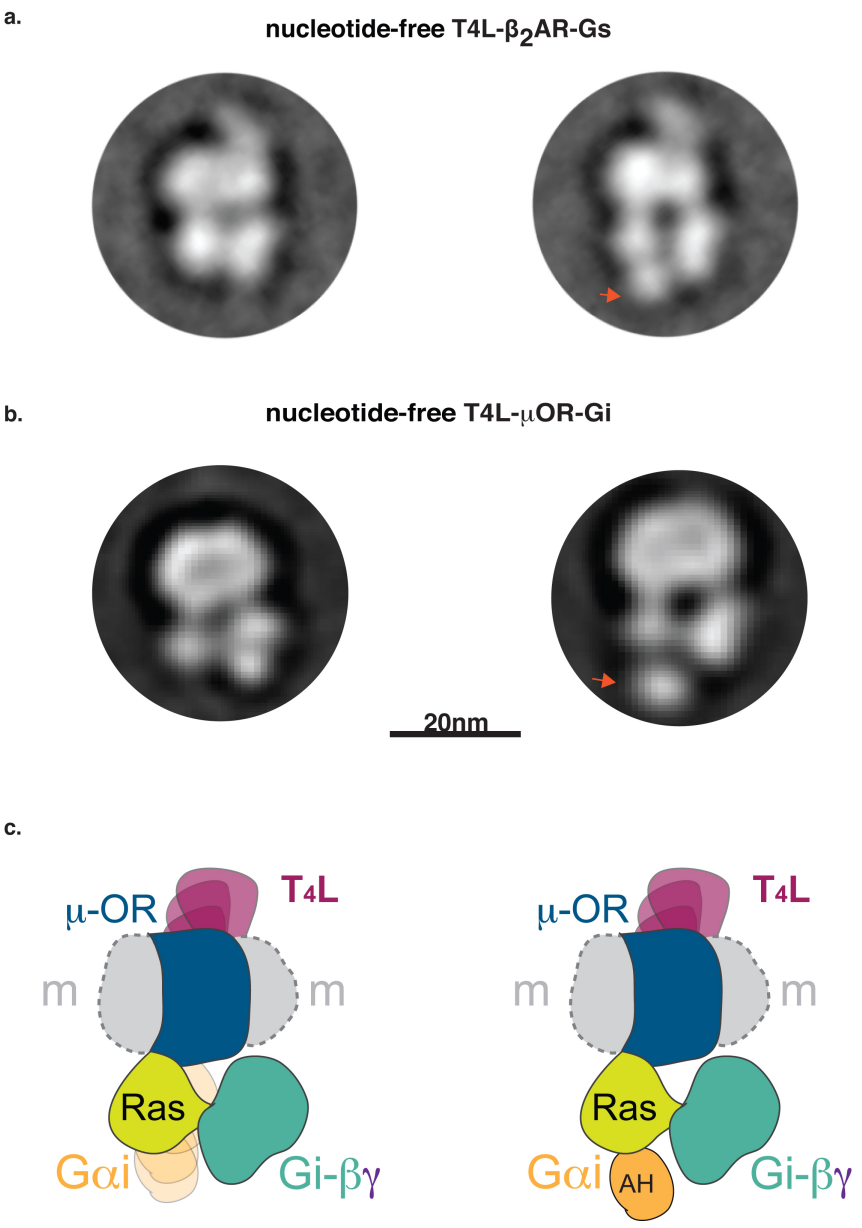

Figure 3-5 Side-by-side comparison 2D class averages from β2AR-Gαs complex and MOR-Gαi complex.
a, representative 2D class averages form the β_2AR-Gs complex in a nucleotide-free state (Courtesy to Gerwin Westfield). b, representative 2D class averages of MOR-Gi complex in a nucleotide-free state .c, model for the domain assignment in the T4L-MOR-Gi complex with both invisible AH domain (left) and fully extended AH domain (right).

As in the case with β2AR-Gαs, the additional density around the receptor is attributed to the large detergent micelle (Rubinstein et al., 2007).

The Gi heterotrimer was assigned to lie on the diametrically opposite side of the T4L with at least 2 domains clearly visible in each of the class averages (Figure 3-5). The domain that visibly made a connection to the micelle of the receptor was attributed to the catalytical domain of the Gi, the Ras domain. Also, in few of the class averages, an extra density was observed protruding below the Ras domain (Figure 3-5). In the crystal structure of the Gi heterotrimer, the AH domain is found in this extended conformation and below the Ras domain (Wall et al., 1995). In addition, the crystal structure of Gαs-GTPγS alone reveals the same positioning of the AH domain (Sunahara et al., 1997). Therefore, we assigned this additional density to the AH domain (Figure 3-5 right panels). This visual variability of the AH domain in the 2D class averages was also observed in the β_2AR-Gαs complex EM studies (Westfield et al., 2011) and was shown to be nucleotide-dependent. Therefore, observing an inherent flexibility in another GPCR-G-protein complex is not surprising. Finally, the Ras domain also appeared to make a contact with an additional larger domain, not connected to the receptor. We assigned this domain as the βγ subunit of Gi heterotrimer (Figure 3-5).

The flexibility of the AH domain of Gi

One of the main aims of these studies was to observe the positioning of the AH domain in the context of the MOR-Gi complex and compare it directly to the β2AR-Gαs complex. Interestingly, careful examination of the 2D class averages from our reference-free alignment also revealed variability in the positioning of the density corresponding to the AH domain with respect to the Ras-like domain (Figure 3-6).

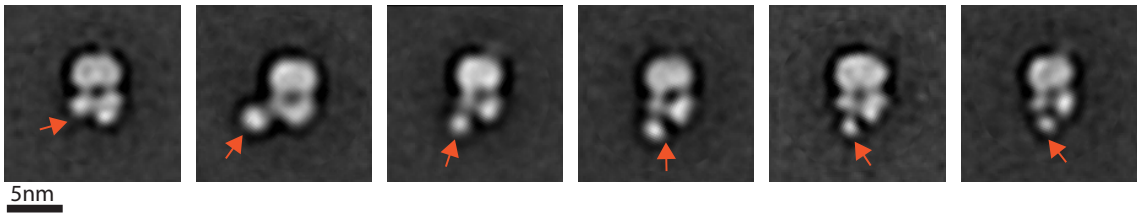

Figure 3-6 Representative class averages displaying the variability in the positioning of the AH domain.

The position of the AH domain with respect to the Ras-like domain and the βγ varied with many degrees. In some class averages the AH domain was not visible likely due to its positioning directly on top of the Ras domain (Figure 3-5 left). In the class averages where the AH domain was clearly visible, it assumed various positions with respect to the βγ dimer (Figure 3-5). The striking similarities between the two GPCR-G-protein complexes of β2AR-Gαs and MOR-Gi, respectively, suggest an inherent flexibility of the AH domain. Further biochemical studies would be needed in order to elucidate the significance of the striking conformational changes of the AH domain in complex with the receptor. The possibility of its role in activation of the G-protein is plausible as previous studies suggest that the AH domain may limit the accessibility of the nucleotides within the nucleotide exchange pocket on the Ras-like domain.

The significance of homo-oligomers of the MORs

Past structural and functional studies have suggested the existence of functional homo-dimers of the MOR (Granier et al., 2012; Manglik et al., 2012). In the case of the β_2AR, it was shown that the existence of such species in the signaling context is unjustified (Rasmussen et al., 2011b; Westfield et al., 2011). EM and other biochemical and biophysical studies support the fact that the detergent micelle contains only one receptor. However, the gel filtration profile of the purified MOR-Gi complex also revealed some higher order species and we wanted to investigate further their overall conformation. We visualized ~4,500 particle projections, which were classified with a reference-free alignment into 100 classes (Figure 3-7a). The class averages displayed both monomers and what appeared as dimers of two complexes next to each other. However, upon closer examination of the classes containing the dimeric species, it appeared that the two detergent micelles, containing the receptors, were positioned at the opposite ends of the particles, forming anti-parallel dimers. (Figure 3-7b). Also, the βγ subunits of one complex seem to be making a 'weak' connection to the micelle of the opposite receptor/complex unit. These anti-parallel conformations were not observed in subsequent purifications and they certainly do not represent functional units. The dimerization artifact could be attributed to hydrophobic groups within the βγ that are

being inserted in the micelles but whether this effect is concentration dependent is not entirely clear at this point.

Interestingly, the MOR was crystallized as a parallel dimer, most likely due to the lowest energy needed for the crystal packing (Manglik et al., 2012). In our first analysis of the MOR-Gi complex, solubilized in detergent and analyzed with negative stain EM, we observed both monomeric and dimeric particles of the MOR-Gi complex. A closer look at the dimeric formations revealed that the dimer is actually formed in an antiparallel fashion (Figure 3-7).The EM analysis provides a view of the complex in solution and an anti-parallel dimer would have no physiological significance. Therefore, the parallel dimer of the receptor observed in the crystal structure may not have any biological significance.

a.

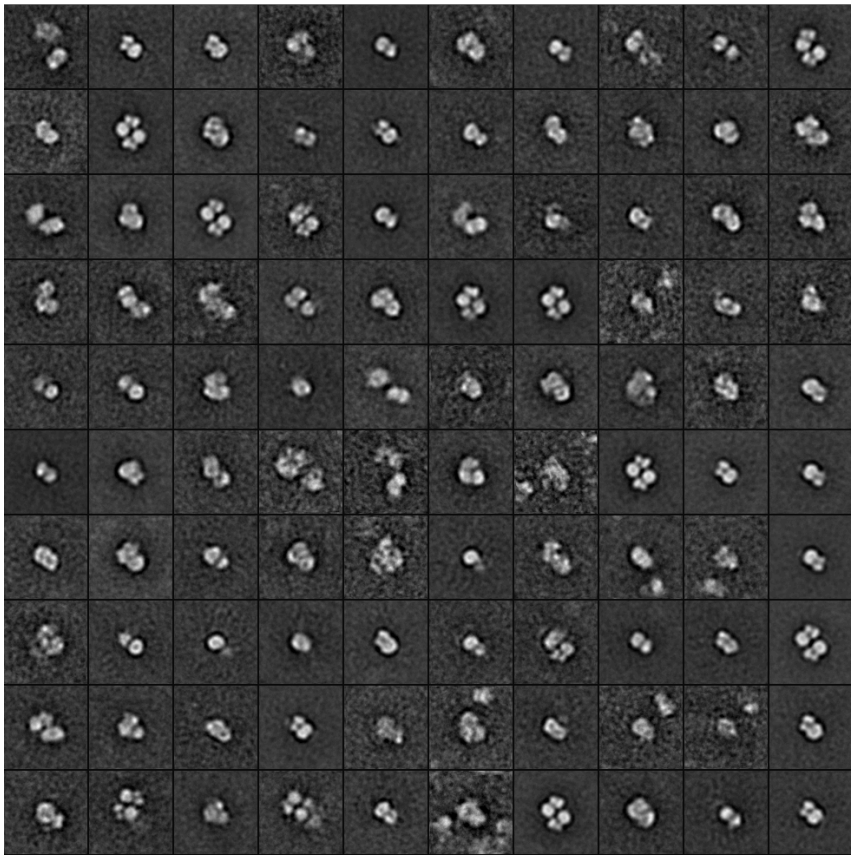

b.

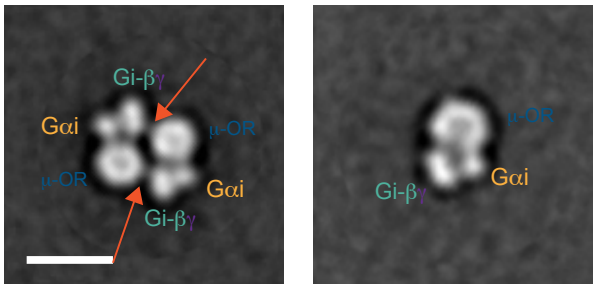

Figure 3-7 The artificial antiparallel dimer of the MOR-Gi complex.
a, 2D class averages of the ~4,500 particle projections grouped into 100 classes. b, side-by-side comparison of the dimer to the monomer also revealing the weak interaction between the βγ subunit of one complex and the receptor micelle of another.

3.5 Three-dimensional reconstructions of the T4L-MOR-Gi complex.

In order to further investigate the overall architecture of the complex and obtain more discernable details of its conformations, we used the random conical tilt approach to calculate a three dimensional reconstruction of the complex. Initial 3D reconstructions were calculated from particle projections either with or without the density corresponding to the AH domain below the Ras-like domain (Figure 3-8 a, b). The initial reconstructions were in excellent agreement to the corresponding 2D class averages (Figure 3-8). Furthermore, the 3D reconstructions where the AH domain is either invisible or positioned below the Ras-like domain, closely resemble the 3D volumes for the β_2AR-Gs complex (Figure 3-8). We could not perform experiments in the presence of nanobody 37 to enhance the density of the AH domain due to time constraints. Nevertheless, our 3D volumes of the MOR-Gi complex are in excellent agreement with the 3D volumes of the β_2AR-Gs complex in the absence of Nb37. In addition, the 3D reconstruction from the population of particle projections with "fully-extended" AH domain, provides enough volume below the Ras-like domain to fully accommodate the AH domain in this region. It should be noted that one of the disadvantages of negative stain is that the proteins lose the hydration shell and collapse on the carbon support. Therefore, the AH domain does not appear to have a designated density protruding either in the front or the back of the 3D reconstructions. More experiments with stabilizing nanobodies or nucleotides are needed to confirm our findings. However, these initial structural studies provide an insight not only into the overall structural similarity of two GPCRs in complex with their

G-proteins but also into the flexibility of the AH domain in the context of the activated receptor.

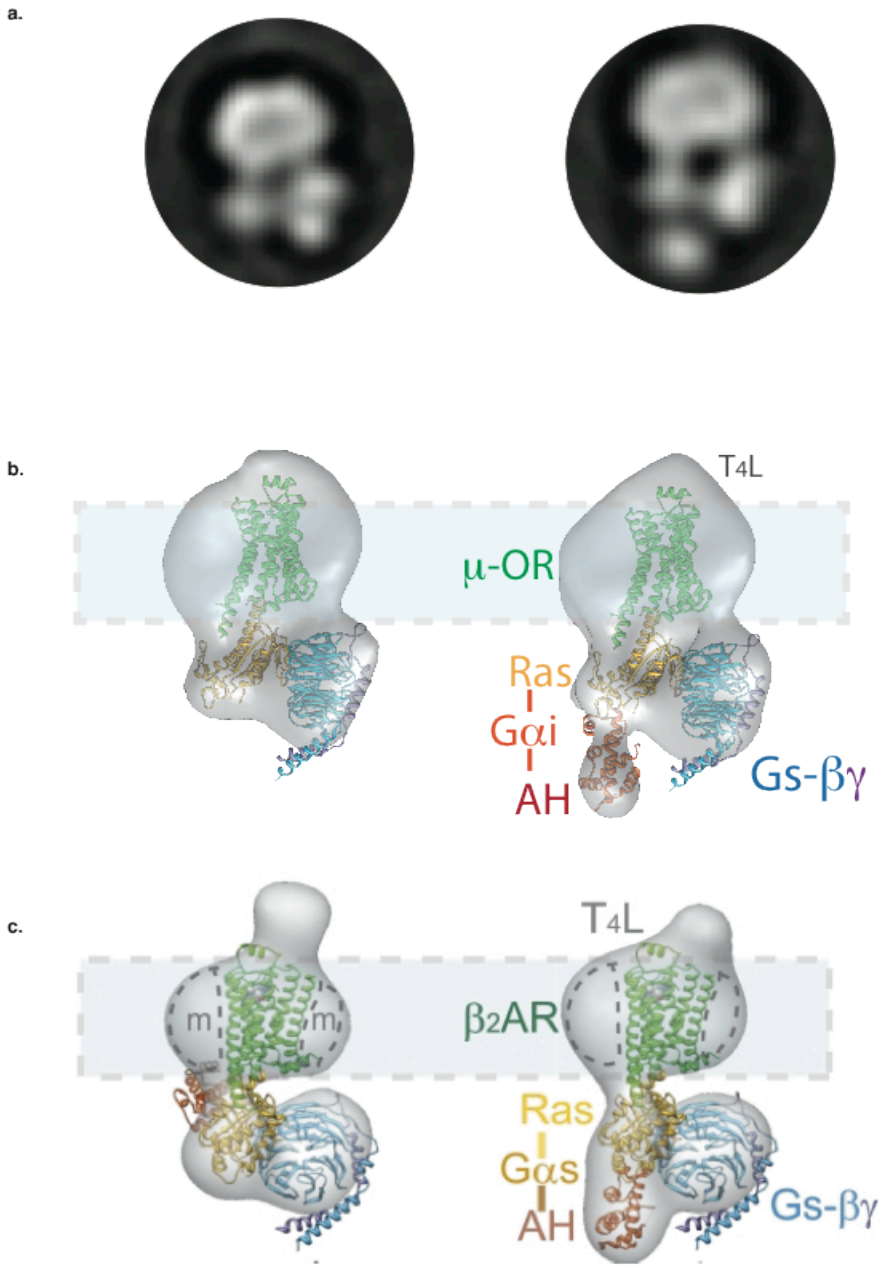

Figure 3-8 Three-dimensional reconstructions of the MOR-Gi complex in a nucleotide-free state.
a, Representative class averages of the corresponding 3D reconstructions in b, of particles in each category to show the variability in the positioning of the AH domain in the nucleotide-free complex. In the reconstruction to the left, the AH domain is not visible because of its flexibility and highly variable particle population. In the reconstruction to

the right, the AH domain is modeled within the EM density and right below the Ras-like domain of Gi, as suggested in the 2D class averages. c., 3D reconstructions of the β_2AR-Gs complex with the docked crystal structure, also displaying the variability in the positioning of the AH domain. (c., Courtesy of Gerwin Westfield).

3.6 Discussion

The EM studies of the MOR-Gi complex provide important insights into the inherent flexibility of AH domains of Gα proteins. The crystal structures are able to provide snapshots of these complexes in certain nucleotide states. However, the flexibility of distinct domains within the complexes that reflect the dynamics of such protein machineries have just begun to unravel. Despite the artifacts from negative staining such as protein dehydration and particle collapse, single particle analysis allows for obtaining new insights into the dynamic features of inherently flexible protein assemblies. Here, we visualized the MOR-Gi complex, embedded in negative stain with EM and applied single particle analysis to elucidate overall domain organization as well as assess the flexibility of the AH domain in the Gαi subunit.

The 2D class averages of MOR-Gi complex and the side-by-side comparison with the β_2AR-Gs complex allowed for the domain assignment. Our analysis revealed striking similarities in the overall architecture of the two GPCS-G-protein complexes, β_2AR-Gs and MOR-Gi (Figure 3-5). As in the case for β2AR-Gs, the 2D class averages revealed a large density in the middle, corresponding to the μ-opioid receptor (MOR) solubilized in detergent. Additionally, an N-terminal T4L was present in some class averages and missing in others. The well documented artifact due to the particle "rock" and "roll" (Westfield et al., 2011) is contributing to this partial visibility in few of our class averages. Moreover, we were able to distinguish the Ras domain from the Gα subunit making its connection to the receptor as well as the variably visible density contributing to the AH domain of Gαi. The globular density contributing the AH domain was observed in various positions compared to the Ras domain, from fully extended to completely positioned on the Ras domain (Figure 3-6).

Interestingly, the AH domain displays the same inherent flexibility in a nucleotide-free state of the complex as is the case with β_2AR-Gs complex. The mode of action of Gs and

Gi proteins is different in how they are able to effect downstream signaling targets either activating adenylyl cyclase (AC) or inhibiting AC, respectively. Indeed, the flexibility of the AH domain was inferred in a study with the activated rhodopsin-Gi complex as a change in the relative distances between the Ras and AH (Van Eps et al., 2011). In addition, the EM and Deuterium exchange coupled to mass spectrometry (DXMS) studies of the β_2AR-Gαs complex (Westfield et al., 2011) (Chung et al., 2011) also support the receptor-induced AH domain flexibility of the G-protein. In addition, it has been demonstrated that the nucleotide exchange lies in the interface between the Ras and the AH domain (Sprang, 1997) and the presence of the AH domain slows the nucleotide exchange (Markby et al., 1993). Therefore, it is possible that the AH domain may play a role in the activation of the G-protein by capturing the nucleotide when positioned directly on Ras or providing an escape route of the nucleotide when in fully-extended conformation. Furthermore, the functional role of the structural flexibility of the AH domains could be explained in the context of bacterial toxins' mode of action as well as nucleotide analogs able to lock the AH domain in certain positions and affect downstream signaling.

More studies need to be conducted to fully assess the effect of different nucleotides on the stability of MOR-Gi complex. However, considering the conservation in the overall domain organization between β_2AR-Gs and MOR-Gi, as well as the inherent flexibility of the AH domains in both Gs and Gi subunits, it is likely that the flexibility of the AH domain in the MOR-Gi complex would be affected by nucleotide analogs in a similar manner. For example, it is suggested that the binding of PPi-mimic foscarnet substitutes for the binding of the α- and β- phosphates in GDP. (Westfield et al., 2011). In addition, only foscarnet is able to stabilize the AH domain on Ras by acting as a ligand fragment in the nucleotide binding pocket (Westfield et al., 2011). If the activating mechanisms of MOR-Gi and β_2AR-Gs are indeed similar, one would expect to find the AH domain of Gi being stabilized on the Ras domain in the presence of foscarnet which presumably interacts with the nucleotide binding pocket on Ras, trapping the Gα subunit in a certain conformation.

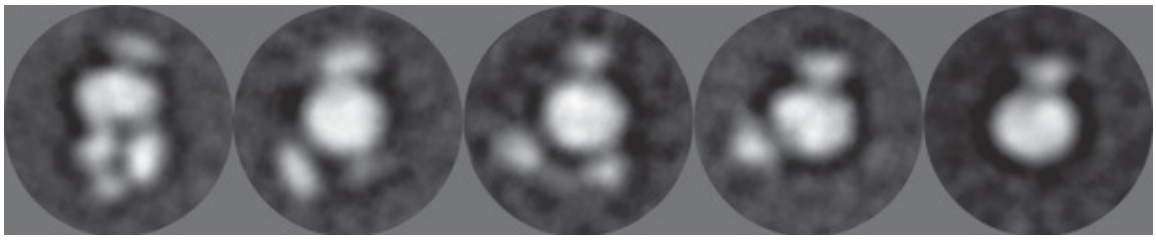

Figure 3-9 Different dissociation states of the β2AR-Gs complex in the presence of 1uM GTPγS.
Left is fully intact complex, right - fully dissociated G-protein hetertrimer (Courtesy of Gerwin Westfieled).

In contrast to PPi and foscarnet, the non-hydrolyzable GTP analog, GTPγS would be expected to mimic bound GTP and lead to dissociation of the G-protein from the receptor. This was the case for β_2AR-Gαs complex (Westfield et al., 2011).

To facilitate obtaining a high-resolution structure of the MOR-Gi complex, we will also investigate the effect of nanobodies on complex stabilization. The nanobodies are clonable variable domains of heavy chain only antibodies that can be obtained by immunizing a Llama with purified GPCR-G-protein complexes (Rasmussen et al., 2011a). Nanobody 35 (Nb35) was found to bind at the interface of Gα and Gβγ stabilizing the complex and facilitating the crystallization the receptor-G-protein complex. More importantly, Nb35 did not interfere with the stability of the AH domain (Rasmussen et al., 2011b; Westfield et al., 2011).

The single particle EM analyses of GPCR-G-Protein complexes serve as a tool to gain important insights into dynamic changes taking place upon receptor activation or nucleotide exchange in the G-protein. In addition, the EM studies allow for the capturing of transient state snapshots of the complex which otherwise may not be present in the crystal structure and thus help reveal mechanism of action.

Acknowledgements

The T4L-μ-opioid receptor Gi complex was purified by Aashish Manglik from the Kobilka Lab.

References

Choe, H.W., Kim, Y.J., Park, J.H., Morizumi, T., Pai, E.F., Krauss, N., Hofmann, K.P., Scheerer, P., and Ernst, O.P. (2011). Crystal structure of metarhodopsin II. Nature *471*, 651-655.

Chung, K.Y., Rasmussen, S.G., Liu, T., Li, S., DeVree, B.T., Chae, P.S., Calinski, D., Kobilka, B.K., Woods, V.L., Jr., and Sunahara, R.K. (2011). Conformational changes in the G protein Gs induced by the beta2 adrenergic receptor. Nature *477*, 611-615.

Coleman, D.E., and Sprang, S.R. (1996). How G proteins work: A continuing story. Trends in biochemical sciences *21*, 41-44.

Frank, J., Radermacher, M., Penczek, P., Zhu, J., Li, Y., Ladjadj, M., and Leith, A. (1996). SPIDER and WEB: processing and visualization of images in 3D electron microscopy and related fields. Journal of structural biology *116*, 190-199.

Fredriksson, R., Lagerstrom, M.C., Lundin, L.G., and Schioth, H.B. (2003). The G-protein-coupled receptors in the human genome form five main families. Phylogenetic analysis, paralogon groups, and fingerprints. Molecular pharmacology *63*, 1256-1272.

Granier, S., Manglik, A., Kruse, A.C., Kobilka, T.S., Thian, F.S., Weis, W.I., and Kobilka, B.K. (2012). Structure of the delta-opioid receptor bound to naltrindole. Nature *485*, 400-404.

Katzung, B.G. (2009). Basic & clinical pharmacology. (New York, Lange Medical Books/McGraw Hill).

Linder, M.E. (2004). the Gi Family and Heterotrimeric G Proteins. Encyclopedia of Biological Chemistry *2*, 181-185.

Ludtke, S.J., Baldwin, P.R., and Chiu, W. (1999). EMAN: semiautomated software for high-resolution single-particle reconstructions. Journal of structural biology *128*, 82-97.

Manglik, A., Kruse, A.C., Kobilka, T.S., Thian, F.S., Mathiesen, J.M., Sunahara, R.K., Pardo, L., Weis, W.I., Kobilka, B.K., and Granier, S. (2012). Crystal structure of the micro-opioid receptor bound to a morphinan antagonist. Nature *485*, 321-326.

Markby, D.W., Onrust, R., and Bourne, H.R. (1993). Separate GTP binding and GTPase activating domains of a G alpha subunit. Science *262*, 1895-1901.

Ohi, M., Li, Y., Cheng, Y., and Walz, T. (2004). Negative Staining and Image Classification - Powerful Tools in Modern Electron Microscopy. Biological procedures online *6*, 23-34.

Palczewski, K., Kumasaka, T., Hori, T., Behnke, C.A., Motoshima, H., Fox, B.A., Le Trong, I., Teller, D.C., Okada, T., Stenkamp, R.E.*, et al.* (2000). Crystal structure of rhodopsin: A G protein-coupled receptor. Science *289*, 739-745.

Radermacher, M., and Ruiz, T. (2006). Three-dimensional reconstruction of single particles in electron microscopy image processing. Methods in molecular biology *319*, 427-461.

Raffa, R.B., Martinez, R.P., and Connelly, C.D. (1994). G-protein antisense oligodeoxyribonucleotides and mu-opioid supraspinal antinociception. European journal of pharmacology *258*, R5-7.

Rasmussen, S.G., Choi, H.J., Fung, J.J., Pardon, E., Casarosa, P., Chae, P.S., Devree, B.T., Rosenbaum, D.M., Thian, F.S., Kobilka, T.S*., et al.* (2011a). Structure of a nanobody-stabilized active state of the beta(2) adrenoceptor. Nature *469*, 175-180.

Rasmussen, S.G., DeVree, B.T., Zou, Y., Kruse, A.C., Chung, K.Y., Kobilka, T.S., Thian, F.S., Chae, P.S., Pardon, E., Calinski, D*., et al.* (2011b). Crystal structure of the beta2 adrenergic receptor-Gs protein complex. Nature *477*, 549-555.

Satoh, M., and Minami, M. (1995). Molecular pharmacology of the opioid receptors. Pharmacology & therapeutics *68*, 343-364.

Shukla, A.K., Xiao, K., and Lefkowitz, R.J. (2011). Emerging paradigms of beta-arrestin-dependent seven transmembrane receptor signaling. Trends in biochemical sciences *36*, 457-469.

Sprang, S.R. (1997). G protein mechanisms: Insights from structural analysis. Annual review of biochemistry *66*, 639-678.

Sunahara, R.K., Tesmer, J.J., Gilman, A.G., and Sprang, S.R. (1997). Crystal structure of the adenylyl cyclase activator Gsalpha. Science *278*, 1943-1947.

Van Eps, N., Preininger, A.M., Alexander, N., Kaya, A.I., Meier, S., Meiler, J., Hamm, H.E., and Hubbell, W.L. (2011). Interaction of a G protein with an activated receptor opens the interdomain interface in the alpha subunit. Proceedings of the National Academy of Sciences of the United States of America *108*, 9420-9424.

Waldhoer, M., Bartlett, S.E., and Whistler, J.L. (2004). Opioid receptors. Annual review of biochemistry *73*, 953-990.

Wall, M.A., Coleman, D.E., Lee, E., Iniguez-Lluhi, J.A., Posner, B.A., Gilman, A.G., and Sprang, S.R. (1995). The structure of the G protein heterotrimer Gi alpha 1 beta 1 gamma 2. Cell *83*, 1047-1058.

Westfield, G.H., Rasmussen, S.G., Su, M., Dutta, S., DeVree, B.T., Chung, K.Y., Calinski, D., Velez-Ruiz, G., Oleskie, A.N., Pardon, E*., et al.* (2011). Structural flexibility of the G alpha s alpha-helical domain in the beta2-adrenoceptor Gs complex. Proceedings of the National Academy of Sciences of the United States of America *108*, 16086-16091.

Wu, H., Wacker, D., Mileni, M., Katritch, V., Han, G.W., Vardy, E., Liu, W., Thompson, A.A., Huang, X.P., Carroll, F.I.*, et al.* (2012). Structure of the human kappa-opioid receptor in complex with JDTic. Nature *485*, 327-332.

Chapter 4 Discussion and Future Directions

4.1 The leptin receptor system

Despite the wealth of biochemical information on the leptin/leptin receptor signaling pathway, there are many structure-function related questions that remain to be resolved. The structural information concerning the atomic detail of the ligand binding domain alone and in complex with leptin is still lacking. Increasing the resolution of structures for this interaction could also lead to development of small molecule agonists and antagonist that can modulate leptin signaling. Additionally, it is still not well understood how ligand binding at the extracellular side of the receptor instigates intracellular signaling. The details regarding the transmission of structural information through the membrane are still lacking. Because LepR relies on intracellularly bound JAK2s for signaling, obtaining structural information about the ligand-receptor-kinase complex is crucial for our understanding not only of leptin-LepR system but also for the whole family of cytokine receptors.

Crystallization trials

The gene for LepR was discovered and cloned about seventeen years ago by Tartaglia and colleagues (Tartaglia et al., 1995). Yet, since then, very limited information regarding the structure of the leptin/LepR complex has become available. Because LepR is an integral membrane protein, its solubilization and purification have proven to be very difficult. In addition, the lack of posttranslational modification mechanisms in bacterial cells such as glycosylation, proteolytic maturation of the overexpressed protein or limited capacity for the formation of disulfide bridges have also contributed to the difficult recombinant production of LepR (Kamionka, 2011). Insect cells and Baculovirus expression systems have emerged as a novel tool for production of recombinant proteins

with the necessary posttranslational modifications (Becker-Pauly and Stocker, 2011). However, the quantities of the recombinant expressed proteins and their solubilization can still pose challenges for the crystallographic studies.

Portions of the extracellular domains of other members of the class I cytokine receptors have been successfully crystallized. For example the N-terminal five domains of LIF-R in complex with LIF have been crystallized, revealing an addition LIF-receptor interaction within the Ig-like domain (Huyton et al., 2007). The structure of the ligand interacting domains of GCSF-R in complex with GCSF was also solved (Tamada et al., 2006). In addition the entire ecto domain of the gp130 was successfully crystallized (Xu et al., 2010). These crystallographic studies give precedent for the crystallization of parts or the entire the region of LepR.

Flexible regions

The EM negative stain studies on the full length extracellular LepR revealed a flexible hinge, at the level of CHR2 which is stabilized upon ligand binding. Moreover, long linkers at the very N-terminus as well as within the CHR1 putative module could also present potential sites of flexibility. Receptor's sequence analysis and homology modeling contribute to this hypothesis. In fact, sequence analysis of LepR reveals long linkers at the N-terminal region of the receptor that are not attributed to any domain. There are ~40 residues between the end of the signal sequence and the first putative domain of the CHR1 module. Additionally, a stretch of 57 residues divides the distance between the two CHR1 domains within the first module (Figure 4-1). Furthermore, the 2D class averages from both full length and truncated extracellular LepR display increased "fuzziness" at the very N-terminal tips, also suggesting flexibility in these regions.

Protein engineering can help alleviate the problem of flexibility by adding more conformational constraints and rigidity in the receptor. Engineering of shorter constructs lacking the flexible regions may aid in the stabilization of the protein and thus enhance

the chances of its crystallization. For this purpose, constructs lacking the entire CHR1 module and one composed only of the CHR2 and IgD could be further examined. Preliminary data from the designing, cloning and expression of the CHR-IgD protein construct is already available (Figure 4-2).

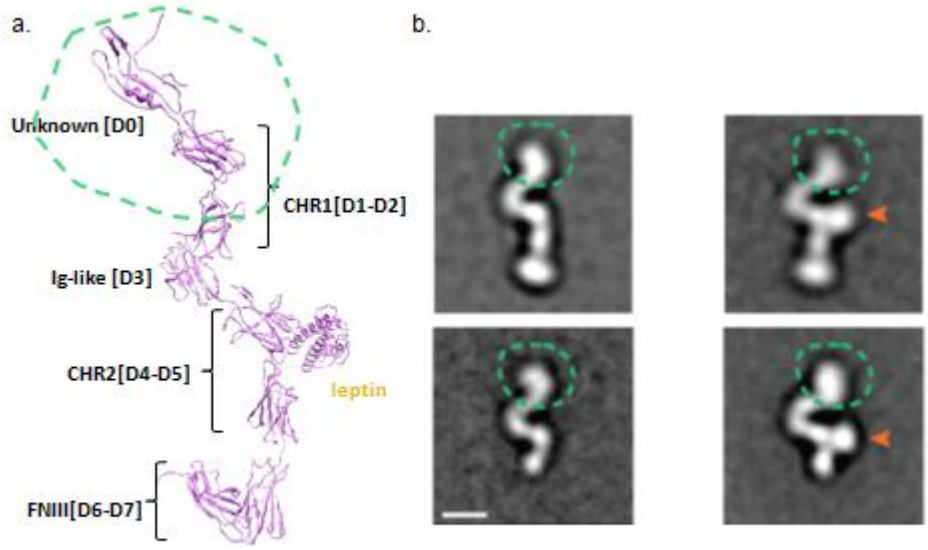

Figure 4-1 a, Homology model of the entire extracellular domain of LepR and 2D class averages of both full length and truncated extracellular Lep-R.
a., Homology model of the entire ecto domain of LepR; all seven domain D1-D7 are modeled according to known structures of the same family of receptors. The first 57 residues, termed D0, are also modeled to a random crystal structure in the PDB (Courtesy of Steven Z. Chou). b, class averages of full length extracellular and truncated LepR where green circles represent flexible regions.

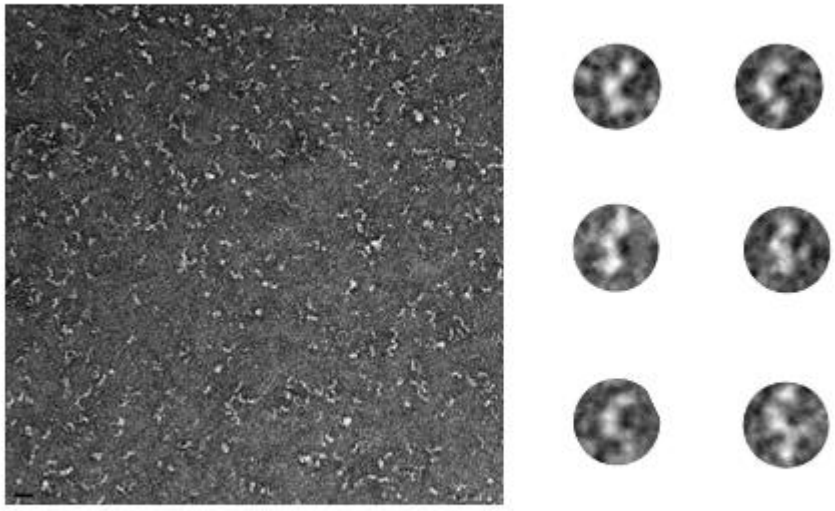

Figure 4-2 Raw images of purified CHR2/IgD construct.

Raw images from negatively stained particles from the purified protein reveal a homogeneous population of monodispersed particles with the characteristic kink at the level of CHR2 domain. In addition, the optimized protocol for the purification of the full length extracellular LepR is also applicable for the shorter constructs, allowing for the production of large quantities of protein that are also needed for the crystallization trials.

Heterogeneity

In addition, our analysis of the leptin/LepR complex consistently revealed complexes composed of two receptor chains and two ligands and a very small population (~15%) of single receptor chains bound to leptin. Because of the dynamical process of these interactions and the shape of the molecules, we were never able to separate the two populations with any biophisical method. Furthermore, it is possible that the monomer-dimer heterogeneity is not present at higher protein concentrations.

Previous mutagenesis studies on the ligand binding domain of the leptin receptor define important functional residues that play roles in leptin binding and LepR activation (Iserentant et al., 2005; Peelman et al., 2006). Precisely, a mutation (L503A) within the CHR2 domain of the receptor completely abolishes leptin binding while a (L370A) within the Ig-like domain leads only to an impaired ability to activate downstream signaling. Interestingly, in the EM studies of the leptin receptor signaling complex, the L370A mutant is still able to bind leptin, thus, stabilizing the hinge region at the CHR2 while unable to form the quaternary complex. The L370A mutant can be useful in the crystallization of the complex by creating a homogeneous population of binary complexes consisting of one receptor chain bound to one leptin.

Furthermore, adding a leucine zipper at the C-terminus of the extracellular portion of the receptor could create a homogeneous population of the quaternary signaling complex. An engineered GCN4 coiled-coil will aid in the stabilization of the quaternary complex by

not allowing the dissociation due to the weaker interaction of epitope 3 of leptin and the Ig-like on the receptor. The design and cloning of this construct is already in progress.

Longer constructs of the LepR

The recent EM studies of the extracellular leptin receptor signaling complex provide important insights into the mechanism of activation upon binding of leptin. Previous biochemical studies suggests that the receptor exists a preformed dimer and binding of ligand induces conformational changes that result in activation of downstream signaling (Devos et al., 1997; Zabeau et al., 2005).We hypothesize that the receptor exists as a preformed dimer at the plasma membrane. Upon leptin binding at the extracellular side, a conformational change on the receptor is transmitted through the membrane and allows for the precise positioning of intracellulary bound JAK2s to transphosphorylate and activate downstream signaling. The EM studies of the extracellular LepR clearly demonstrated that the extracellular LepR exists as a monomer and it dimerizes upon ligand binding. Therefore, it will be interesting to examine further whether the dimerization interface can be attributed to the transmembrane helices or the intracellular receptor tails. For this purpose, longer receptor constructs will aid in the analysis. Moreover, reconstitution of the full-length receptor in the presence of the ligand and the Janus kinase could provide invaluable insights onto how the kinase gets activated. In addition, an in vitro reconstitution of all the components of the signaling machinery could also provide more clues onto how transmembrane receptors translate ligand-induced structural information through the membrane to instigate downstream signaling.

4.2 The μ-opioid receptor - Gαi complex system

In both the β2AR-Gαs and the μ-OR-Gαi complexes, the AH domain of the α subunit of their respective G-protein seems to possess an inherent flexibility. The flexibility of the AH domain can be implicated in the activation mechanism of the G-protein. Because G-proteins play a central role in signal transduction and mediate the extracellular signaling

through the largest family of receptors, the GPCRs, they are poised for further examination.

The flexibility of the α-helical domain of the G-protein

Crystal structures of G-proteins reveal important insights into their activation mechanism. Conformational changes can be exerted within three regions, termed Switch I-III, which lie within the Ras domain and Switch I connects the Ras to the AH domain (Sprang, 1997). The nucleotide exchange occurs at the interface between the Ras and the AH domain and it is presumably dependable on their uncoupling. In fact, it was demonstrated that the rate of nucleotide exchange is slowed in the presence of AH domain suggesting the role of the AH domain in the activation of the G-protein (Markby et al., 1993). Additionally, experiments with chimeric Gα subunits from plant G-proteins showed that the more disordered AH domain contributes to higher basal activity (Jones et al., 2011). In other words, a more extended conformation, where the AH domain is further away from the Ras domain, provides for more accessibility of the nucleotide to be shuffled in and out. Moreover, in the crystal structure of the β_2AR-Gαs complex, the βγ subunit does not interact with the receptor where the Gαs contacts the receptor with both its N- and C-termini (Rasmussen et al., 2011). A snapshot of the G-protein bound to the receptor in its nucleotide-free state also reveals the displacement of the AH domain away from Ras thereby, suggesting their dissociation and exposing the nucleotide binding pocket. Aside from the structural information about the AH domain in the crystal structure of the β2AR-Gαs complex, past biochemical and biophysical studies also have revealed the flexibility of the AH domain. In one study, the author applied double electron-electron resonance spectroscopy and measured the change in probes between the Ras and the AH domains in Gαi. Interestingly, the increase in distance between the two domains corresponded with nucleotide release (Van Eps et al., 2011). In hydrogen deuterium exchange studies, the solvent accessibility at the Ras-AH domain increases upon receptor binding (Chung et al., 2011). Thus, it appears that upon receptor activation the AH domain moves away exposing the nucleotide binding pocket. Moreover, the single

particle EM studies of the β2AR-Gαs complex also revealed that the conformation of the AH domain undergoes from being stabilized on the Ras domain in the more inactive state, to becoming more flexible in a fully extended orientation in active state. In fact, the MOR-Gi complex also exhibits flexibility of the AH domain. It seems likely that the separation of the AH domain from Ras is correlated to release of nucleotide in all of the above mentioned studies.

AH domain as a drug target

G-proteins have a high degree of sequence similarities with the greatest conservation being within the Ras, particularly the switch regions, and the least conservation within the AH domain (Dohlman and Jones, 2012). The EM studies of the MOR-Gi complex were able to reveal and confirm the previously suggested flexibility of the AH domain of Gαi. In addition, it has been demonstrated that the presence of the AH domain slows the nucleotide exchange within the α subunit (Markby et al., 1993). Interestingly, the crystal structure of a plant G-protein that is structurally similar to its mammalian counterparts, reveals a self-activating function attributed to the intrinsic disorder within the AH domain (Jones et al., 2011). Therefore, it is possible that the AH domain plays an important role in the activation of the G-protein, making it a potential drug target.

The sequence variability within the AH domains makes them attractive pharmacological targets for finding small molecules that can bind to unique residues and potentially modulate signaling. In addition, finding potential downstream binding partners that uniquely interact with the AH domain of the Gα could also provide new modes of regulation of G-protein signaling.

Thus, recent advances in structural biology provide new opportunities for developing novel therapeutics not limited only to the receptors. With the growing understanding the role of the AH domain on the activity of the G-proteins come new possibilities for influencing signal regulation.

4.3 Concluding remarks

The investigation of the signaling complex between leptin and its receptor with electron microscopy has provided important insights in the activation mechanism not only for the leptin system but also for the rest of the class I cytokine members. The structural analysis from electron microscopy allowed for the visualization of the flexible regions on the leptin receptor, specifically at the CHR2 domain, which are stabilized upon ligand binding. In addition, the stoichiometry of the complex which was a matter of debate for a long time was also deduced. Most importantly, the electron microscopy allowed for the observation of transient states of the proteins, forming the signaling complex. Here, a technique such as x-ray crystallography could have provided only a snapshot of the mechanism. Yet, detailed and high resolution structural information between the ligand and receptor binding domain could provide very useful information for the development of novel therapeutics. Thus, further investigation with x-ray crystallography and/or high-throughput screening for potential drugs is needed to gain more understanding on how the leptin signaling can be modulated.

The electron microscopy studies of the MOR-Gi complex will not only aid in the crystallization efforts of the complex but also extend the previous observations of the flexible nature of the AH domain. A crystal structure of the MOR-Gi complex would undoubtedly provide a high resolution information about the AH domain interaction with the rest of the complex. However, further studies regarding the AH domain can also shed light into development of novel therapeutics. Small molecule and protein-protein interaction studies would be an invaluable addition to our further understanding of the mechanism of action of G-proteins.

4.4 References

Becker-Pauly, C., and Stocker, W. (2011). Insect Cells for Heterologous Production of Recombinant Proteins. Biol Inspir Syst *2*, 197-209.

Chung, K.Y., Rasmussen, S.G., Liu, T., Li, S., DeVree, B.T., Chae, P.S., Calinski, D., Kobilka, B.K., Woods, V.L., Jr., and Sunahara, R.K. (2011). Conformational changes in the G protein Gs induced by the beta2 adrenergic receptor. Nature *477*, 611-615.

Devos, R., Guisez, Y., Van der Heyden, J., White, D.W., Kalai, M., Fountoulakis, M., and Plaetinck, G. (1997). Ligand-independent dimerization of the extracellular domain of the leptin receptor and determination of the stoichiometry of leptin binding. The Journal of biological chemistry *272*, 18304-18310.

Dohlman, H.G., and Jones, J.C. (2012). Signal activation and inactivation by the Galpha helical domain: a long-neglected partner in G protein signaling. Science signaling *5*, re2.

Huyton, T., Zhang, J.G., Luo, C.S., Lou, M.Z., Hilton, D.J., Nicola, N.A., and Garrett, T.P. (2007). An unusual cytokine:Ig-domain interaction revealed in the crystal structure of leukemia inhibitory factor (LIF) in complex with the LIF receptor. Proceedings of the National Academy of Sciences of the United States of America *104*, 12737-12742.

Iserentant, H., Peelman, F., Defeau, D., Vandekerckhove, J., Zabeau, L., and Tavernier, J. (2005). Mapping of the interface between leptin and the leptin receptor CRH2 domain. Journal of cell science *118*, 2519-2527.

Jones, J.C., Duffy, J.W., Machius, M., Temple, B.R., Dohlman, H.G., and Jones, A.M. (2011). The crystal structure of a self-activating G protein alpha subunit reveals its distinct mechanism of signal initiation. Science signaling *4*, ra8.

Kamionka, M. (2011). Engineering of therapeutic proteins production in Escherichia coli. Current pharmaceutical biotechnology *12*, 268-274.

Markby, D.W., Onrust, R., and Bourne, H.R. (1993). Separate GTP binding and GTPase activating domains of a G alpha subunit. Science *262*, 1895-1901.

Peelman, F., Iserentant, H., De Smet, A.S., Vandekerckhove, J., Zabeau, L., and Tavernier, J. (2006). Mapping of binding site III in the leptin receptor and modeling of a hexameric leptin.leptin receptor complex. The Journal of biological chemistry *281*, 15496-15504.

Rasmussen, S.G., DeVree, B.T., Zou, Y., Kruse, A.C., Chung, K.Y., Kobilka, T.S., Thian, F.S., Chae, P.S., Pardon, E., Calinski, D*., et al.* (2011). Crystal structure of the beta2 adrenergic receptor-Gs protein complex. Nature *477*, 549-555.

Sprang, S.R. (1997). G protein mechanisms: Insights from structural analysis. Annual review of biochemistry *66*, 639-678.

Tamada, T., Honjo, E., Maeda, Y., Okamoto, T., Ishibashi, M., Tokunaga, M., and Kuroki, R. (2006). Homodimeric cross-over structure of the human granulocyte colony-stimulating factor (GCSF) receptor signaling complex. Proceedings of the National Academy of Sciences of the United States of America *103*, 3135-3140.

Tartaglia, L.A., Dembski, M., Weng, X., Deng, N., Culpepper, J., Devos, R., Richards, G.J., Campfield, L.A., Clark, F.T., Deeds, J*., et al.* (1995). Identification and expression cloning of a leptin receptor, OB-R. Cell *83*, 1263-1271.

Van Eps, N., Preininger, A.M., Alexander, N., Kaya, A.I., Meier, S., Meiler, J., Hamm, H.E., and Hubbell, W.L. (2011). Interaction of a G protein with an activated receptor opens the interdomain interface in the alpha subunit. Proceedings of the National Academy of Sciences of the United States of America *108*, 9420-9424.

Xu, Y., Kershaw, N.J., Luo, C.S., Soo, P., Pocock, M.J., Czabotar, P.E., Hilton, D.J., Nicola, N.A., Garrett, T.P., and Zhang, J.G. (2010). Crystal structure of the entire ectodomain of gp130: insights into the molecular assembly of the tall cytokine receptor complexes. The Journal of biological chemistry *285*, 21214-21218.

Zabeau, L., Defeau, D., Iserentant, H., Vandekerckhove, J., Peelman, F., and Tavernier, J. (2005). Leptin receptor activation depends on critical cysteine residues in its fibronectin type III subdomains. The Journal of biological chemistry *280*, 22632-22640.

Appendix A

Structural Studies of Isobutyryl Co-A Mutase Fusion – A G-protein Chaperone

*This project has been in collaboration with Ruma Banerjee's Lab at University of Michigan.

Isobutyryl-CoA mutase (ICM) is a radical enzyme that uses Coenzyme B12 to catalyze carbon skeleton rearrangements. It is a $\alpha_2\beta_2$-heterotetramer that catalyzes the rearrangement of isobutyryl-CoA to n-butyryl-CoA.

The Banerjee Lab has shown that ICM is fused to the P-loop GTP-ase in >70 bacteria and named this protein Isobutyryl Co-A Mutase Fusion (IcmF). Structural information about the domain organization and interdomain interaction in this newly discovered protein is lacking. I have been exploring these interactions using purified protein of the holo complex of IcmF using negative stain EM.

I investigated different constructs of the complex, in the presence of different nucleotides and performed reference-free alignment on all samples (Figure A 1-6).

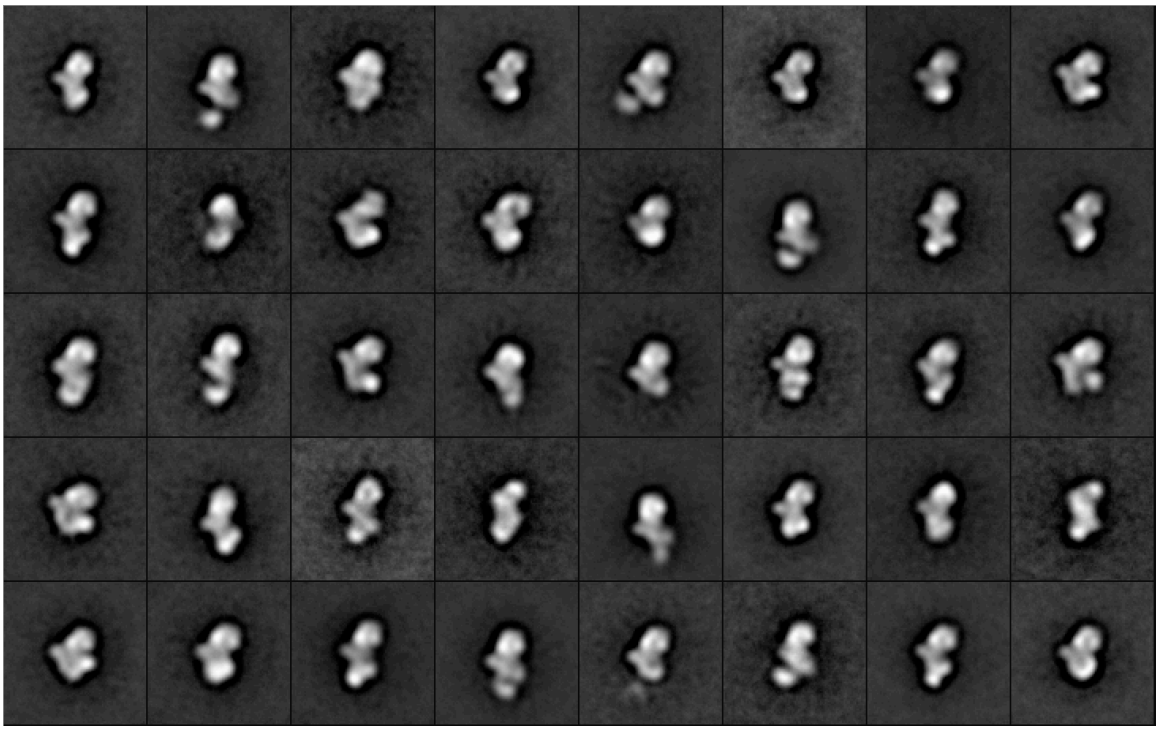

Figure A 1 Reference-free alignment of the holo ICMF complex.
19,515 particle projections classified into 40 classes.

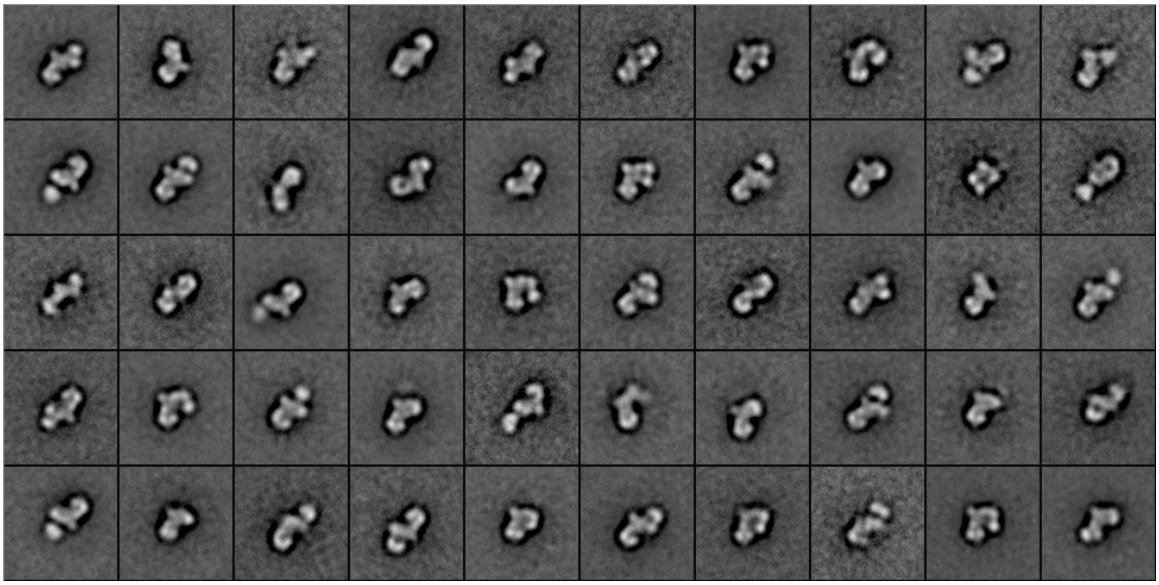

Figure A 2 Reference-free alignment of Apo-IcmF – 4,688 particle projections split into 50 classes

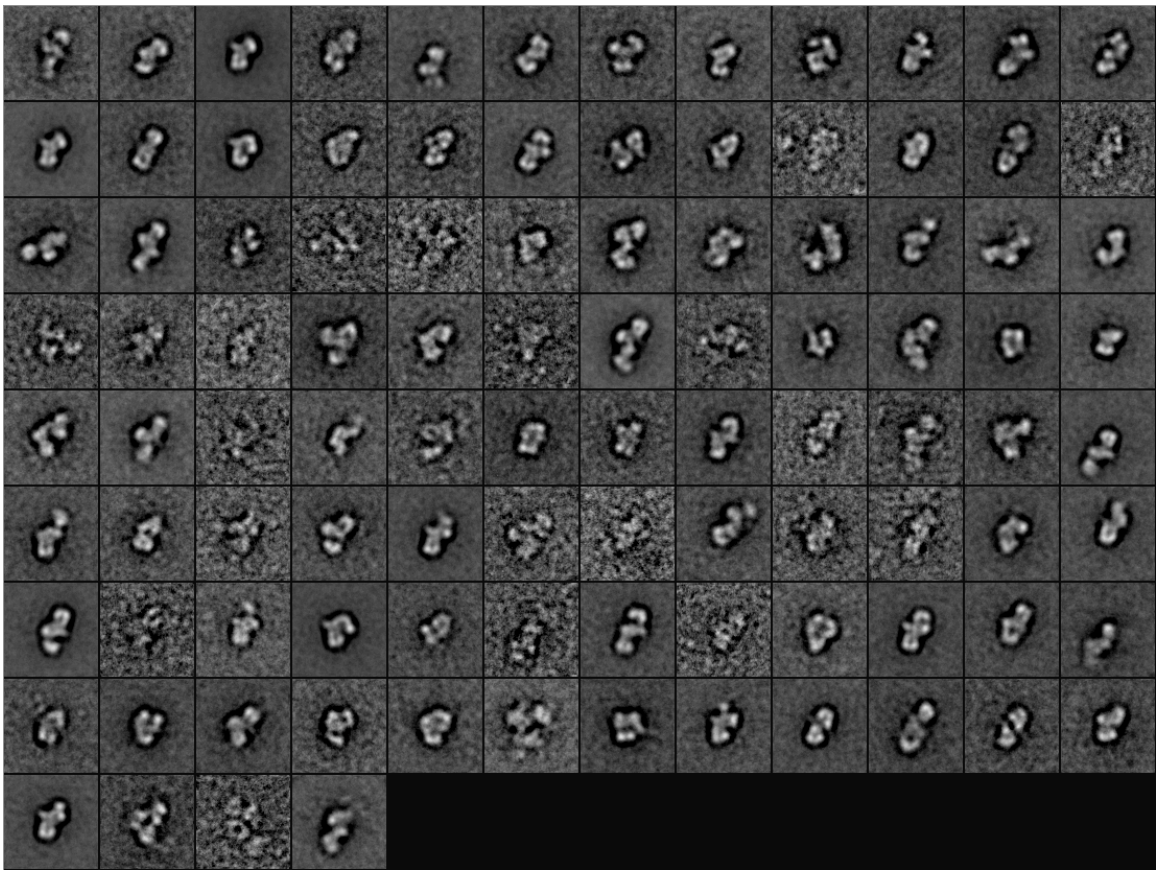

Figure A 3 Reference-free alignment of IcmF_Apo_GDP_IcsobutyrylCoA – 3,226 particle projections into 100 classes.

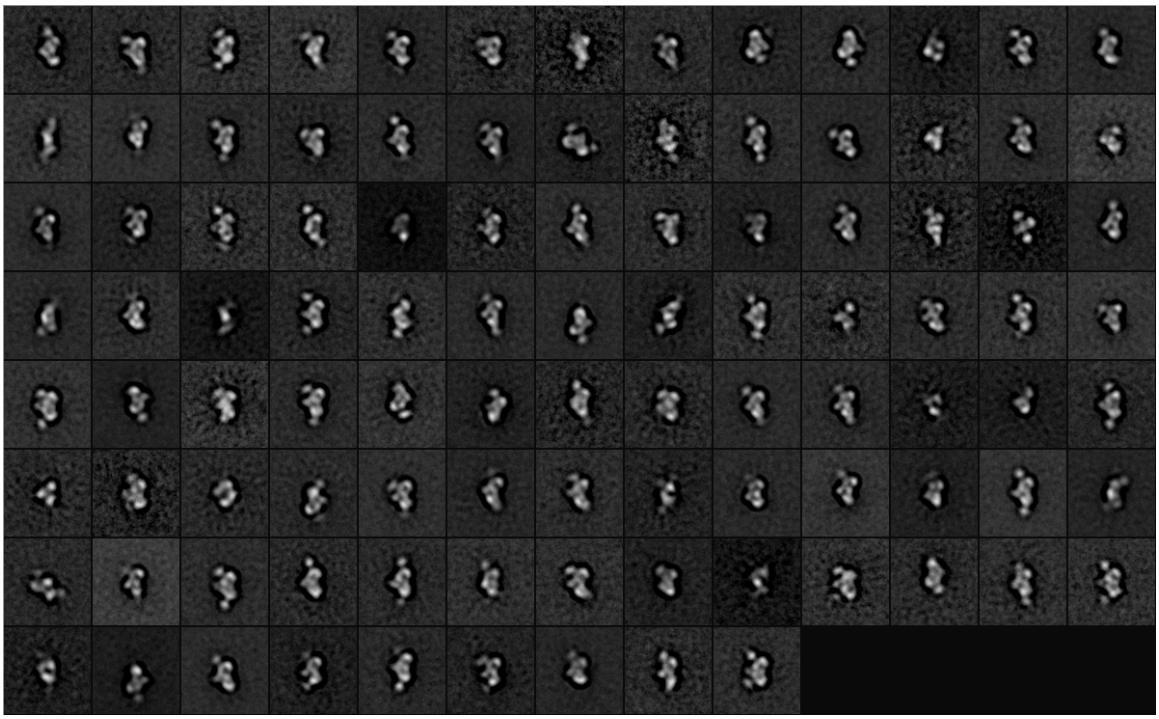

Figure A 4 Reference-free alignment of truncated IcmF, lacking the B12 binding domain – 14,588 particle projections into 100 classes.

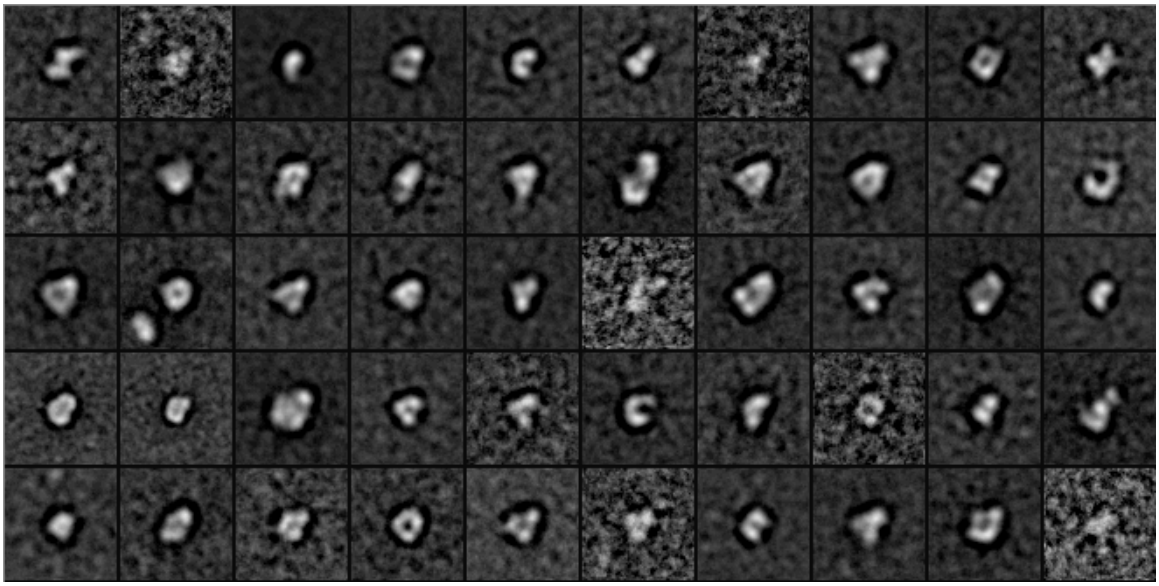

Figure A 5 Reference-free alignment of MeaI, a single domain of IcmF, possibly defining the interface between the two subunits.

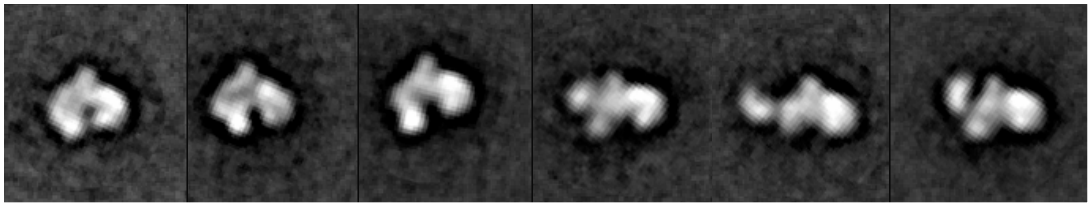

Figure A 6 Gallery of different IcmF conformations

During our analysis of the 2D class averages of the holo complex, we observed that while one half of the molecule remained consistently similar when compared between class averages, the other half varied dramatically. We wanted to further investigate this phenomenon and calculated a three dimensional reconstructions using the Random Conical Tilt approach. The three dimensional envelop closely resembles the 2D averages. However, due to the limited biochemical data, we could not explain the significance of the "movement" od one of the domains.

In conclusion, due to the limited biochemical information, our EM results were inconclusive and we didn't pursue further investigation.

Appendix B

Vps13

*This project has been in collaboration with Bob Fuller Lab at University of Michigan, Ann Arbor.

Mutations in human orthologs of the yeast VPS13 result in hereditary disorders chorea acanthocytosis and Cohen syndrome. VPS 13 functions to transport proteins to the vacuole in yeast and also plays an important role in the formation of prospore membrane that eventually gives rise to spores. Because of the established role of yeast VPS13 in vacuolar transport, it has been inferred that the human phenotypes result from comparable defects in membrane transport.

We carried out some initial EM negative stain analysis of VPS13 to gain more insights into its overall topology. We carried out the 2D classification with reference-free alignment and split the 7,639 particle projections into 50 classes (Figure B 1).

The class averages revealed a highly elongated and flexible molecule. Some of the 2D averages revealed a distinct loop at one end and a characteristic hook at the other diametrically opposite end. However, because of the highly flexible nature of the particles and their subsequent alignment, these features were lost form most of the classes. We attempted to isolate only these averages that clearly displayed either the loop or the hook and reclassify the particles with a subsequent round of reference-free classification. As a result we split ~3,000 remaining particles into 15 classes and performed another round of averaging (Figure B 2).

Figure B 1 Reference-free alignment of VPS13 - ~7,600 particle projections classified into 50 classes.

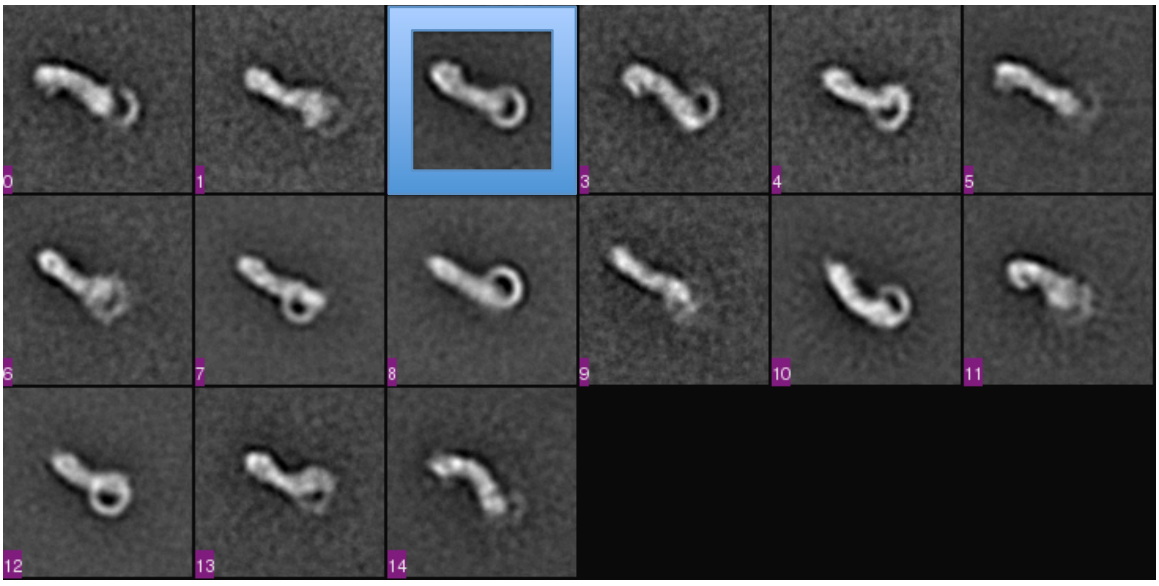

Figure B 2 Reference-free alignment of VPS13 - ~3,000 particle projections classified into 15 classes.

In addition, we generated three-dimensional reconstructions, using the Random Conical Tilt Approach from three classes that most clearly displayed both characteristic features (Figure B 3).

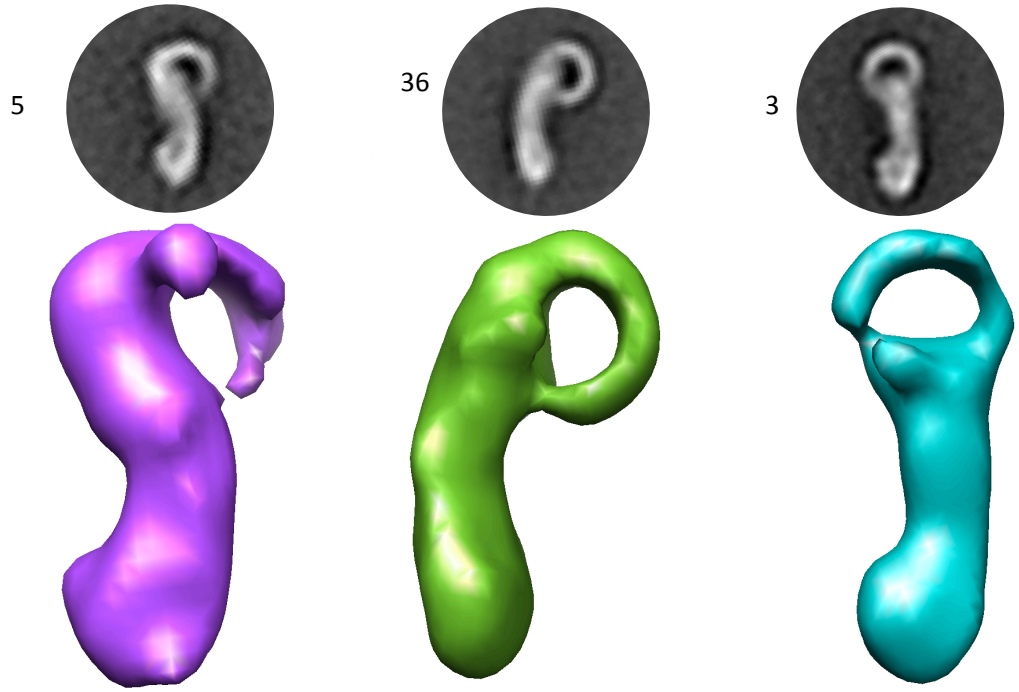

Figure B 3 three-dimensional reconstructions from the respective 2D class averages, using Random conical tilt approach.

In conclusion, these analysis require further and more thorough investigation. Additionally, optimizing sample preparation and staining is also of critical importance in order to aid in the negative stain analysis.